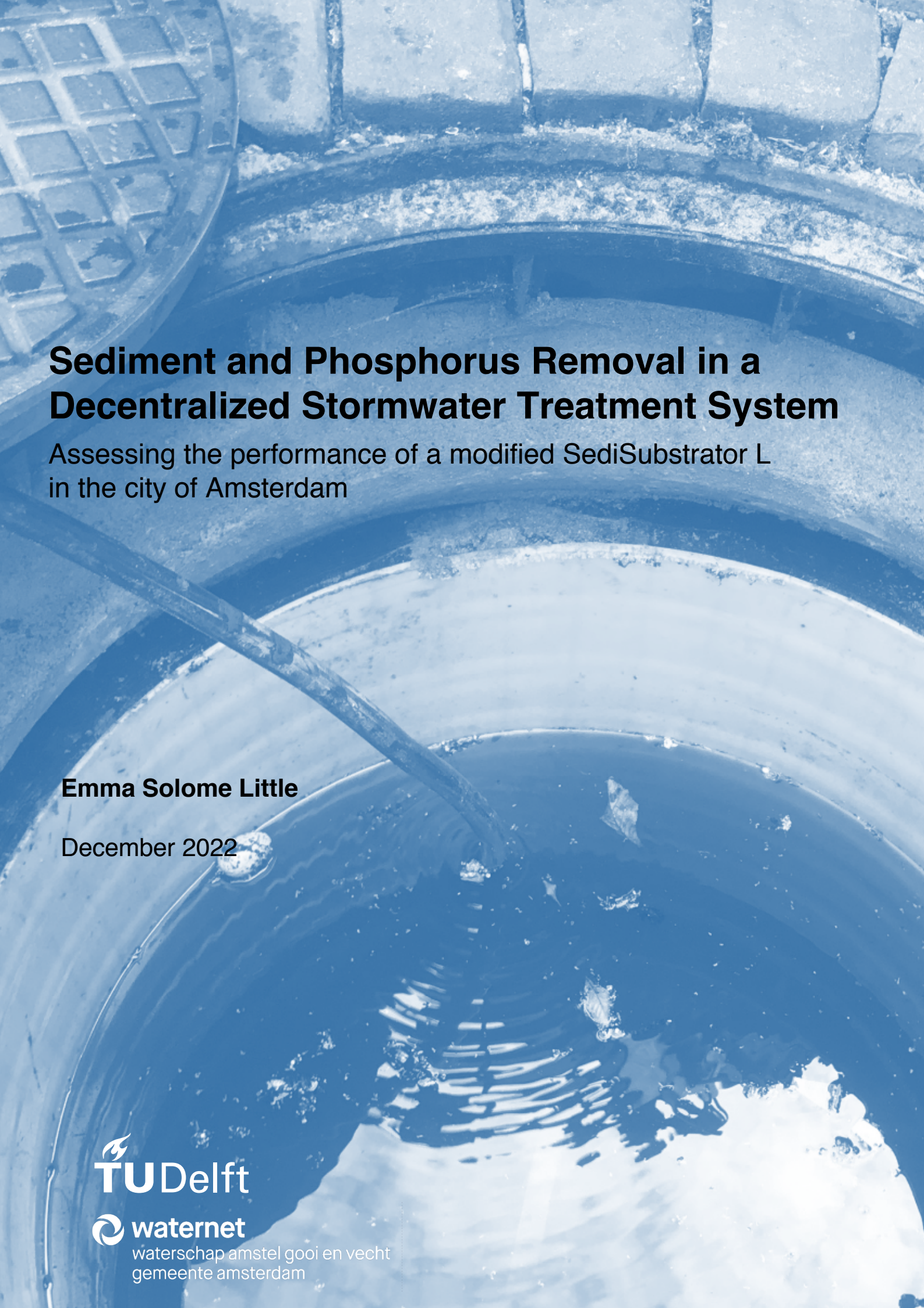

Sediment and Phosphorus Removal in a Decentralized Stormwater Treatment System

Assessing the performance of a modified SediSubstrator L in the city of Amsterdam

Emma Solome Little

December 2022

TU Delft

waternet
waterschap amstel gooi en vecht
gemeente amsterdam

Sediment and Phosphorus Removal in a Decentralized Stormwater Treatment System

Assessing the performance of a modified SediSubstrator L
in the city of Amsterdam

Emma Solome Little

Student Number: 5364396

in partial fulfilment of the requirements for the degree of

Master of Science
in Civil Engineering, Environmental Technology

To be defended in public on the 2nd of December 2022
An electronic version of this thesis is available at *http://repository.tudelft.nl/.*

Thesis Committee

Committee Chair:	**Prof. dr. ir. Jan Peter van der Hoek**	*TU Delft & Waternet*
Daily Supervisors:	**Frank Smits, MSc**	*Waternet & TU Delft*
	Dr. Winnie Rip	*Waternet*
Committee Members:	**Dr. ir. Jeroen Langeveld**	*TU Delft & Partners4UrbanWater*
	Dr. ir. Martine Rutten	*TU Delft & The Green Village*
External Advisors:	**Dr. ir. Frans van de Ven**	*Deltares*

TU Delft

waternet
waterschap amstel gooi en vecht
gemeente amsterdam

With research funded in part by the province of North Holland

Preface

This document presents the culminating thesis report for the Master of Civil Engineering, track Environmental Technology at TU Delft. I am extremely grateful for my time at Waternet and collaborations with Fränkische Rohrwerke these past nine months. From start to finish, this project presented me with all the ingredients of fulfilling research—navigating uncertainty, the "aha" moments, the unexpected findings with big implications, the collaboration with many, many enthusiastic colleagues, the data cleaning, the lab work and the hands-on maintenance of a full-scale installation in the city. These are just a few of the highlights.

I am grateful for the guidance and support I received throughout this project, first and foremost from my thesis committee filled with "echte liefhebbers" of the water sector. Thank you, Frank, for exemplifying inclusive, purpose-driven work every day—through your tireless efforts, bottomless enthusiasm and out-of-the-box thinking. Winnie, Jan Peter and Frans, thank you for your sound guidance and for inspiring me to follow crucial (and very interesting) aspects of this project of this field. Martine, thank you for trusting in me (throughout the past two years) and for being a role model of how interdisciplinary, ethical engineering can be carried out. And thank you Jeroen for your candid feedback and advice, making sure lessons learned from past full-scale experiments are carried forward.

Working in the field, further—in the city—definitely requires flexibility. Simon Holsteijn (and colleagues) are familiar with this, and I'm unbelievably appreciative of the continuous stream of communication on pipe status, maintenance and sampling that took place in the past months as settings and equipment were adjusted and re-adjusted. Thanks to Wilko, Arjen, Nico, Michael, Frans and Wesley for the past work making this possible and continuous, warm support for any question or need of mine now. I'm indebted to Volkert and the sewer cleaning colleagues of Waternet as well as to Peter and the colleagues from BAM who were meticulous, quick and eager to think along. Thanks to Jasper, Paul, Mark, Erik, Henco, Juan, Liesanne, Cheryl, Petra and Joost (to name just a few) for introducing me to your work. Finally, I'm grateful for the opportunity I had to present this work at the Waternet Innovation Day, on multiple bike excursions and at the Groundwater Colloquium.

The past two years have been a period of marked growth and opportunity for me. I feel incredibly lucky to have met and lived alongside some truly amazing people. You know who you are, and in case you don't I will profess my gratitude to you in person at some point soon. Thank you for sharing ideas, musings and ambitions with me. Finally, although quite far away in distance I am grateful for my family, who have always been campaigners of working hard, playing hard and making sure the work is something I truly love. I think I have found that here.

Emma Solome Little
Amsterdam, December 2022

Abstract

In the context of climate change and urbanization, sustainable urban drainage systems (SUDS) are widely adopted measures to manage stormwater in the city on-site. However, their performance in practice often differs from modelled and laboratory-scale predictions due to the variability in properties of real sediments (in terms of size, shape, density and coagulation) compared to the silicate standard Millisil®W4. Clogging is a common source of failure.

The *SediSubstrator L* is a decentralized stormwater treatment device installed as a pre-treatment step to mitigate clogging in a storage and infiltration system on the Rooseveltlaan in Amsterdam. It consists of a sedimentation pipe with a flow-separating grate, the *SediPipe*, and a filter-adsorbent, the *SediSorp+.* It is purported to remove 80% of TSS by DiBT (the technical authority in the German construction sector) test principles that use Millisil®W4 to simulate real sediments. The full-scale unit was monitored in the city throughout May-September 2022 to assess its performance.

The stormwater runoff discharged from the catchment had high concentrations of lead (54 µg/L) and zinc (790 µg/L), likely due to contact with gutters and old roofing material, amplified by the relative contribution of these roofs to the total catchment discharge (accounting for 50% of the area contributing to runoff). The sediment (TSS) concentration was low, equivalent to 20 mg/L on average. The sediments were also light and fine—with an organic fraction of 66% and with 78% of diameter smaller than 63 µm.

In the SediSubstrator L, the TSS removal efficiency was 34% on average. This corresponds to an estimated caught load of 2.7 kg for this period. The removal efficiency was shown to increase with an increasing stormwater TSS concentration, with longer antecedent dry periods and with lower TSS organic fractions. Turbidity dynamics in the system suggest that while a net sequestration of solids occurs in the SediPipe, there is a resuspension of fine solids. This was observed in a camera inspection to occur from solids which settle on or near the grate. In an extreme rainfall event on September 28th 2022, water collected on the section of the street connected to the SediSubstrator, the cause of which is still subject to speculation. The observed SediSorp+ filter resistance across the summer was not indicative of gradual clogging, but an inspection showed signs of decayed organic matter throughout the full length of the filter bed as well as traces of cement in two of the four cartridges. It is possible that these two effects together with turbulent inflows prompted the acute clogging behavior.

There is interest in using the SediSubstrator beyond the city of Amsterdam to reduce phosphorus loadings in the road runoff discharged to sensitive nature areas. On the Rooseveltlaan, the average total phosphorus removal efficiency was 18% (50% for dissolved, readily bioavailable ortho-phosphate). Interactions with settled sediments generated ortho-phosphate in the SediPipe, and fine particulate and colloidal organic phosphorus was shown remobilized in both the SediPipe and SediSorp+. The removal of ortho-phosphate in the SediSorp+ in natural rainfall was good (on average 50%) and was shown to be consistent at different contact times (approximately 10-30 minutes).

The installed unit should be monitored over a longer time period of two years for statistical significance and to capture seasonal variation in loads. Nevertheless, the removal efficiency observed on site is consistent with the results of a sedimentation model developed according to Ferguson & Church (2004), using a stormwater sediment particle density as measured at another location in the city. Design adaptations are recommended to improve the SediSubstrator L to the conditions observed in Amsterdam: namely, better site selection, a longer SediPipe section (24 m) and a second filter stage to better capture the fine suspended solids.

List of Figures

List of Tables

List of Abbreviations

SUDS – Sustainable Urban Drainage Systems
TSS – Total Suspended Solids [mg/L]
TSS_{63} – Total Suspended Solids of Particle Diameter < 63 µm [mg/L]
Total P – Total Phosphorus [mg/L]
PO_4^{3-} – Ortho-Phosphate [mg/L]
CSO – Combined Sewer Overflow
WFD – Water Framework Directive
GRP – Municipal Sewerage Plan 2018-2021 ("*Gemeentelijk Rioleringsplan*")
BAT – Best Available Technology
SP1/SP2/SP3 – Sampling Point 1, 2 and 3
EMC – Event Mean Concentration
PSD – Particle Size Distribution [vol. %]
I_{max5} – Rainfall Maximum Intensity, 5-Minute Average [mm/h]
ADP – Antecedent Dry Period [d]

Table of Contents

1 Introduction

1.1 General Introduction

The movement towards making better use of natural drainage mechanisms in the city—under the moniker of Sustainable Urban Drainage Systems (SUDS)—has been underway since the 1970s (Davies & Butler, 2011; Duffy & McKay, 2015). The associated systems are widely applied, nevertheless, there often still exists significant discrepancies between their modelled or laboratory-scale performance to that in practice (Conley et al., 2020; Lieske et al., 2021; Neupert et al., 2021; Vollaers et al., 2021).

On the Rooseveltlaan in Amsterdam, a stormwater treatment unit, the *SediSubstrator L*, was installed as a full-scale test to mitigate clogging in an infiltration system situated under the tram tracks. There is a particular interest in quantifying the total suspended solids (TSS) load removed by the SediSubstrator L, to determine to what extent it lengthens the lifetime of the infiltration system. Beyond the city, the SediSubstrator L is being considered for a different purpose—to reduce phosphorus loadings to the Loosdrecht lakes, which are located in a Natura2000 area and regularly exceed the Water Framework Directive guidelines.

1.2 Problem Statement and Aim

The research objective is to leverage the installed SediSubstrator L to not only evaluate its performance in an urban setting on the Rooseveltlaan but also to provide an outlook for its application in sensitive nature areas. To do so, the unit's efficiency of sediment (TSS) and phosphorus removal will be estimated over a summer season (May-September 2022). This will be done through in-situ monitoring and sampling with natural rainfall and with a pumped, controlled phosphorus dosing experiment. Lessons learned from this evaluation will be supported through the development of a sedimentation model to guide proposed design adaptations.

1.3 Thesis Layout

This thesis is organised in seven chapters. This initial chapter provides a general overview of the SediSubstrator L as a decentralized treatment technology in the SUDS movement and highlights an interest in the removal of sediment and phosphorus loading in stormwater discharge.

Chapter 2: *Project Background* outlines the motivation for the installation of the Sedi-Substrator L on the Rooseveltlaan as a climate adaptation measure. Past research on the unit and on sediments in stormwater is summarized. Current interest in the SediSubstrator L to remove phosphorus from stormwater discharge in sensitive nature areas, and the greater issue of phosphorus loading in stormwater is introduced.

Chapter 3: *Research Questions* enumerates the guiding research questions in response to the background information and the identified knowledge gaps.

Chapter 4: *Research Methodology* describes the methodology for the site preparation, monitoring and experimental work on the Rooseveltlaan. The development of a sedimentation model is explained. Data analysis, including an assessment of the filter resistance across the experimental period to corroborate observations is also explained.

Chapter 5: *Results* presents hydrological information, the stormwater composition and the long-term removal efficiency of sediments and phosphorus with an estimation of the total load removed. Model results are used to support experimental results and guide design recommendations. Relationships between the removal efficiency and environmental factors are presented, and the change in filter bed resistance over time is analyzed.

Chapter 6: *Discussion* compares the results to literature and elaborates upon the implications of these findings. The limitations of the methodology are discussed. An outlook on the performance of the Rooseveltlaan SediSubstrator in the context of sensitive nature areas is provided.

Chapter 7: *Conclusions and Recommendations* lists the conclusions of the research project. It includes recommendations for future research and for design adaptations to better suit the situation in the city of Amsterdam.

2 Project Background

2.1 Study area: the Rooseveltlaan, Amsterdam

The Rooseveltlaan is situated in the Rivierenbuurt, a subsided area located in the south of Amsterdam, which suffers from flooding after extreme rainfall and low groundwater levels during drought. The importance of introducing rainproofing measures there was deemed extremely urgent by Amsterdam Rainproof (see Figure 1). This characterization applies in cases in which there is a risk of serious damage to, for example, real estate, vital infra-structure, hospitals and museums, with a serious traffic nuisance in the area (City of Amsterdam, 2022), and should be resolved on a 5 year time-frame. As such, many water infiltration and storage projects are currently in progress, such as bioswales, permeable pavements, green areas and infiltration zones.

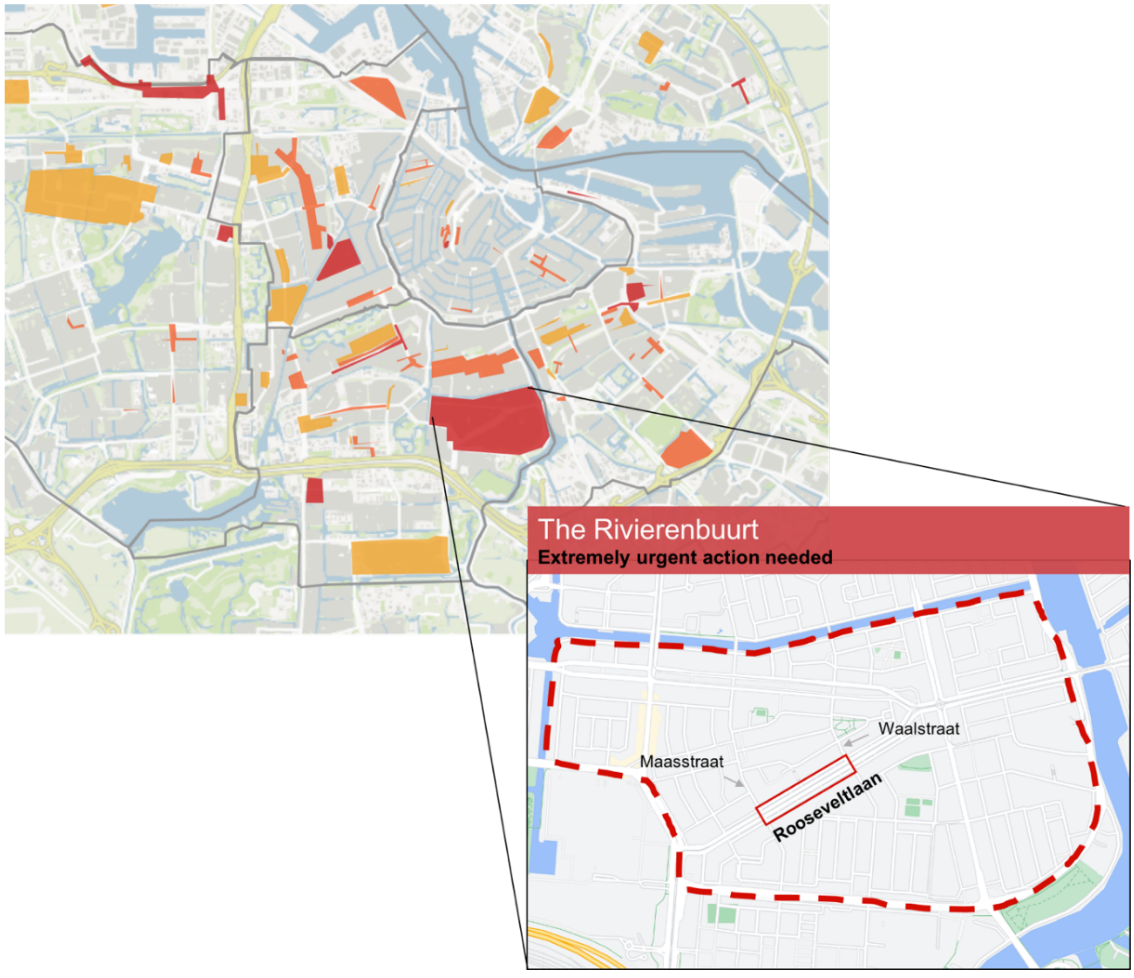

Figure 1: Map of Amsterdam with urgency of rainproofing measures marked by neighbourhood (*yellow: urgent, orange: very urgent, red: extremely urgent*); the Rivierenbuurt and the system boundary for the Rooseveltlaan study area marked in red. Adapted from the City of Amsterdam (2022)

Along the Rooseveltlaan, between the Maasstraat and Waalstraat, an infiltration system has been installed below the tram tracks to store and infiltrate stormwater from the service road,

the main road, sidewalks, adjacent green strips and roofing—acting as both a heat-proof (improving drought tolerance) and a rain-proof intervention.

2.2 The AquaBASE

The stormwater infiltration system installed under the tram tracks on the Rooseveltlaan is the AquaBASE, supplied by the company of the same name. It is intended to act as a water storage and infiltration facility in extreme rainfall events and as a buffer in drought to maintain groundwater levels, protecting the surrounding dwellings' wooden pile foundations from decay. Its composition is shown in the side view in Figure 2.

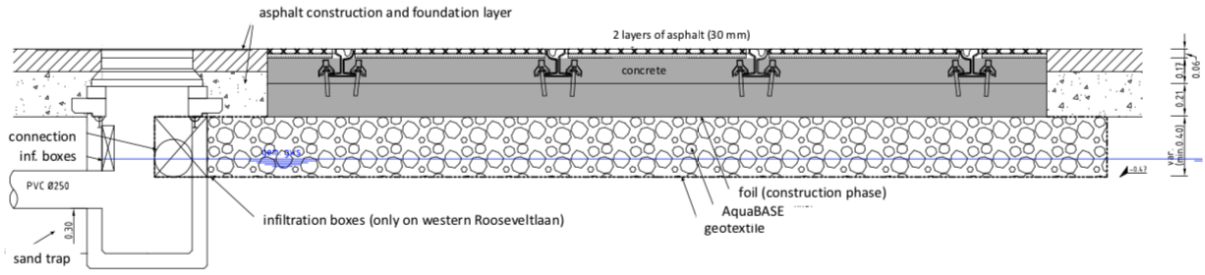

Figure 2: Side view of the AquaBASE infiltration system below the tram tracks (Goess-Enzenberg, 2020)

The inflow from the separated stormwater sewer on the block enters the system through the PVC pipe of diameter 250 mm shown on the left side of the figure. It has a total storage capacity of 523 m^3, comprised of infiltration boxes and a coarse aggregate bulk material, the EcoBASE A5 8/32. The aggregate material accounts for the most of the infiltration system, with a length, width and depth of 290 m, 7 m and 0.55 m respectively and pore space of 35% (*EcoBASE A5*, n.d.). This material risks clogging long-term due to the suspended solids loadings in urban stormwater. This concern is not unique to the AquaBASE – in infiltration systems, clogging has been cited as the most common technical failure in occurrence, and is a current subject of research at various institutions (Conley et al., 2020; Niëns, 2015; Vollaers et al., 2021; Votel et al., 2022). Accessing the space below the tram tracks is extremely difficult and disruptive, making maintenance on the system unfeasible. It follows that two SediSubstrators, accompanying decentralized water treatment devices, were installed to remove sediments from stormwater runoff pre-infiltration to reduce the risk of clogging.

2.3 The SediSubstrator L

The SediSubstrator L is a decentralized stormwater treatment unit from Fränkische Rohrwerke which functions based on the principles of sedimentation and filtration. It is the feature of the study on the Rooseveltlaan and was installed upstream to the AquaBASE infiltration system. The unit is designed to remove particulates, heavy metals, nutrients and light oils from stormwater (*Product Brochure: SediPipe L / L plus; SediSubstrator L*, 2019). As shown in Figure 3, it consists of a start shaft, a horizontal pipe with a sedimentation-promoting flow separator (the SediPipe) and an end shaft housing a filter adsorbent (the SediSorp+). The filter

adsorbent distinguishes the SediSubstrator from the SediPipe (a similar unit installed with a vacant end shaft).

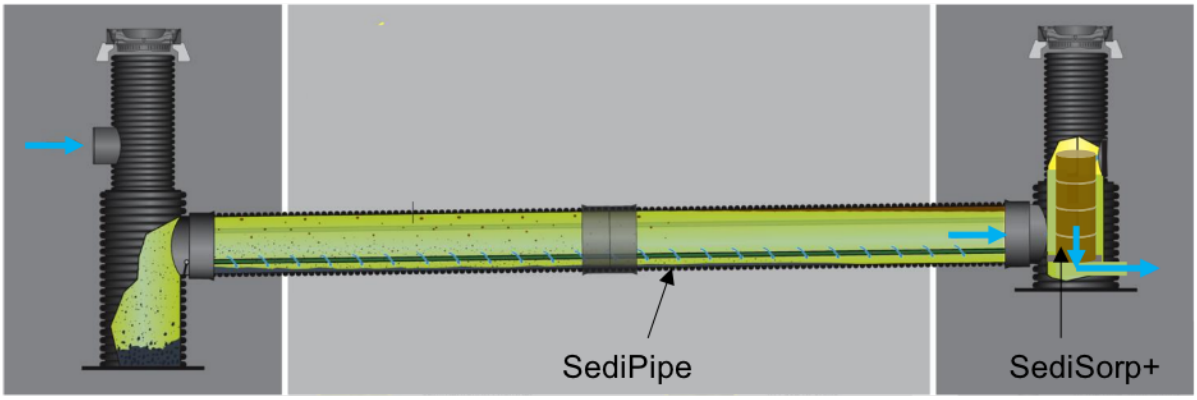

Figure 3: The SediSubstrator L (adapted from: Product Brochure: SediPipe L / L plus; SediSubstrator L, 2019)

The performance is advertised to be compliant with the German Association for Water, Wastewater and Waste DWA-A 102-2 regulations for TSS removal. In particular, the removal efficiency for sediments with diameter smaller than 63 µm (TSS_{63}) is said to be 80% according to methods in Section 6.1.2 of DWA-A 102-2 (*SediSubstrator® L*, n.d.).

Over 40 SediPipe systems (without filter) have been installed in the Netherlands to date (Klappe, 2022), but it appears none of them are being monitored beyond scheduled maintenance activities. On the south-side of the Rooseveltlaan, two SediSubstrator L 600/12s were installed in the period between December 2021-April 2022. The model is named for the diameter (600) and length (12) of the SediPipe.

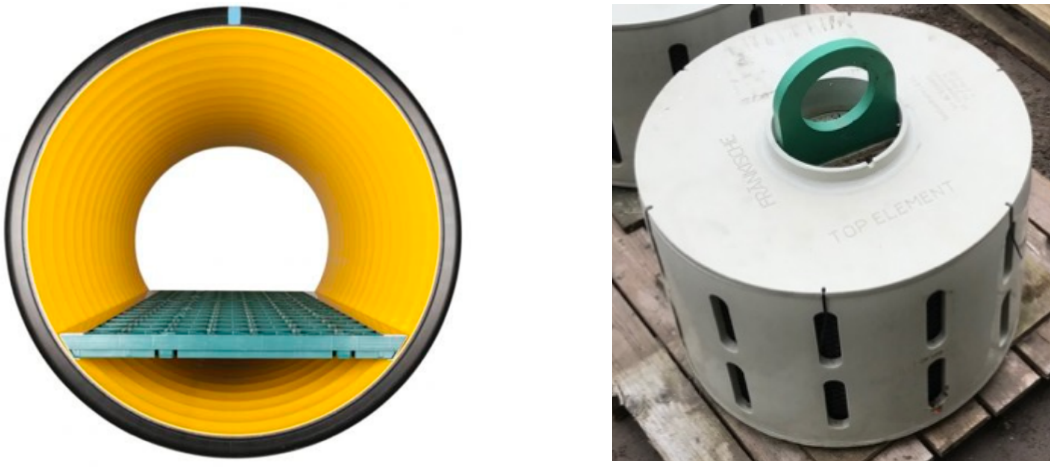

Figure 4: SediPipe cross-section (left, from Fränkische Rohrwerke) and SediSorp+ filter cartridge (right)

Sedimentation takes place in the SediPipe, with adsorption as well as filtration in the SediSorp+ in the end shaft (*Product Brochure: SediPipe L / L plus; SediSubstrator L*, 2019). The flow separator (the green grate visible on the left side of Figure 4) drives the sedimentation and solids collection process in the SediPipe, as the lower section of the end of the pipe is closed, creating a stagnant storage space for settled solids below it. This aspect is designed to reduce the resuspension of solids with inflow to the system and was validated in tracer tests

(Boogaard, 2015). The SediSorp+ filter cartridges in the end shaft (as shown in Figure 4) are cylindrical with slots down the sides and with a hollow core; the lid of the top element is sealed such that flows enter the filter laterally. Further information on the filter material is protected by a non-disclosure agreement.

2.4 Past Research on the SediSubstrator

A full-scale SediPipe XL 600/24 (the system without a SediSorp+ filter, with a 24 m long SediPipe section) was tested in the Hydraulic Laboratory of the TU Delft, using Millisil®W4 quartz to simulate stormwater sediments as a part of the PhD thesis of Floris Boogaard (2015). Results from these experiments demonstrate that for flowrates of 10 L/s a removal efficiency of nearly 100% is expected for particles over 63 µm, and a maximum 45% removal efficiency for particles smaller than 25 µm (Figure 5).

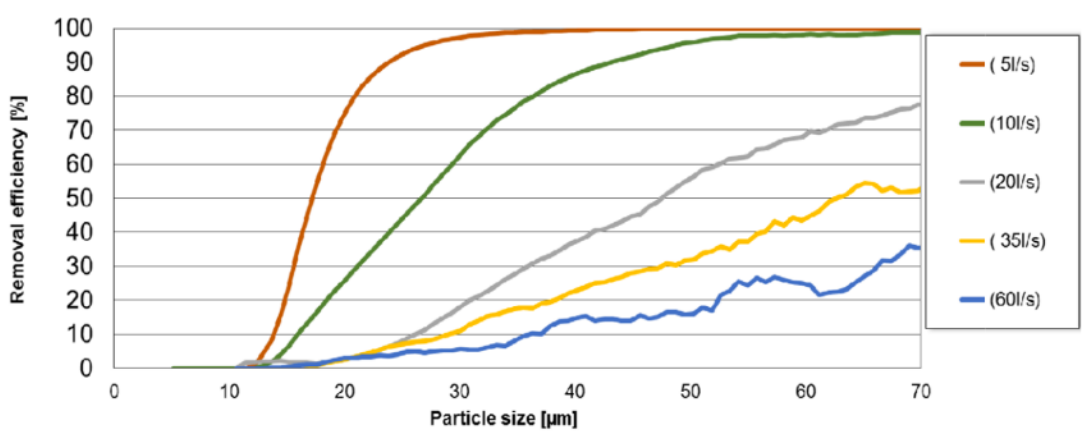

Figure 5: Measured removal efficiency of the SediPipe XL 600/24 for various flowrates (Boogaard, 2015)

A theoretical model for the SediPipe was also developed in 2020 as part of the MSc thesis of Isabelle Goess-Enzenberg. This model, using experimentally-determined particle densities from literature, predicted improved removal efficiencies as compared to the experimental results of Boogaard, especially at mid-range flowrates (Figure 6).

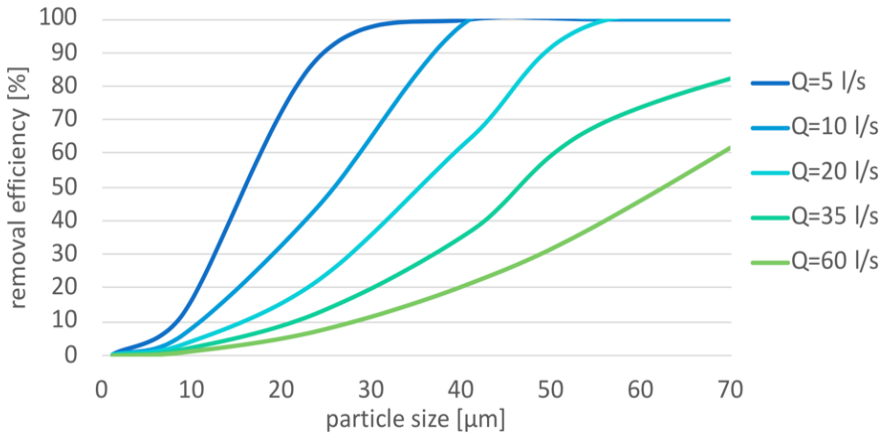

Figure 6: Modeled removal efficiency of the SediPipe L 600/12 for various flowrates (Goess-Enzenberg, 2020)

Furthermore, the model results show that the influence of precipitation and runoff volumes on the TSS removal efficiency is small: for a normal rainfall event the efficiency varies only within a range of 6% (Appendix A, Figure A - 2). Nevertheless, for fine sediments, ie. stormwater with a TSS_{63} fraction greater than 40%, the average annual solids removal efficiency during flow-phase ranges in between 17 and 78%, as shown in Figure 7. This same figure demonstrates the extent to which stormwater with sediments with a greater coarse fraction have a significantly improved removal efficiency (increased by 10% for each 10% reduction in TSS_{63}).

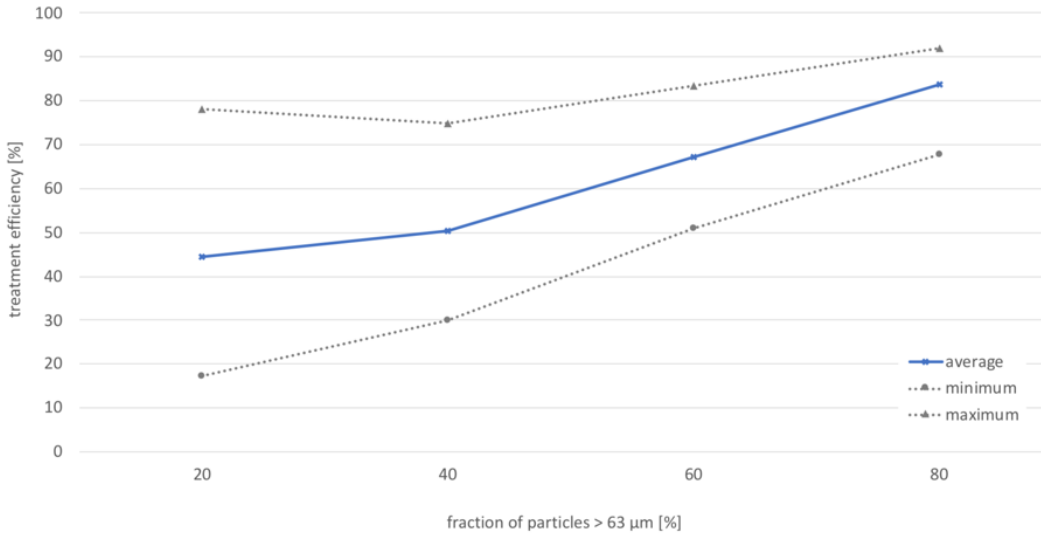

Figure 7: Influence of sediment particle fraction on modeled removal efficiency (Goess-Enzenberg, 2020)

There are two multi-year in-situ research projects being conducted on the SediPipe: in Münster, which started in 2017 and in Hamburg, which started in July 2022. In Münster, 19 rainfall events were sampled between January 2018 and June 2019 with a mean and median intensity of 1.8 mm/h and 0.9 mm/h, respectively. Results from Münster show a long-term removal efficiency of TSS of 29% for the 2018-2020 period (Lieske et al., 2021). These results are justified by the particle size distribution of the suspended solids—with 78% finer than 63 µm in size (TSS_{63}) that do not have a sufficient residence time to settle. The removal efficiency for TSS_{63} is estimated to be 16%, and for the remaining coarse fraction 59%. The authors conclude that in-situ treatment is not consistent with lab results, and that the treatment of urban stormwater runoff with a significant TSS_{63} fraction requires a filtration step as sedimentation alone is not sufficient (Lieske et al., 2021). The results have been contested by Fränkische Rohrwerke, however, as the product of a biased sampling method that favoured heavier rainfall events. With more water flowing through the system, the samples have benefitted relatively less from the "batch effect" (water which has previously been stagnant in the system with more time to settle and is effectively pushed out). This means the discharge from the SediSubstrator would consist of more water which has directly flowed through the system during the event with less time for sedimentation. When input into a hydraulic model that is being developed with academic partners, they claim that they are able to mediate this bias, and removal efficiencies more similar to lab-scale estimations are expected.

Research on the removal efficiency of the filter medium has reportedly been privately conducted by the supplier; however, results from lab or in-situ experiments including the filter cartridge performance have not been published. The impact on nutrients such as phosphorus in real stormwater has not been investigated.

2.5 Suspended Solids in SUDS

In controlled testing of SUDS systems Millisil®W4 is typically used. Nevertheless, it has limitations due to the variability of actual urban suspended solids' particle size distribution, density, non-uniform shape and coagulation properties per catchment (Boogaard, 2015). Differences in density are driven primarily by the organic and mineral fractions of the sediments, which vary within the fraction categories as well.

In real stormwater sediments, the mineral fraction consists of compounds originating from soils (ie. quartz and clay-forming materials), from road wear, vehicle abrasion (brakes and tires) and from atmospheric deposition (Gelhardt et al., 2021). Quartz-like materials typically account for most of the mineral fraction and have a density around 2600 kg/m^3. In general minerals from road wear and atmospheric deposition have been reported to have densities in the range of 2040 to 2940 kg/m^3 (Gruber, 1985). The average mineral fraction in stormwater in the Netherlands is 44% (Liefting et al., 2020).

The organic fraction of sediment stems from vegetation debris (ie. leaf litter or soil-based material) or from traffic, such as tire and bitumen wear. Vegetation debris accounts for most of the organic fraction of sediments and its bulk density can range between 200 to 1350 kg/m^3, depending on the type of material (Li et al., 2020; Swenson & Enquist, 2008). Tire and bitumen-based material account for a small mass proportion and have a density around 1000 kg/m^3, although different tire formulations can contain more metals or other compounds affecting this value (Alves et al., 2020; Faizah et al., 2019).

The season (impacting especially the composition of the organic fraction of sediments), catchment use (impacting both organic and mineral fractions) and antecedent dry period (influencing the particulate size through contribution of atmospheric dry deposition and as well as the load in stormwater) all influence the properties of stormwater sediments (van de Ven, 2016). Therefore, properties vary not only by location but also with time. Millisil®W4 has a uniform density of 2650 kg/m^3, a property which is not representative of the complex and variable composition of stormwater sediments. The stormwater sediments at the inlet to a settling facility in the Ookmeerweg in Amsterdam have been measured to have an average density of 1144 kg/m^3 (Nijman et al., 2015). Sedimentation time is a function of density, suggesting that Millisil®W4 experiments may overestimate the removal efficiency of sedimentation facilities. Indeed, experiments on this topic demonstrate consistent over-estimations between lab-scale installations using Millisil®W4 and in-situ systems (Neupert et al., 2021). The average removal efficiency in-situ has been observed to be 10-23% lower for TSS and 13-40% lower for TSS_{63} as compared to lab-scale results (Neupert et al., 2021).

In stormwater, the most pollutants are bound to the finest particles due to their relatively large surface area to volume ratio (van de Ven, 2016). In particular, 74 to 88% of the heavy metals (Zn, Cu and Pb) are absorbed by the particles of a size smaller than 63 µm (Fuchs et al., 2019). This highlights the importance of ensuring the fine fraction of sediments is removed by SUDS systems to maintain or improve environmental quality.

2.6 Phosphorus in SUDS

Phosphorus in stormwater runoff is generated from organic matter (like vegetation, leaf litter and animal droppings) as well as detergents, added fertilizers and to a small extent from dry atmospheric deposition (Figure 8) (*Loosdrecht Site Visit*, 2022; Mandemakers & Holstein, 2019). The relative loading from each of these sources is likely to vary seasonally and with use. Urbanization increases phosphorus concentrations in runoff, as impervious surfaces reduce the entrapment, sorption and uptake of particle-bound P in soils and vegetation (Hobbie et al., 2017). Rainfall intensity, runoff volume and duration, the mass of street leaf litter and antecedent dry days have all been identified as predictors of phosphorus concentrations in runoff (Allison et al., 1998; Li et al., 2015; Wang et al., 2022).

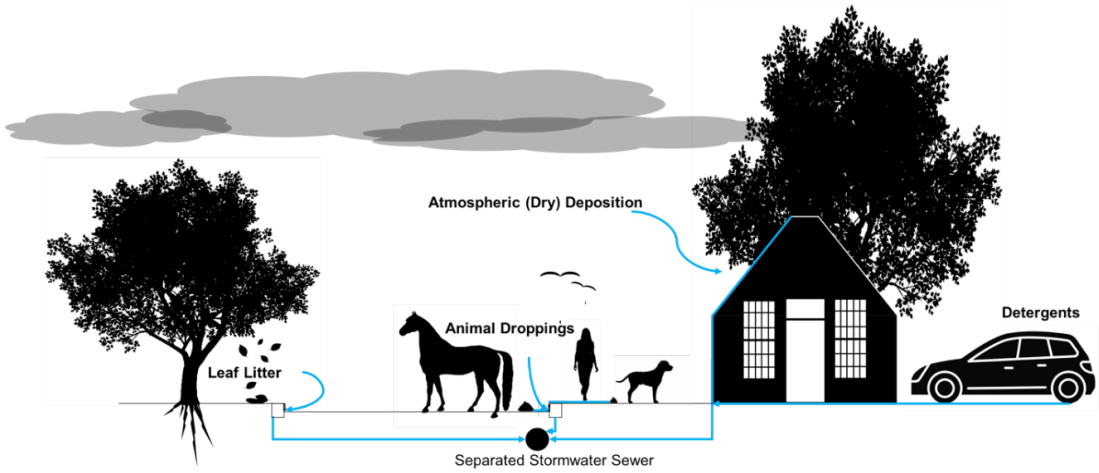

Figure 8: Environmental sources of phosphate contributing to phosphorus loadings

Phosphorus in stormwater is both dissolved and particle-bound. The dissolved fraction consists of mostly ortho-phosphate (PO_4^{3-}), which is readily bio-available for uptake by algae and microorganisms, and some dissolved organic phosphate (Y.-Y. Yang & Toor, 2018). Particulate phosphorus is predominantly found in organic matter (leaves, vegetation, etc.), in mineral form and adsorbed onto clays which may find their way into waterways with soil erosion (Schulz, n.d.). Decomposition processes play a crucial role in liberating usable phosphorus, converting the organic-bound P to soluble reactive phosphorus (PO_4^{3-}), as P is quickly solubilized from decomposing organic matter like leaf litter (Bratt et al., 2017). In terms of speciation, PO_4^{3-} is present in the forms of $H_2PO_4^-$ and HPO_4^{2-} between pH 6-8, which hovers around the average pH of stormwater in the Netherlands, equal to 7 (Liefting et al., 2020).

2.6.1 Impacts of Discharge on Receiving Waters

The discharge of phosphorus-loaded stormwater to surface waters accelerates eutrophication, a process marked by the domination of harmful algal blooms that reduce both light penetration and dissolved oxygen levels (Y.-Y. Yang & Toor, 2018). Consequently fish deaths occur and the growth of submerged water plants, which are crucial for a healthy water system, is inhibited. Stormwater phosphorus concentrations must be maintained below a critical limit to promote clear receiving waters with aquatic plants, in turn supporting the ecosystem and bolstering biodiversity.

Beyond the city of Amsterdam, there is interest in the SediSubstrator as a potential solution to reduce phosphorus loadings in road runoff that discharges to the Loodrecht lakes which are situated in a designated Natura2000 area. Although a standard of 0.03 mg P/L applies for the Loosdrecht lakes according to the European Water Framework Directive (WFD), this limit is often exceeded (*Oostelijke Vechtplassen | Natura 2000*, n.d.)(Mandemakers & Holstein, 2019). In the stormwater discharge, total phosphorus concentration is 0.21 mg/L P, of which 30% is readily bioavailable ortho-phosphate (PO_4^{3-}) and 70% is particle-bound (Mandemakers & Holstein, 2019). The overall stormwater quality in the area and further information on this case is summarized in Appendix A.

2.6.2 Phosphorus Removal Strategies

There are various chemical and physical techniques that may be used to remove phosphorus from stormwater in theory. Dissolved phosphorus may be removed from stormwater through chemical dosing to induce precipitation, the use of adsorptive media, ion exchange and biological removal (Bunce et al., 2018), while sedimentation and filtration are typical methods used to remove particle-bound phosphorus. Nevertheless, many of these methods are unfeasible in a full-scale situation in which available space is limited, cost is a crucial factor and both loadings and residence times vary per event. In practice, filtration-adsorption by $Fe(OH)_3$, iron-coated sand or bioswales are commonly applied (Shokri et al., 2021; J. Stroom, personal communication, September 2022).

3 Research Questions

The central question of this research project is:

How does the Rivierenbuurt SediSubstrator L perform as a decentralized stormwater treatment system with the potential to be deployed as a SUDS in the city of Amsterdam and the surrounding rural areas?

The main research question should be answered through the following sub-questions:

1. *What is the stormwater sediment composition in the Rivierenbuurt, and what are the sources of the pollutants in this system?*
2. *What is the efficiency of sedimentation and filtration-adsorption of the SediSubstrator L on TSS and P, and what is the contribution of the SediPipe and the SediSorp+ to this efficiency?*
3. *What key factors influence the removal efficiency?*
4. *How can the efficiency of the SediSubstrator L be improved?*
5. *How does sediment loading in the SediSubstrator L over time change the behavior of the system?*

4 Research Methodology

In order to answer the proposed research questions, the ensuing methodology was followed. This chapter focuses on the definition of the system boundaries and the SediSubstrator L technical details, on the experimental strategy, on the subsequent data analysis and the modelling that was performed.

4.1 Site Description

4.1.1 Layout

The Sedisubstrator L "S4" and the adjacent measurement location is situated on the south-west side of the Rooseveltlaan service road (coordinates 52°20'39.0"N 4°54'01.5"E), as shown in Figure 9. The service road is a quiet, tree-lined one-way route for local traffic (estimated 50 vehicles/day), parallel with the busier main road. A 5 storey-apartment block (age 1930-1945) lines one side, opposite the row of trees (Spaan & BAG, 2015).

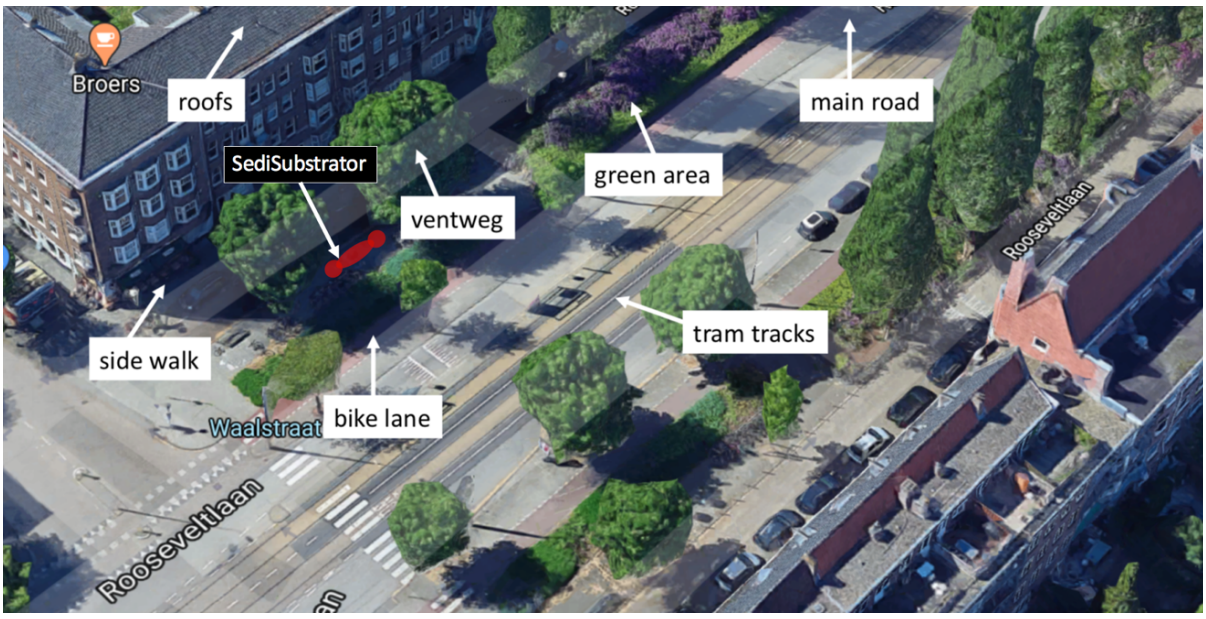

Figure 9: The location of the SediSubstrator and its surroundings on the Rooseveltlaan, adapted from (Goess-Enzenberg, 2020)

The catchment feeding into S4 consists of mostly sloped roofs, sidewalks, a service road, and green strips (shrubs and mature trees), with a total area of 6197 m^2 (Table 1). However, findings by Goess-Enzenberg show that the green areas contribute to the runoff just 0.02% of the time, making the effective area contributing to the runoff discharge into the SediSubstrator 4753 m^2 (Goess-Enzenberg, 2020).

Table 1: Contribution of surface types in the catchment feeding into the SediSubstrator L

	Roofs	Sidewalks	Service Road	Green Zones	Total
Area [m^2]	2508	1118	1127	1444	6197
Percentage [%]	41%	18%	18%	23%	100%

The stormwater runoff drains through 26 gully pots along the service road and is transported by a separated stormwater sewer of diameter 315 mm into the SediSubstrator. The system is shown in Figure 10. The system boundaries were set by placing blockages in the stormwater sewer to ensure that all discharge measured in the SediSubstrator enters into the AquaBASE infiltration system, and to isolate S4 (the studied unit) from S3 (the non-studied unit). The overflow weir to the Waalstraat stormwater sewer (Figure 10, right) was raised from the original NAP -0.80 m, level with the rest of the line and the AquaBASE inlet, to NAP -0.35 m, just above the target water level of the surrounding surface water bodies. In this system, stormwater runoff discharged from the main road does not flow through the SediSubstrator but directly into the AquaBASE. Due to expected high metals concentrations in the stormwater runoff from the tram tracks, this flow is connected directly to the dry weather sewer, sent to the wastewater treatment facility.

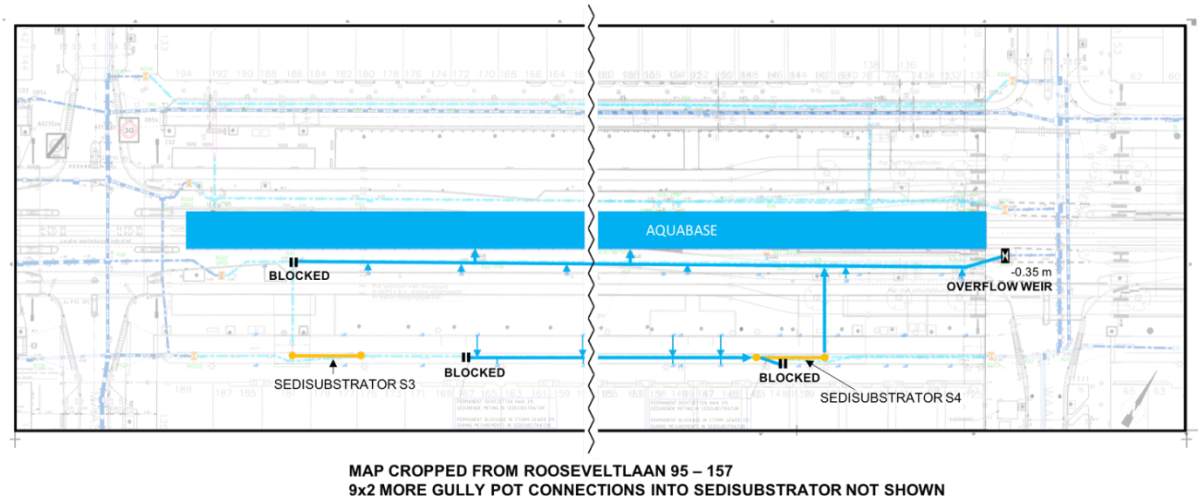

Figure 10: Plan of water flows in the Rooseveltlaan SediSubstrator-AquaBASE system, adapted from (de Leeuw, 2022)

4.1.2 The SediSubstrator L

The SediSubstrator was modified to suit the situation in Amsterdam, with the installation depth reduced from 4 m to 3 m, the end shaft enlarged from DN600 to DN800, and the inlet and exit shafts connected at the same depth as the surrounding stormwater drainage system. With the elevation of the manhole covers shown in the figure, this yielded a maximum available head of 1.3 m in the system (assuming a minimum stagnant water level equivalent to the minimum surrounding groundwater level measured the past 5 years, see Appendix E, Figure E - 1).

The SediPipe is 12 m long with a 2° counter-gradient, to encourage the suspended solids to settle below the flow separator earlier in the pipe, and to gather closer to the start shaft. Four SediSorp+ filter cartridges are stacked in the end shaft. The complete specifications, including modifications, are shown in detail in Figure 11. In this figure, the permanent water level indicates the maximum stagnant water level that can occur in the system, set by the weir on the right of Figure 10. In no-flow conditions, the water level in the system will vary between

the height of the surrounding groundwater and the invert outlet (NAP -0.84 m) to the AquaBASE. The system is designed to be flooded (permanently filled with water).

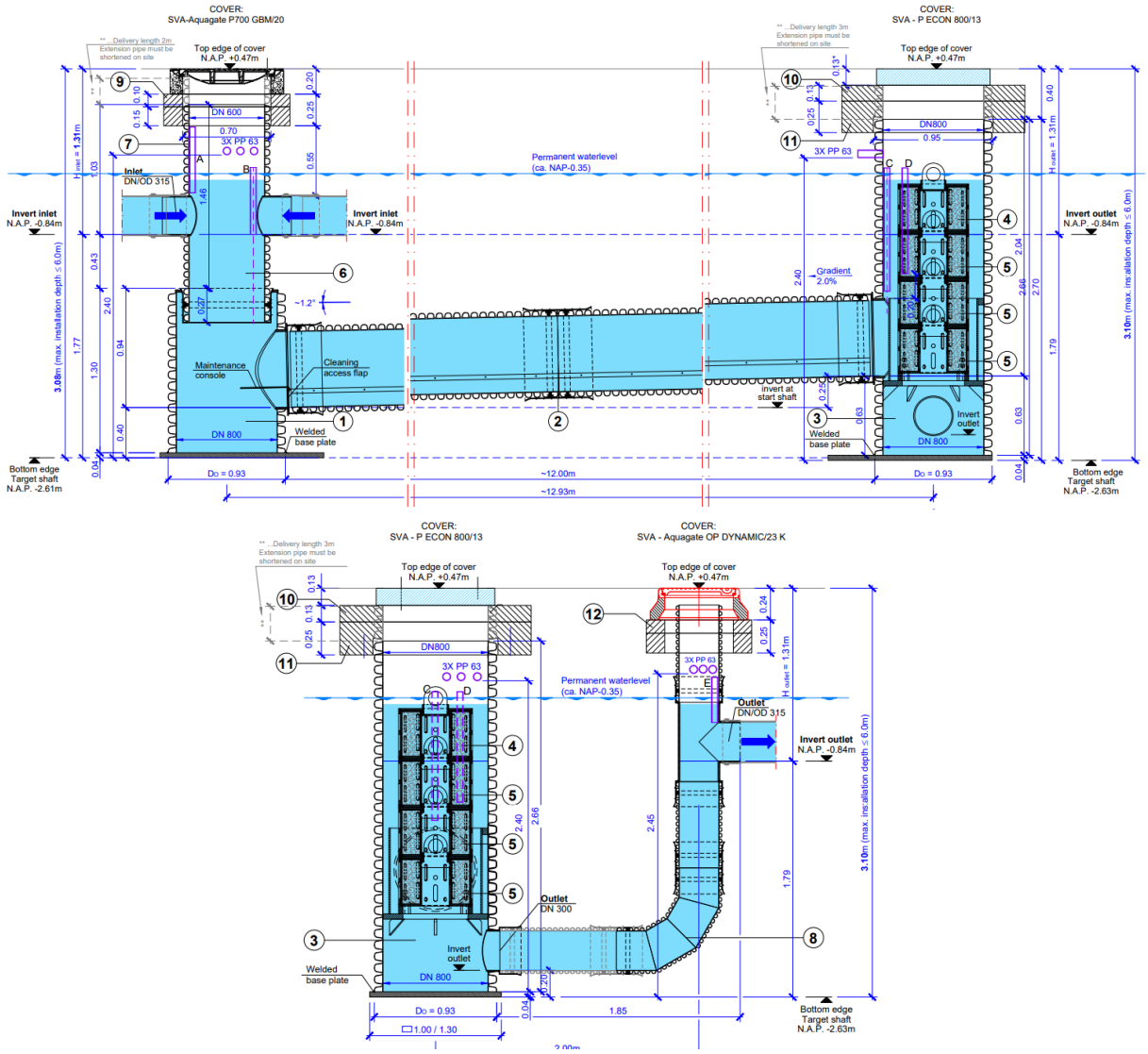

Figure 11: Side view of the SediSubstrator (Schönherr et al., 2020)

4.2 Site Preparation

Several preparation measures were taken to standardize the experiment. Firstly, the service road, the stormwater sewer, all gully pots, manholes and the two SediSubstrators on the southern service road were cleaned. The manhole and gully pot sinkers were filled with paving stones, to reduce their contribution to solids removal (see Appendix C for photos). The time period for a gully pot sand trap to fill is typically 6 months (M. Nijman, personal communication, July 2022), while this experimental period spans just 4 months. The addition of the paving stones was also intended to simulate the real situation in Amsterdam, for which inspections have shown that the bed depth equilibrium is reached in 95% of gully pots (M. Nijman, personal communication, July 2022). Street and sewer cleaning in the city typically occur less consistently than planned due to impediments such as parked cars. In accordance with advice from Fränkische Rohrwerke, the SediSubstrator was filled with clean water from

an adjacent hydrant prior to start-up, to immediately promote sedimentation with the arrival of the first rainfall event.

4.3 Monitoring and Sampling

4.3.1 Precipitation

Precipitation is measured by a tipping bucket rain gauge installed on the top of the Gerrit Rietveld Academie on the Frederik Roeskestraat (52.34175, 4.86026), 2.77 km away from the Rooseveltlaan site. Tips are recorded on a per-minute basis, and each tip represents 0.2 mm of rainfall.

4.3.2 Continuous Monitoring

In the SediSubstrator, the parameters measured on a per-minute basis are summarized in Figure 12. The runoff discharge, or flowrate into the SediSubstrator, is measured by a flowmeter (Promag W 400, 5W4C2H, DN200) installed in a dry manhole preceeding the start shaft. A constricted diameter magnetic flowmeter was selected for sensitivity to low flows, as the surrounding stormwater line is of DN 315. The water level is monitored in the start shaft (SP1) by a pressure transducer, the Waterpilot FMX21, sheathed by an open-ended PVC pipe to reduce motion induced by turbulence. The electrical conductivity is measured at SP1 by an Indumax CLS50D. Turbidity sensors—the Turbimax CUS51D—are installed at SP1, SP2 and SP3, connected to air spargers which run hourly to mitigate fouling. All of the aforementioned instrumentation is supplied by Endress+Hauser. The water samplers consist of an inlet tube (DN20) feeding a suction hose connected to a pump.

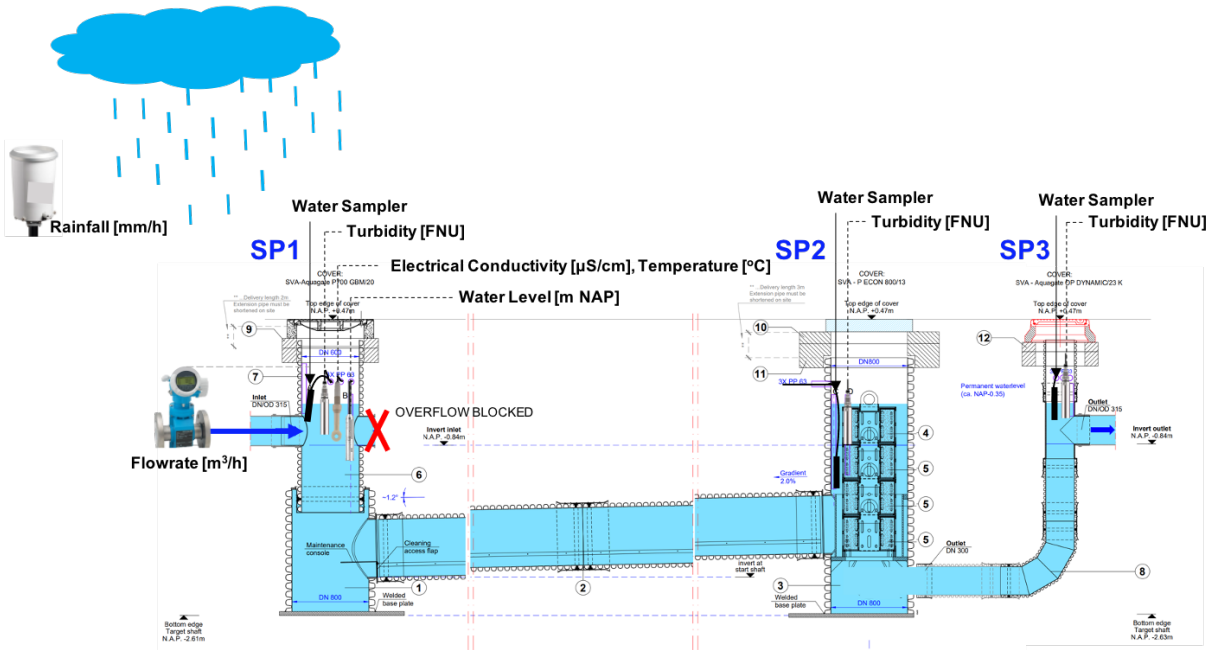

Figure 12: Sampling points marking the locations of the different devices: flowmeter, automatic sampler, turbidity sensor, pressure transducer, electrical conductivity and temperature sensor

4.3.3 Sampling

Automatic water samplers at the three positions in the system (SP1, SP2, SP3) took volume-proportional subsamples triggered by inflows to the SediSubstrator greater than 0.1 m^3/h. This discharge is equivalent to approximately 0.02 mm/h of rainfall on the effective connected area. Above this threshold, 200 mL was sampled for every 0.25 m^3 through the flowmeter. The collected subsamples per rainfall event composed one complete sample for laboratory analysis of the event mean concentration (EMC, see Figure 13).

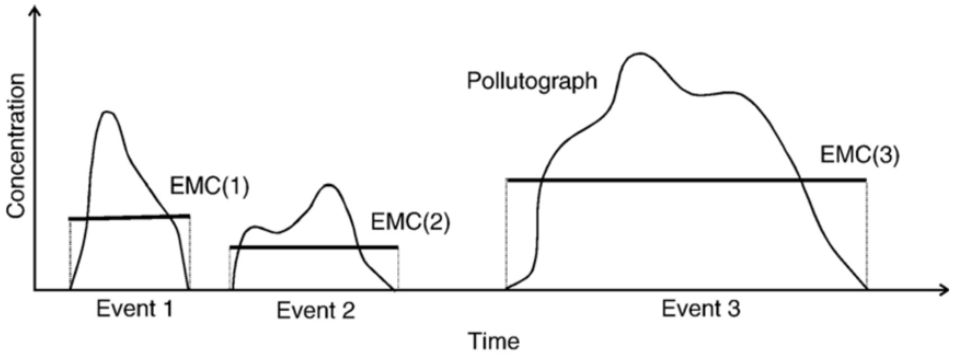

Figure 13: Event Mean Concentration (EMC) method used as a basis for the volume-proportional samples (Göbel et al., 2007)

Between sampling and analysis, samples were temporarily stored in refrigerated sampling carousels (4-6°C) for SP1, SP2 and SP3 prior to pick-up (see Figure 14, right). The samples were then transported 2 km by bike, transferred to the correct vessels for analysis, then stored again at 4-6 °C for pick-up by the laboratory. The sampling carousel bottles were emptied, cleaned with a sponge and drinking water and the sampling program reset. The analysis took place within 48 hours of the rainfall event to adhere to the shortest mandated timeframe for analysis, corresponding to the requirement for TSS (C. Wagemakers, personal communication, June 1, 2022).

Figure 14: Installed instrumentation container adjacent to the service road (left) with samplers inside (right)

4.3.4 Water Quality Analysis

4.3.4.1 Total Suspended Solids, Phosphorus and Organic Fractions

For the volume proportional sample collected from each rainfall event, the TSS, total P and PO_4^{3-} and the organic fraction of the suspended solids were measured (Table 2). These measurements were conducted by Waterproef, one of the laboratories of Waternet.

Table 2: Methods followed in the Waterproef lab per water quality indicator

Indicator	Method (Waterproef B.V.)
TSS [mg/L]	Vacuum filtration, drying and weighing
Organic fraction [%]	Change in mass after 45 minutes in a 600 °C oven
Total P [mg/L P]	Acid digestion (H_2SO_4) followed by photometric analysis
PO_4^{3-} [mg/L P]	Pre-filtration with a 0.45 µm filter and photometric analysis

4.3.4.2 Supplementary Ortho-Phosphorus Pumped Surface Water Experiment

The concentration of PO_4^{3-} in the Rooseveltlaan service road stormwater was below the reporting limit in May and June 2022 (as described by the phosphorus proficiency tests in Appendix A). To compensate, a supplementary pumped surface water experiment was done to increase the number of PO_4^{3-} measurements in the SediSubstrator. Water from the Sloterplas, a lake in Amsterdam which is known to have high PO_4^{3-} concentrations (0.42 mg/L P in May 2022), was used for this purpose (J. Stroom, personal communication, September 2022). In preparation, 12 m^3 of water was pumped into a truck from the south-west side of the Sloterplas (shown in Figure 15) the morning of the experiment and was transported to the Rooseveltlaan.

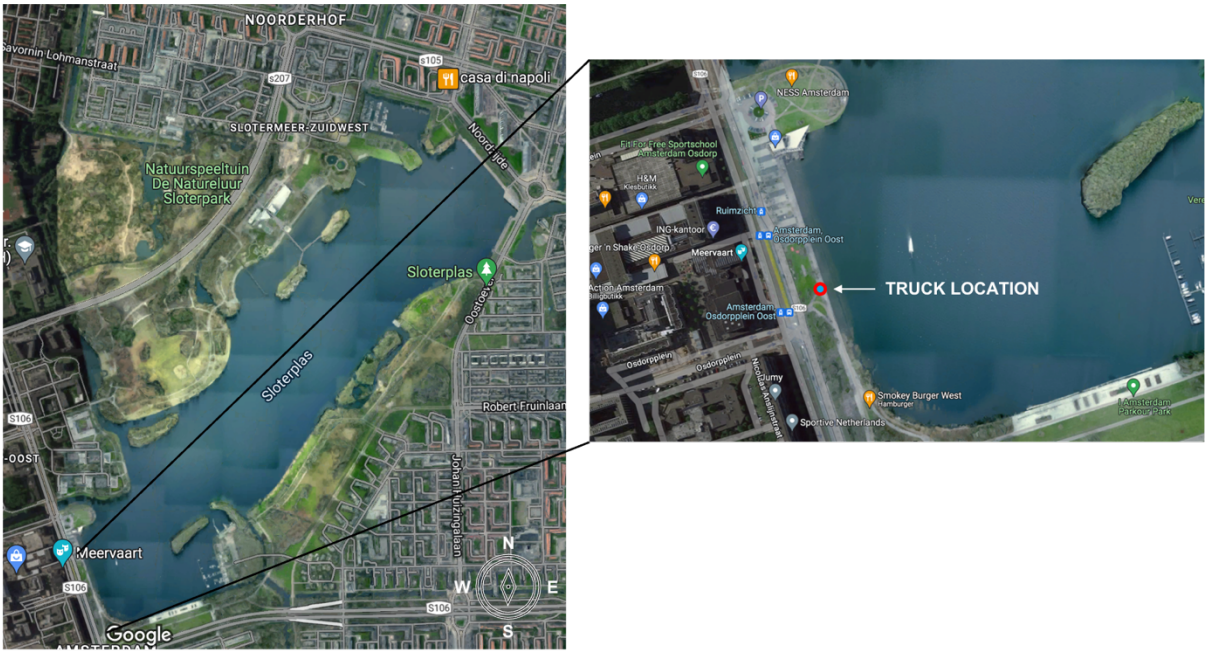

Figure 15: Truck pumping location

On the Rooseveltlaan service road, the experiment was run on S3, the south-west SediSubstrator which is not being studied, to avoid affecting the monitoring in natural rainfall that was underway on S4, the unit on the east side of the block. Temporary blockages were installed in the locations marked in Figure 16, to block flows to the AquaBASE and S4 and to avoid backward flow through S3. To reduce interference with sediments in the horizontal shaft and to require less water volume, the end shaft (before the filter, shown by arrow marked "IN" in front of house number 181) served as the inlet for the experiment.

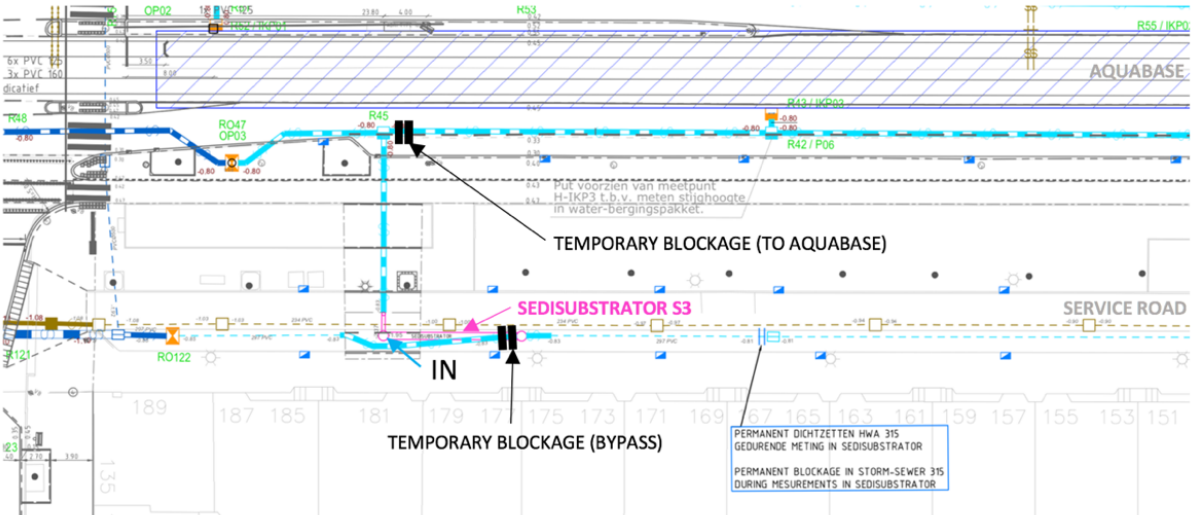

Figure 16: Locations of temporary blockages during the experiment

Discharge into the SediSubstrator measured in the first half of the summer season showed that low to moderate rainfall events yielded average discharges of approximately 4 m^3/h (0.8 mm/h on the catchment area) and only the larger events exceeded 8 m^3/h (1.7 mm/h on the catchment area). From this information, three flow regimes were defined to capture the impact of rainfall intensity on the phosphorus removal efficiency in the filter (summarized in Table 3). These flowrates were set using practical methods—measuring the time to fill a 40 L bucket and adjusting the pumping pressure accordingly—as the vacuum truck was not equipped with a flowmeter (see Appendix C for photos). Throughout the experiment, the water level marked on the side of the truck was monitored to ensure there was sufficient water remaining for the rest of the tests.

Table 3: Experimental flow regimes with associated settings

Regime	Discharge		Pressure Applied	Hose	Pre-flush Period
	Inflow [m^3/h]	Equiv. Rainfall [mm/h]	[bar]		[min]
Low	3	0.6	45	Small	30
Medium	4	0.8	70	Small	20
High	10	2.0	110	Large	10

Samples in the end shaft (before the filter) were manually taken using a telescopic water sampler, and samples at the outlet were taken simultaneously using an Eijkelkamp standard peristaltic pump (12 VDC) at a depth of NAP -1.5 m, to avoid the influence of stagnant water

at the top of the column above the connection to the AquaBASE (Figure 17, left). The final set-up on the street is shown on the right side of Figure 17.

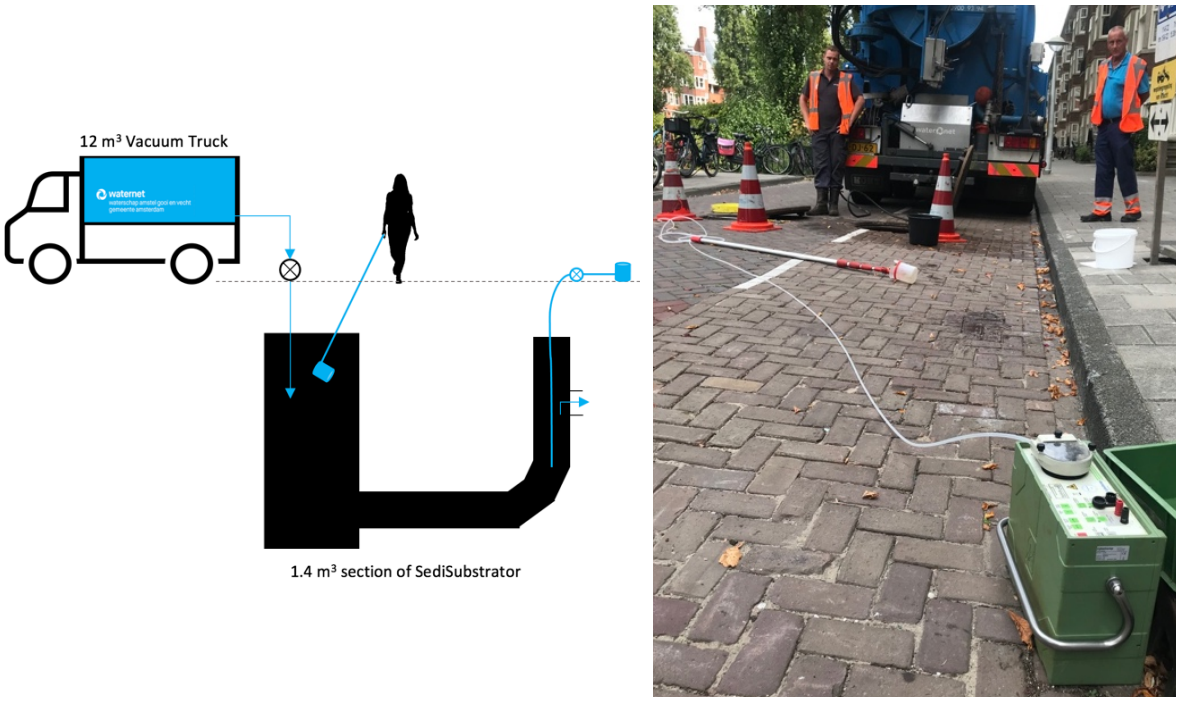

Figure 17: Design sampling strategy - manual sampling (end shaft) and simultaneous pumped sampling (outlet) (left); equivalent set-up on site (right)

4.3.4.3 Particle Size Distribution

The particle size distribution of the suspended solids in two rainfall events, of June 5th and June 6th 2022, were analyzed in the TU Delft WaterLab using two methods: by a PAMAS OLS4031 particle counter, and a particle size analyzer from BLUEWAVE by Microtrac (see Figure 18).

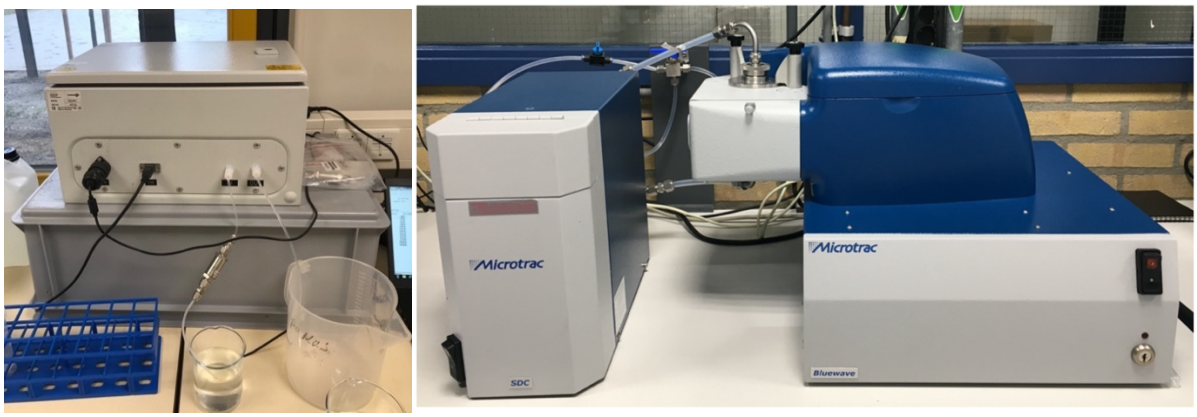

Figure 18: The PAMAS OLS4031 particle counter (left), and the BlueWAVE particle size analyzer (right, from Goess-Enzenberg, 2020) of the WaterLab

Specifications for these methods are listed in Table 4. The loading factor is a unitless benchmark used in the BlueWAVE particle size analyzer to indicate the concentration of the sample. The analyzed stormwater sample had a loading factor just below the optimal range limit, equivalent to 0.27. It was advised to provide the particle counter data for the same sample as a comparison.

Table 4: Operating limits and methods for particle size analysis

Indicator	Concentration Limit	Particle Size Range	Standard
Particle Counter	Max. 24 000 particles/mL	<1-200 µm	ISO 21501
Particle Size Analyzer	Loading factor optimal range minimum 0.3 [-]	0.0117-2000 µm	ISO 13320-1

4.4 Data Analysis

The methodology followed for data analysis is summarized in this section, with the complete Python scripts available on the GitHub repository of the project (*github.com/solomelittle/Master-Thesis-2022*).

4.4.1 Determination of Removal Efficiencies

The removal efficiencies (η_i) for TSS, total P and PO_4^{3-} across the SediPipe, the SediSorp+, and the SediSubstrator system were calculated for each sampled rainfall event using Equation 1. In these equations EMC_j [mg/L] refers to the event mean concentrations determined from volume-proportional sampling at the sampling points (j = 1, 2 or 3) during the event, as measured from the water quality lab analyses.

$$\eta_i = \frac{\left(EMC_{SPj} - EMC_{SP(j-1)}\right)}{EMC_{SP(j-1)}} \cdot 100\% \quad (1)$$

In the above equation:

η_i = removal efficiency of indicator *i* (TSS, P) [%]
EMC_{SPj} = event mean concentration at sampling point *j* [mg/L]

The per-event removal efficiency in the system is not representative of the removal from a given influent, as water sampled at SP2 and SP3 is likely to contain water from before the given rainfall event, by the working principle of the SediSubstrator. However, with multiple events sampled over an extended time period, an average flow-weighted removal efficiency may be calculated to more accurately characterize the system's performance.

The long-term removal efficiency $\eta_{wt.avg.}$ was calculated by taking a flow-weighted average of the event-specific removal efficiencies across the summer season (Equation 2). In the scope of this study, the extended time period spans the 4-month experimental period. In this equation, for event *k*, $\eta_{wt.avg.i}$ refers to the removal efficiency of TSS, total P or PO_4^{3-} and Q_k to the total discharge during the event.

$$\eta_{wt.avg.i} = \frac{\sum Q_k \eta_k}{\sum Q_k} \cdot 100\% \quad (2)$$

In the above equation:

$\eta_{wt.avg.}i$ = long-term flow-weighted removal efficiency of (TSS, P) [%]
Q_k = total discharge per event *k* [m^3]
η_k= removal efficiency of event *k* [%]

4.4.2 System Dynamics

To gain insight into the dynamics of TSS removal during rainfall events, a simulated load was calculated from continuous turbidity measurements at SP1, SP2 and SP3. Turbidity measurements were not reliable for much of the experimental period, so a turbidity-TSS relation could not be determined. As an indication, the cumulative turbidity at SP1 as measured in the rainfall event of September 7th was made equivalent to the total load through SP1 for the same event, and turbidity was scaled accordingly. Using this scaled turbidity, the load throughout the event was estimated by Equation 3.

$$q_T = T \cdot Q \quad (3)$$

In the above equation:

q_T = simulated load [g/h]
T= TSS-scaled turbidity, 3-minute averages [g/m^3]
Q = discharge, 3-minute averages [m^3/h]

4.4.3 Discharge-Head Relationship

Discharge into the SediSubstrator, *Q* [m^3/h] on a 3-minute basis, was plotted versus the measured head at SP1 [m NAP] for each of the sampled events to indicate the change in filter resistance over time. This was further quantified for each event by fitting a linear regression during the period of water level decline to compare the slope of the lines. The slope of the line is analogous to the specific discharge—a term borrowed from groundwater hydrology which uses the ratio between the change in discharge to the change in head in a well to compare the throughput (TNO, 1986).

4.5 Hydraulic Model Formulation

The sedimentation model was developed to inform potential design adaptations to improve the performance of the *SediSubstrator L* and to compare findings to previous research by Boogaard and Goess-Enzenberg. This model only applies for the SediPipe. Removal in the SediSorp+ is not considered. The complete Python scripts and approach may be found in the GitHub repository of the project (github.com/solomelittle/Master-Thesis-2022).

4.5.1 Theory

The sedimentation model was constructed according to theory as shown in Figure 19, in which the efficiency of sediment removal (η) is equivalent to the ratio of the rate of sedimentation (or settling velocity, v_s) relative to the surface loading to the system (v_{sl}).

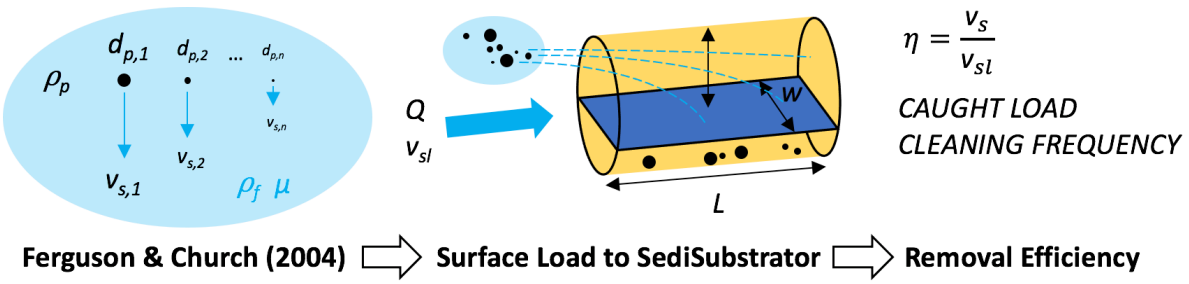

Figure 19: Model design

The ideal rate of sedimentation (or settling velocity, v_s) for a particle in water is governed by Stokes' Law, as shown in Equation 4 (van Dijk, 2020). This expression depends on the force of gravity and the drag force on the particle, which are determined by the particle density and particle diameter, respectively. This expression assumes a spherical particle shape, neglects interactions between particles and assumes laminar flow.

$$v_s = \frac{g d_p{}^2 (\rho_p - \rho_f)}{18\mu} \quad (4)$$

In the above equation:

g = gravitational constant, *9.8* [m^2/s^2]
ρ_p = particle density [kg/m^3]
ρ_f = fluid density, *1000* [kg/m^3]
d_p = particle diameter [m]
μ = kinematic viscosity, *0.001304* at 10°C [m^2/s]

The rate of sedimentation in the SediSubstrator was computed according to Ferguson & Church (Equation 5), which is effectively an extended Stokes' Law expression (Ferguson & Church, 2004). This expression was validated empirically and accounts for expected variable and non-laminar flow patterns in the SediSubstrator as well as angular particle shapes for

natural sand grains and organic particles (Ferguson & Church, 2004). The surface loading to the system (v_{sl}) was described by Equation 6, depending only upon the flowrate through the SediSubstrator (Q).

$$v_s = \frac{g{d_p}^2(\rho_p - \rho_f)}{18\mu + \sqrt{(0.75gCd_p^3)(\rho_p - \rho_f)}} \quad (5)$$

$$v_{sl} = \frac{Q}{w \cdot l} \quad (6)$$

$$\eta = \frac{v_s}{v_{sl}} \quad (7)$$

The above equations contain the same variables as Stokes' Law (Equation 4), as well as:

C = constant, *1* [-]
Q = inflow to the SediSubstrator [m^3/h]
w = width of the flow separator, *0.46* [m]
l = length of the flow separator, *12* [m]

4.5.2 Inputs

The settling velocity distribution was constructed from Equation 5 using the average particle size distribution (vol. %) from the events of June 5th and June 6th in the particle counter. With this distribution, the average particle density (ρ_p) as measured on the Ookmeerweg in Amsterdam (Nijman et al., 2015) and the particle density of Millisil®W4 were input to the model. These are densities of 1144 kg/m^3 and 2650 kg/m^3, respectively. The Ookmeerweg was deemed representative as both the Rooseveltlaan service road and the Ookmeerweg are tree-lined streets, although the Rooseveltlaan service road receives a much lighter traffic load. The Ookmeerweg density was measured by grab-sampling settled solids at the entrance to a stormwater sedimentation facility (Nijman et al., 2015). It follows that it likely overestimates the density of the suspended solids in stormwater but is nevertheless the most accurate measurement available. As a final point of comparison between design and real sediments, a settling velocity distribution was constructed using both the density and the particle size distribution Millisil®W4 (Neupert et al., 2021).

The removal efficiency by particle size was modelled in varied flowrates to compare to the results of Goess-Enzenberg (2020) and Boogaard (2015). A range of particle diameters (d_p between 1-200 µm, with step size 1 µm) used as an input to Equation 5, with the particle density (ρ_p) as measured on the Ookmeerweg once again compared to that of Millisil®W4. To inform recommendations for the design of the SediSubstrator, an additional analysis length-ening the SediPipe from 12 m to 24 m (l, Equation 6) was performed to observe the impact on the removal efficiency.

In both cases, the kinematic viscosity of water (μ) at 10°C was used. The constant C is the asymptotic value of the drag coefficient of a particle in predominantly turbulent flows (1000 < Re < 10 000) (Ferguson & Church, 2004). For natural, angular grains with imperfect sphericity it has been empirically determined to be equivalent to 1.

5 Results

This section summarizes the experimental findings and describes notable discoveries observed across the measurement period (May-September 2022). Hydrological information for the sampled events, the stormwater runoff quality on the Rooseveltlaan service road and removal efficiencies in the SediSubstrator L are presented. Hydraulic dynamics and one extreme rainfall event are described, and a sedimentation model is used to gain more information on the most important parameters contributing to the removal efficiency of the system.

5.1 Hydrology

The rainfall events sampled have varying characteristics (Table 5). In the beginning of May and in July there were few rainfall events, and those that were present weren't sampled as the flowmeter wasn't functioning correctly during these periods. As such, the volume-proportional sampling program wasn't triggered. The nine events that were sampled are marked in Figure 20, alongside the precipitation measurements at Schiphol and the Rietveld Academie. The runoff coefficients are computed on the basis of the entire area of the catchment, including green areas which typically do not contribute to runoff.

Table 5: Key hydrological characteristics of the sampled rainfall events based on the Rietveld Academie tipping gauge

Event	Date	Duration [h]	Sum [mm]	Mean [mm/h]	Median [mm/h]	Maximum Intensity (I_{max5}) [mm/h]	Runoff Coefficient	Antecedent Dry Period (ADP) [days]
A[1]	19/05	10.0	7.4 ± 0.4	0.6	0.0	3.4	0.34	2
B	05/06	10.0	24.0± 0.4	2.4	2.4	19.2	0.29	5
C	06/06	4.5	4.6 ± 0.4	1.0	0.0	7.2	0.39	<1
D	19/06	1.3	3.0 ± 0.4	2.3	0.0	21.6	0.54	10
E	24/06	5.2	22.2± 0.4	4.2	0.0	45.6	0.25	4
F	25/06	15.4	9.0 ± 0.4	0.6	0.0	12	0.38	1
G	31/07	23.9	5.6 ± 0.4	0.2	0.0	2.4	0.28	5
H	15/08	0.2	0.4 ± 0.4	1.6	2.4	2.4	0.73	14
I	07/09	4.8	13.6 ± 0.4	2.8	2.4	12	0.47	20

[1] Hydrological characteristics from this event are determined from the KNMI Schiphol station data due to restricted availability of the Rietveld tipping gauge data for this time period.

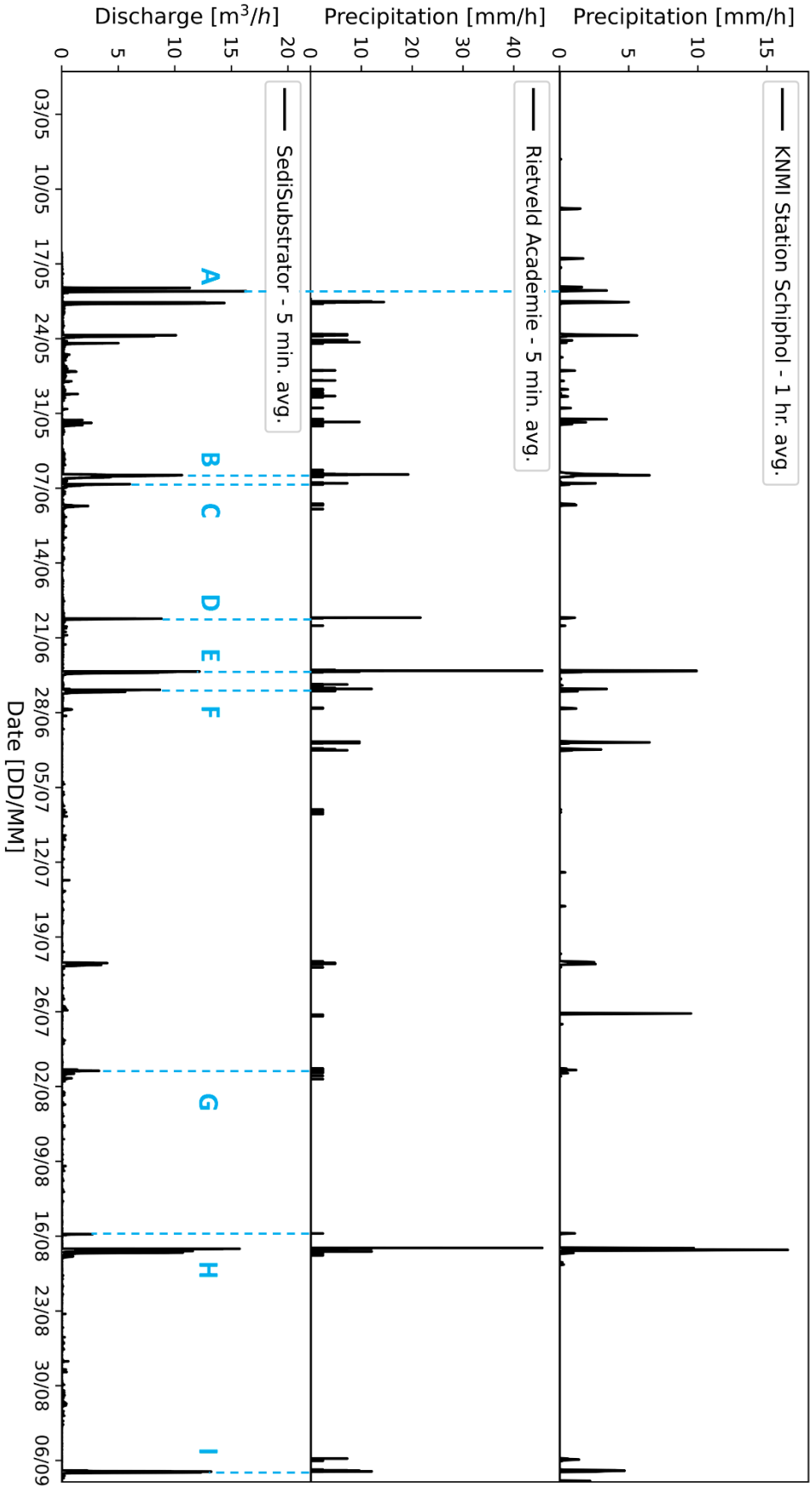

Figure 20: Precipitation as measured at Schiphol (*top*), the Rietveld Academie (*middle*) and discharge in the SediSubstrator (*bottom*)

5.2 Pollutant Loadings and Sources in Stormwater

5.2.1 Rooseveltlaan Stormwater Quality

The quality of the stormwater discharged to the SediSubstrator L is summarized in Table 6. In this table it is compared to national data for stormwater runoff from roofs and roads in residential areas: the average, the median (50th percentile) and the 90th percentile concentrations (Liefting et al., 2020). Of these concentrations, Pb and Ni are notably high compared to the national values, within the top 10% of measured concentrations in the Netherlands.

Table 6: Water quality assessment for the service road runoff (n = 1 event) September 7th 2022, compared to mean, median and 90th percentile concentrations from the STOWA stormwater database (Liefting et al., 2020)

	Concentration			
Indicator	Rooseveltlaan	NL Mean	NL 50%	NL 90%
Total Suspended Solids (TSS) [mg/L][2]	20	38	13	57
Turbidity [FNU]	97	-	-	-
Mineral fraction [%]	34	-	-	-
Ammonium, NH_4-N [mg/L]	2.0	-	-	-
Nitrate, NO_3-N [mg/L]	0.5	-	-	-
Nitrite, NO_2-N [mg/L]	0.03	-	-	-
Total Kjeldahl Nitrogen, TKN [mg/L]	3.3	2.1	1.4	-
Ortho-Phosphate, PO_4-P [mg/L][2]	0.19	-	-	-
Total Phosphorus, P [mg/L][2]	0.29	0.3	0.2	0.54
Chromium, Cr [µg/L]	<2	-	-	-
Copper, Cu [µg/L]	<5	21	12	37
Lead, Pb [µg/L]	53	21	8	53
Nickel, Ni [µg/L]	<5	4.1	2.1	7
Zinc, Zn [µg/L]	790	144	75	330
Mineral Oil, C_{10}-C_{40} [mg/L]	0.06	-	-	-
PAHs, total VROM (10) [µg/L]	0.10	-	-	-

5.2.2 Sources

The pollutant sources are visualized by means of an inventory of surfaces shown in Figure 21. This summarizes the materials of interest in the catchment. Most noteworthy is that rain gutters and bike racks are all zinc-based (zinc or galvanized steel). Consistent with the lush vegetation in the area, sources of organic material were apparent by the greening of certain surfaces (see centre left).

[2] Average concentration across the 9 sampled events

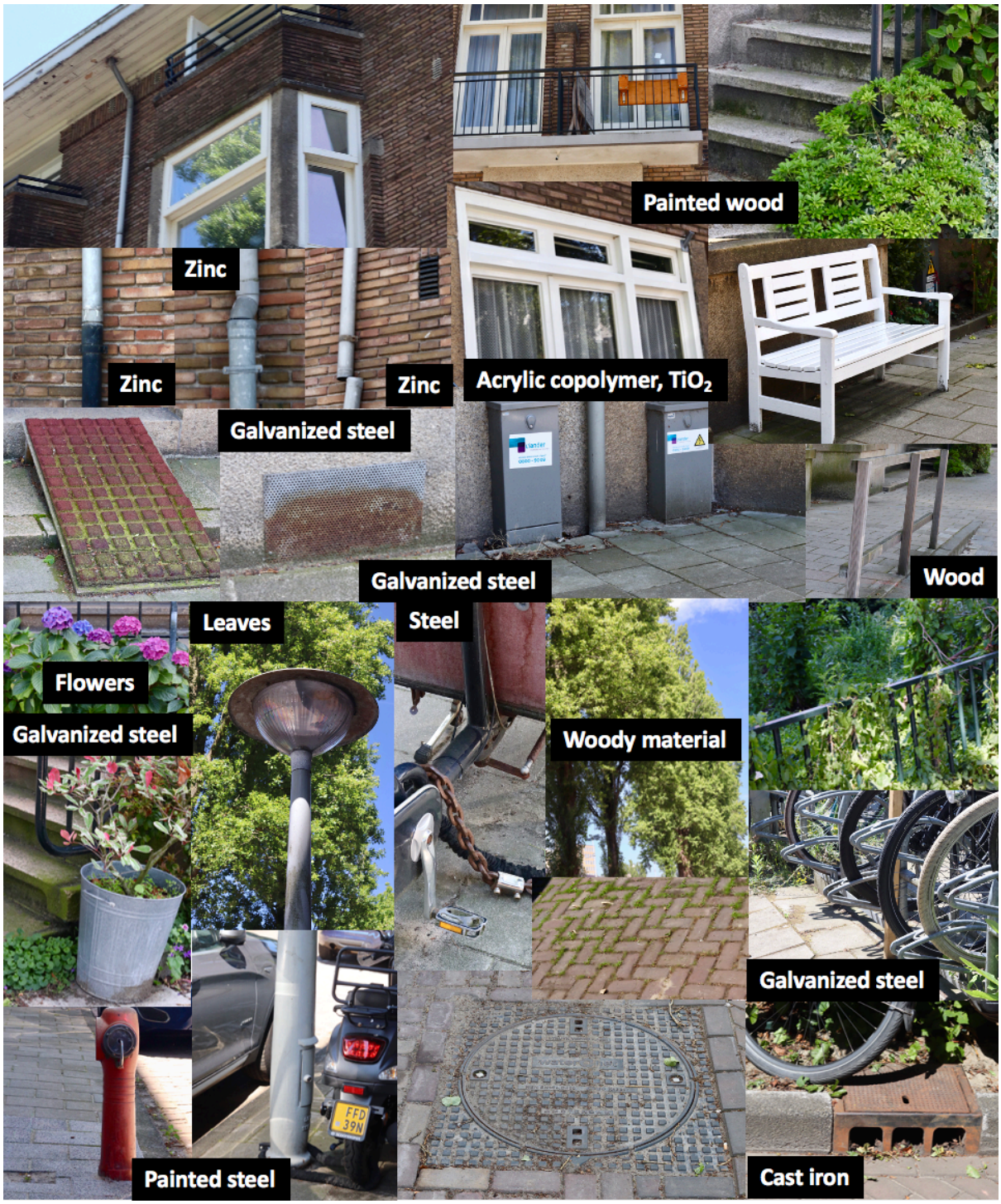

Figure 21: Inventory of surfaces observed in the catchment

5.2.3 Particle Size Distribution

The particle size distribution of the sediments in the stormwater for the events of June 5th and June 6th is shown in Figure 22, in which 78% have a diameter smaller than 63 µm. The darkest blue lines correspond to the particle size distribution of the catchment runoff discharge measured in the start shaft of the SediSubstrator (SP1). Medium blue and light blue lines refer to the particle size distribution in the end shaft (SP2) and at the outlet (SP3), respectively. The solid lines refer to the distribution as measured in the BlueWAVE particle size analyzer (with 140 particle size increments), and the dashed lines to the distribution as measured in the particle counter (with 17 particle size increments).

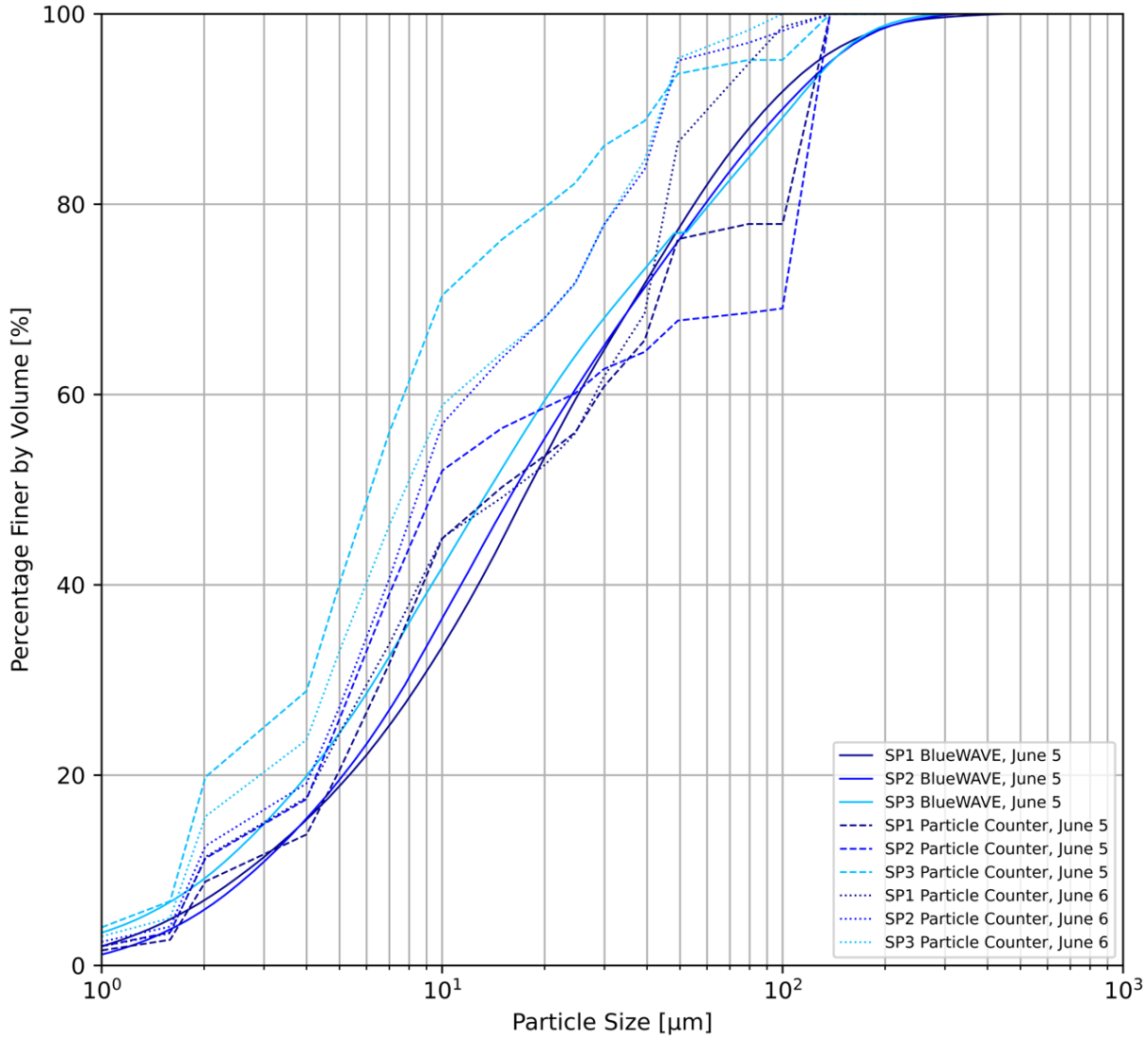

Figure 22: The particle size distribution of the stormwater sediments in the service road runoff

5.2.4 Settling Velocity Distribution

The settling velocity distribution is shown in Figure 23, and was determined from the Ferguson & Church sedimentation model. The average SediSubstrator influent particle size distribution (PSD) as measured in the particle counter for the events of June 5th and June 6th was used, with densities of 1144 kg/m^3 as measured on the Ookmeerweg in Amsterdam (Nijman et al., 2015), and 2650 kg/m^3 corresponding to that of Millisil®W4. The light orange line was generated from applying both the density and particle size distribution of Millisil®W4.

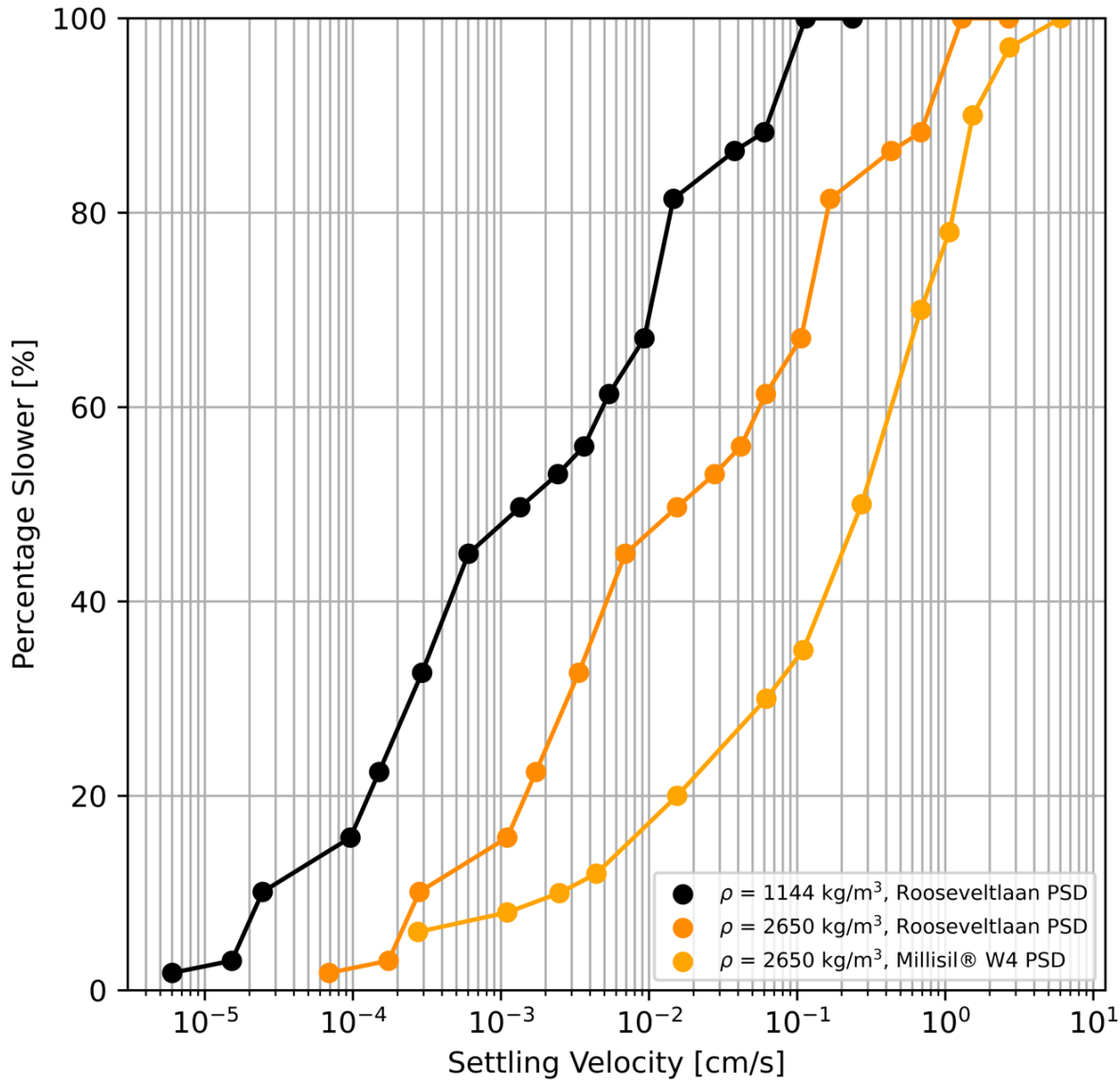

Figure 23: Modeled settling velocities from known particle size distribution (PSD), compared to Millisil®W4

The settling velocity distribution shows that 50% of the particles will settle below the flow separator after 10 hours for real stormwater sediments (in black), 45 minutes for stormwater sediments with silicate densities (in orange) and 3 minutes for Millisil®W4 (in light orange). Further, 80% of the particles will settle below the flow separator after 4 days for real sediments, 9 hours for silicate densities and 51 minutes for Millisil®W4.

5.3 Removal Efficiency TSS, Total P, PO_4^{3-}

The removal efficiencies generated by the measured change in EMC in the SediSubstrator during natural rainfall are summarized in Table 7. Negative removal efficiencies are possible due to interactions with existing settled solids in the SediPipe from previous events. The removal efficiency for particulate and organic phosphorus was generated from the difference between the measured total P and PO_4^{3-} EMCs. More information on the phosphorus forms by analysis method may be found in Appendix B.

Table 7: Weighted average removal efficiencies across the experimental period (April 29th-September 7th)

	Removal Efficiency [%]			
	TSS	Total P	PO_4^{3-}	Particulate and Organic Phosphorus
SediPipe	22	-6	-3	-15
SediSorp+	16	24	52	-14
Overall	34	18	50	-24

The removal efficiencies determined in the constant pumped surface water experiment are shown in Table 8. The concentrations per event are shown on the left side of Figure 24, including the surface water experiments at three constant pumping regimes as a point of comparison. The event-specific loads at the sampling points in the system (Figure 24, right) demonstrate the variability in removal efficiencies that exists within these averages across the experimental period. The loads on the right side of the figure do not include the pumped surface water measurements they were solely concentration-based (with constant flow).

Table 8: SediSorp+ removal efficiencies determined from the constant pumped surface water experiment

			Removal Efficiency [%]		
Regime	Flowrate		Total P	PO_4^{3-}	Particulate and Organic Phosphorus
	[m^3/h]	[mm/h]			
Low	3	0.6	41	66	-25
Medium	4	0.8	35	63	-19
High	10	2.0	42	56	0

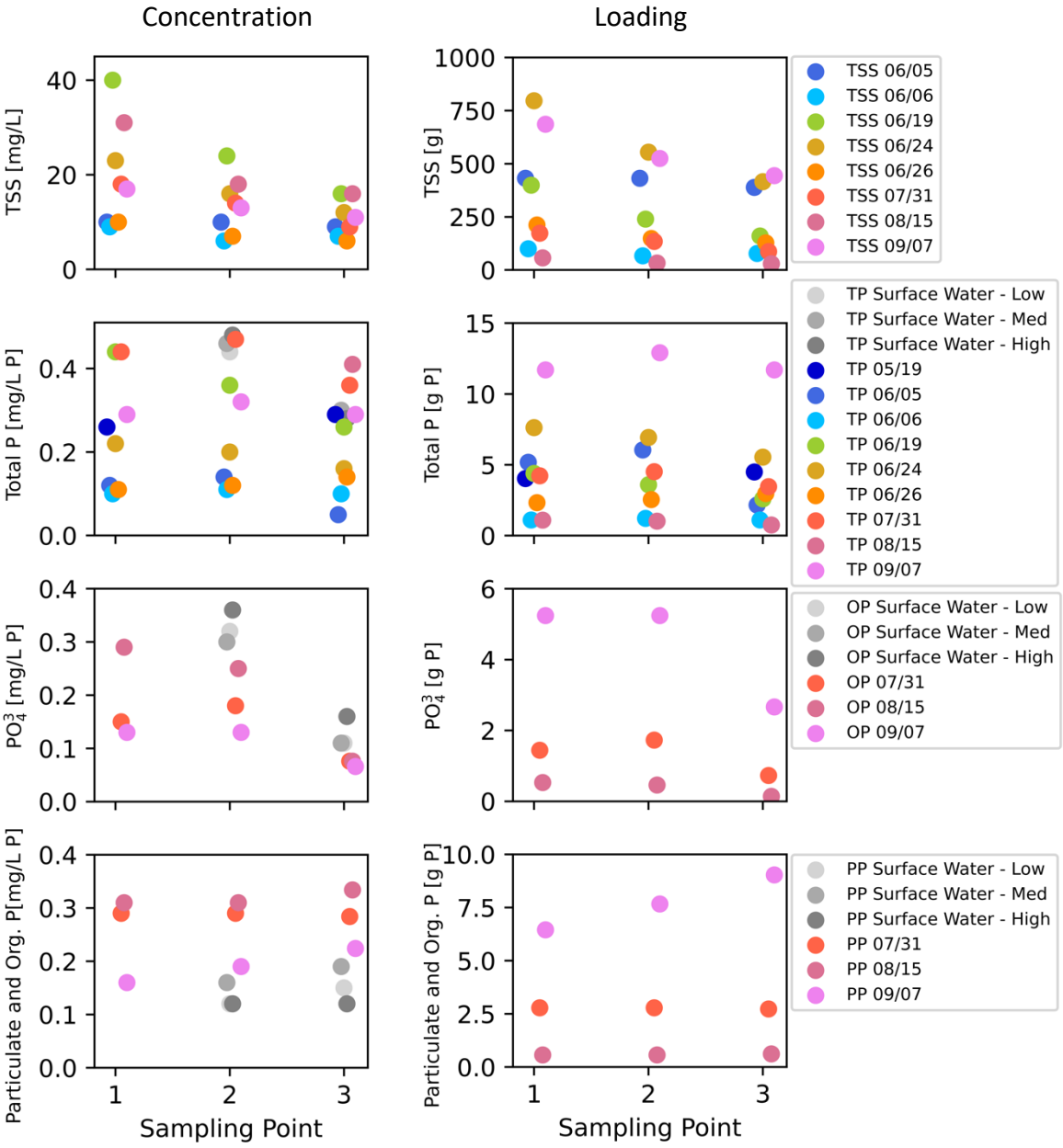

Figure 24: Concentrations and loads by event at the three sampling points (SP1, SP2 and SP3) in the SediSubstrator

5.4 Factors Affecting Removal Efficiency

5.4.1 Hydrological Characteristics

The relationship between the removal efficiency of TSS and Total P with certain rainfall characteristics is shown in Figure 25. The linear regression equation is described for each relationship, and the R^2 value included for an indication of the strength of the relationship.

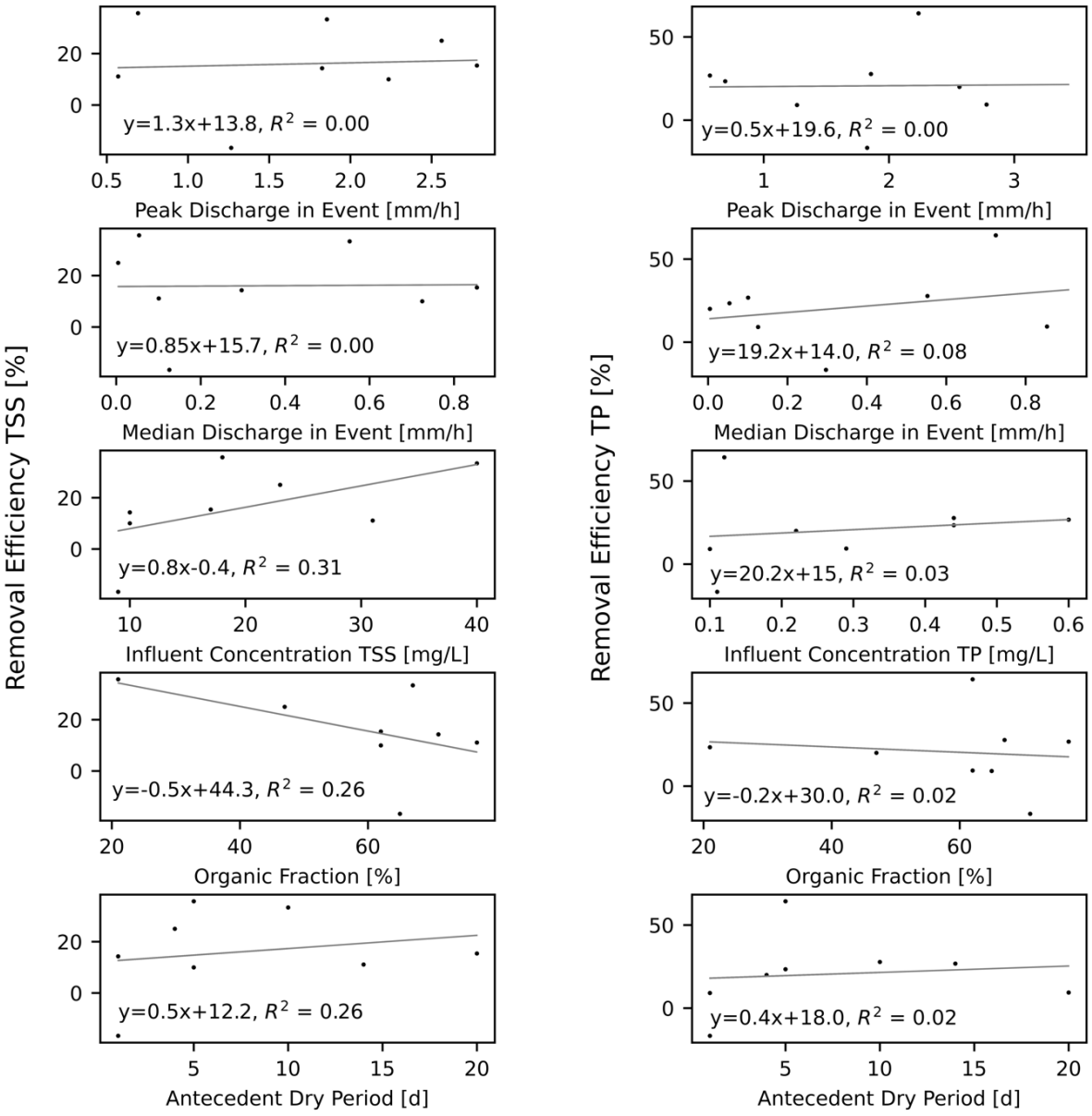

Figure 25: Relationship between removal efficiency and event characteristics

5.4.2 Design Improvements

The sedimentation efficiency modelled for various flowrates is shown in Figure 26. Results from the standard model parameters are shown on the left, namely with a SediPipe length of 12 m and a particle density of ρ_p=1144 kg/m^3 (Nijman et al., 2015). The effect of a longer SediPipe improves this removal efficiency; however, this improvement pales in comparison with that brought upon by using characteristics of silicate Millisil®W4 particles with density ρ_p = 2650 kg/m^3 (right).

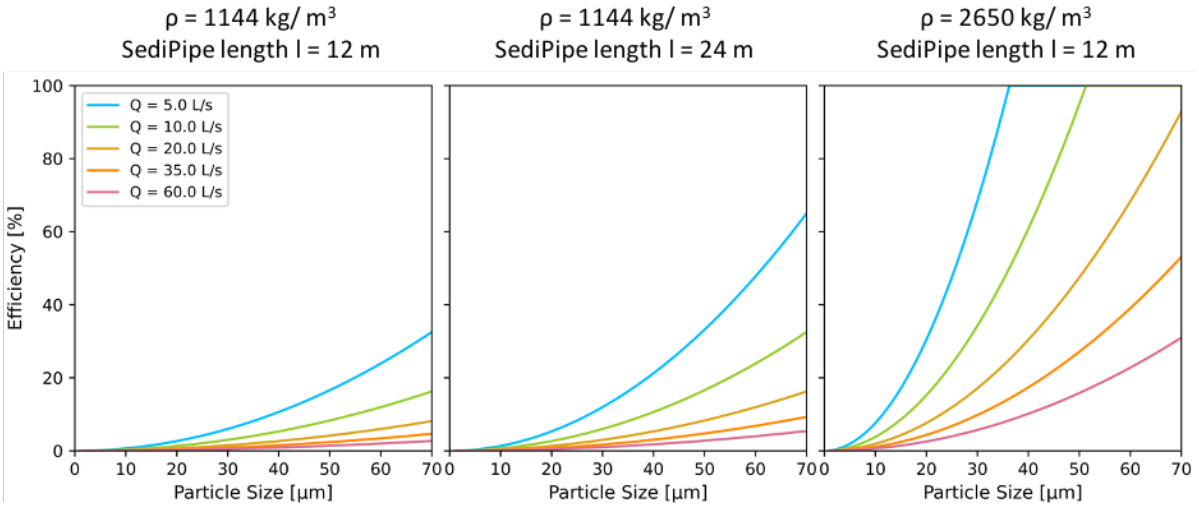

Figure 26: The modeled removal efficiency of TSS of the SediSubstrator L for various flowrates. Particle density ρ = 1144 kg/ m^3 (*left*); SediPipe length l = 24 m (*center*); Particle density ρ = 2650 kg/ m^3 (*right*).

5.4.3 System Dynamics

The dynamics of solids removal in the SediSubstrator is visualized for the event of September 7th in Figure 27. The turbidity [FNU] as monitored in the start (SP1) and end shaft (SP3) is shown with the discharge (top), the turbidity-generated simulated load [g/h] is shown at the same points in the system (middle), as well as the cumulative simulated load [g] (bottom). The cumulative simulated load clearly shows that the outflowing load exceeds the incoming load. This is inconsistent with the TSS loadings from sampling which demonstrate a load reduction from 686 g in the influent to 444 g in the outlet of the SediSubstrator.

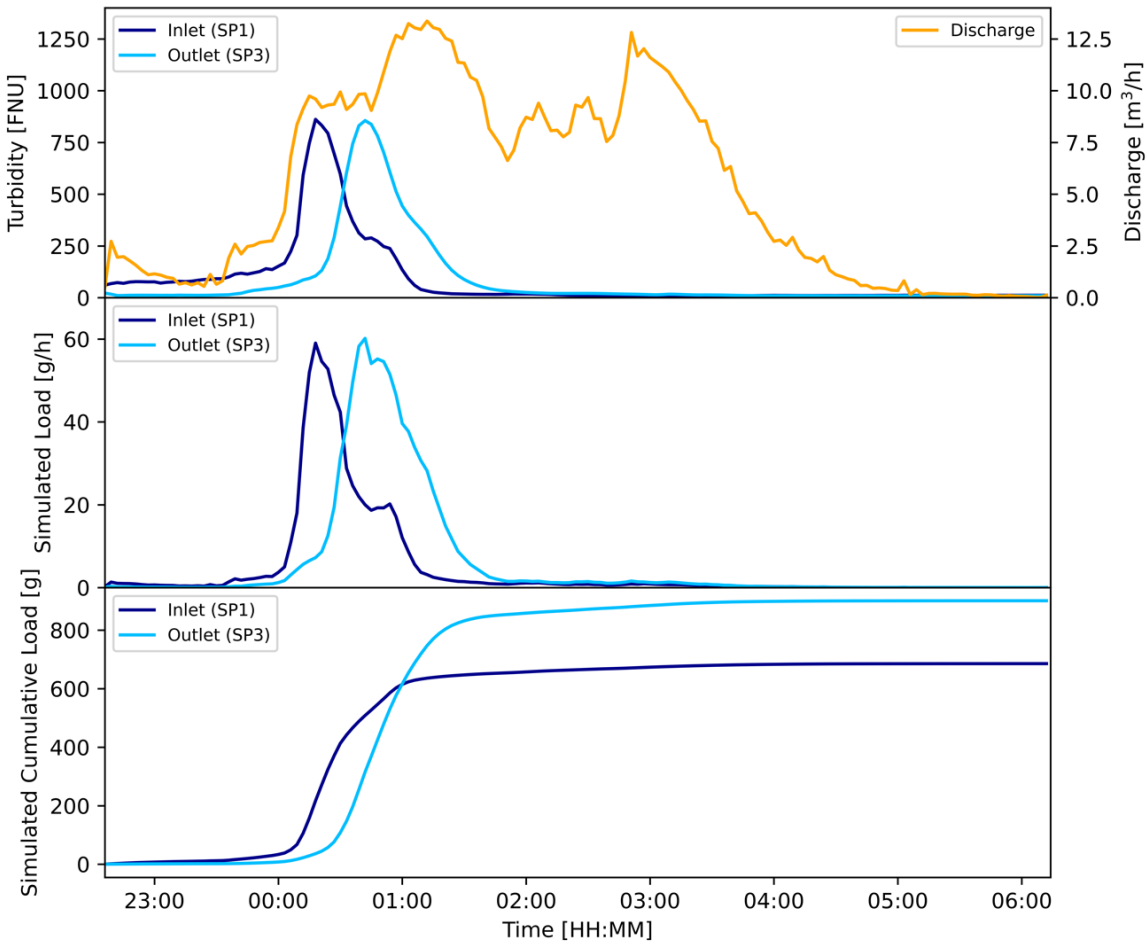

Figure 27: Turbidity-based loads entering and leaving the SediSubstrator, September 7th

5.5 Filter Performance Over Time

The change in filter resistance due to clogging was quantified by the calculation of the discharge-head relation across the nine sampled rainfall events plus a bonus emergency event. A special emphasis on the conditions and timeline of the emergency clogging event that occurred on September 28th 2022 is made.

5.5.1 Discharge-Head Relation

The relationship between discharge through the SediSubstrator (m^3/h) and the head (m) measured in the start shaft (SP1) is shown in Figure 28. In this figure, black represents the rising water level, or the first section of the rainfall event. Red marks the declining water level, or the latter section of the rainfall event.

A trendline is fit through the period of decline (red line), and the slope indicates the relative resistance in the SediSorp+ filter. The higher the slope, the lower the filter resistance as there is relatively more water passing through the system with a smaller change in head. The lower the slope, the more filter resistance (clogging), as less water passes with a larger change in head.

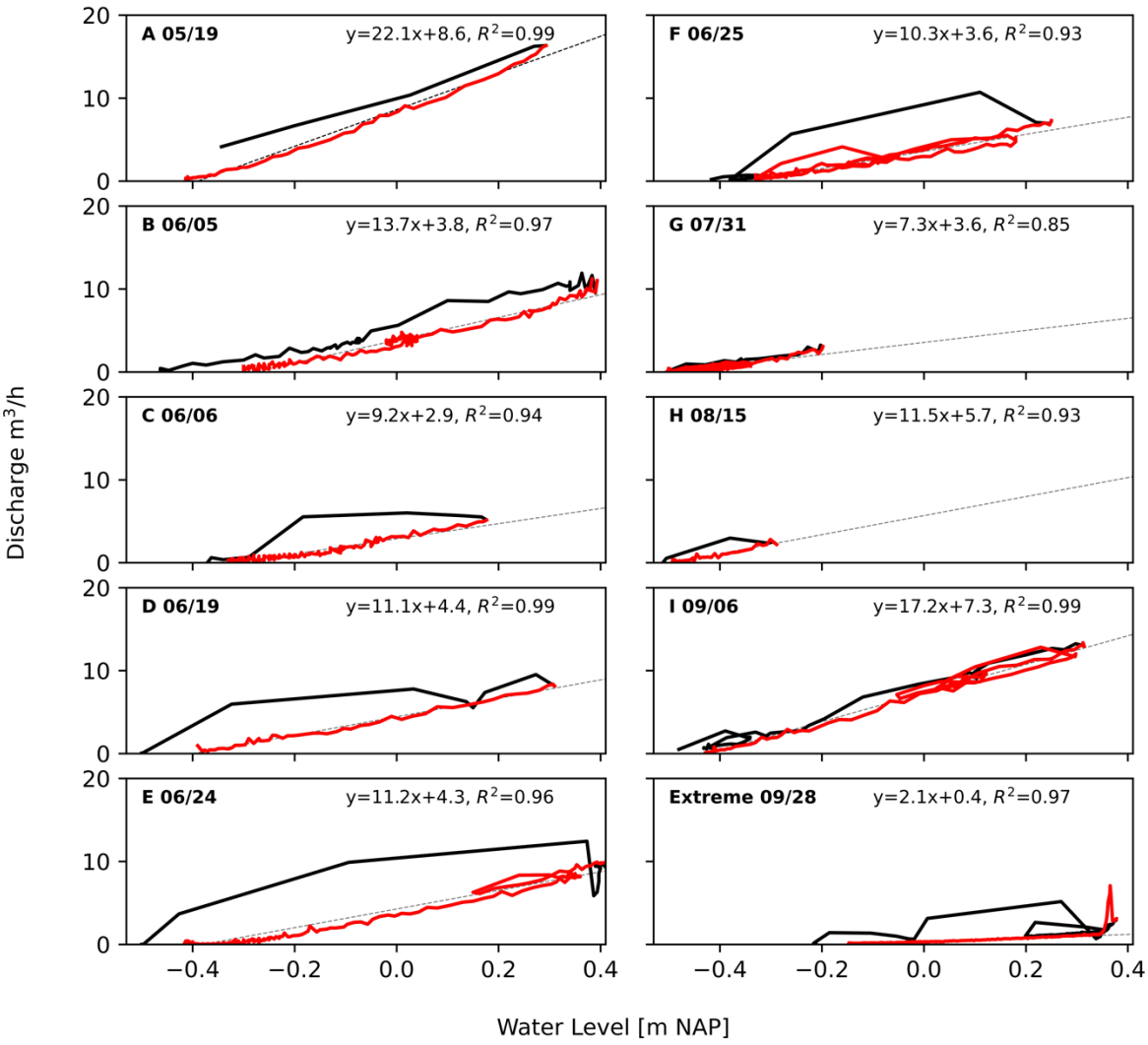

Figure 28: Discharge into the SediSubstrator vs. head for the nine events and the extreme rainfall event of September 28th (“Extreme”)

6 Discussion

In this section the results are interpreted and compared with past research and literature. The applicability of the SediSubstrator L in Loosdrecht is discussed and design recommendations are made for the unit in Amsterdam. Furthermore, the experimental methodology and limitations are reviewed.

6.1 Interpretation of the Results

6.1.1 Hydrology

During the experimental period, there were fewer rainfall events than anticipated. The summer of 2022 ranks among the top 5% driest summers on record (*KNMI - Neerslagtekort / Droogte*, n.d.)—nevertheless, the correct sampling of nine events across the season was deemed satisfactory for the purposes of this study.

The precipitation amount and duration of the sampled events was varied (see Table 5), which was desired to mitigate the shortcomings of the previous monitoring of the SediPipe in Münster (Lieske et al., 2021; M. Schutz, personal communication, 2022). For the most part, the duration of the events were long; however, there were extended dry periods included in these events, as exemplified by the median rainfall intensities being mostly 0.0 mm/h.

The range in runoff coefficients (0.25-0.73) is consistent with expectations based on the surface types in the area (Table 9). Roofs and paved areas account for similar areas in the catchment (41% and 36%, respectively, see Table 1), and the surfaces of the paved areas are covered by bricks and pavers, which are more permeable than uniform paving. The green areas are expected to contribute to the runoff just 0.02% of the time, making their runoff coefficient effectively zero (Goess-Enzenberg, 2020).

Table 9: Typical ranges for runoff coefficients for different surfaces (Waterfall, 2004)

Surface Type		Low	High
Roof	*Metal, gravel, asphalt, shingle, fiber, glass, mineral paper*	0.90	0.95
Paving	*Concrete, asphalt*	0.90	1.00
	Bricks[3]	0.70	0.85
Gravel	*General*	0.25	0.70
Soil	*Flat, bare*	0.20	0.75
Soil	*Flat with vegetation*	0.10	0.60
Lawns	*Flat, sandy soil*	0.05	0.10
	Flat, heavy soil	0.13	0.17

[3] (van de Ven, 2016)

Runoff coefficients for a given area vary inherently as they depend on the state of the depression storage, the moisture content of the subsurface, the temperature of the pavement, current weather conditions and average weather conditions of the recent past (van de Ven, 2016). However, the runoff coefficient of event H is uncharacteristically high considering the rainfall characteristics, with a long antecedent dry period, average intensity and short duration of rainfall. This is likely a byproduct of the functioning principle of the tipping gauge, which records 0.2 mm/tip. Collected rainfall remaining below the tipping threshold is not recorded, which contributes to error at the beginning and end of a rainfall event. For event H this is a significant source of error as the total rainfall measured for the event is equivalent to just 0.4 mm.

6.1.2 Pollutant Loadings and Sources in Stormwater

The runoff from the Rooseveltlaan service road catchment had lower sediment loadings than expected. While the average TSS concentration in the inflow (17 mg/L) was above the national median concentration (13 mg/L), in the city of Amsterdam small rainfall events have been purported to prompt a stormwater TSS concentration between 8-100 mg/L, increasing up to 320 mg TSS/L with intense precipitation (Liefting et al., 2020; Nijman, 2022). Stormwater discharged through the SediSubstrator never even reached 100 mg/L during the most intense event after a long antecedent dry period. This is indicative of the effect of the low traffic load and high contribution of roofs to the catchment area on the Rooseveltlaan service road, and especially the effect of starting up the system clean. The street, preceding gully pots and stormwater sewer were collecting sediments (Appendix C: Figure C - 5, Figure C - 6 and Figure C - 9), contributing to the low concentrations measured in the start shaft of the SediSubstrator. The sediments were fine compared to the Dutch average, similar to those measured by Drapper (1998) and the US EPA (1986) internationally (see Appendix A, Figure A - 1). The storage of coarse material prior to the SediSubstrator likely contributed to this as well.

High nitrogen and phosphorus loadings are consistent with sources of depositable organic matter that were observed in the catchment. Not only is the road green—with trees and shrubs on one side and domestic potted plants on the other (Figure 21)—but it is a local pedestrian walking route, so pets pass through the area. Furthermore, the road appears to be infrequently cleaned: debris from pollination early in the period, landscaping scraps mid-summer and fallen leaves and blooms late in the period gathered in and around gully pots (Appendix C). Nutrients are released as this organic matter decays, for example when submerged in gully pots. Water column stratification can foster anaerobic conditions in settled sediments, which prompt microbially-assisted ammonification and the conversion of particle-bound P to dissolved P (Si et al., 2021; Song et al., 2015). The concentration of N-components have been correlated to rainfall intensity and antecedent dry period (Jani et al., 2020), which are also contributing factors to P mobilization (see section 2.6).

Lead and zinc were the only heavy metals measured above the reporting limit, and were measured in high concentrations, with that of zinc being alarmingly high (the 90th percentile in the Netherlands being almost three times lower, at 283 µg/L) (Liefting et al., 2020). Lead is likely generated from seaming pieces on the old roofs, with zinc from the gutters which are all zinc or galvanized steel Figure 21 (*Lead Sheet on Monuments | Cultural Heritage Agency*, n.d.). The pH of rainwater is typically in the range of 6-9, acidified by the presence of SO_2 and NO_x in the atmosphere, and organic acids generated from decaying moss and bird droppings on roofs may also further lower the pH, corroding these metal components (Hofman-Caris et al., 2019; *Lead Sheet on Monuments | Cultural Heritage Agency*, n.d.). In this catchment, 50% of the runoff is in contact with roofs (neglecting the green spaces which seldomly contribute).

6.1.3 Removal Efficiency of TSS and Phosphorus

The seasonal sediment removal efficiency for the SediSubstrator L 600/12 (η_{TSS} = 34%) is consistent with the findings of the two-year in-situ test in Münster on a SediPipeXL 600/12 (η_{TSS} = 29%) (Lieske et al., 2021). The catchment differs significantly in terms of use—Stadtgraben, Münster is a commercial area close to the city center with a traffic load of 30,000 vehicles per day (Lieske et al., 2021), while the service road at the Rooseveltlaan is an urban residential street that receives a small fraction of the traffic load by comparison (estimated at 50 vehicles per day). Nevertheless, the fine fraction of sediments is the same, with (TSS_{63}/TSS = 0.78). It is likely that there is a higher organic fraction in the Rooseveltlaan service road stormwater sediments (lowering their average density) as the TSS removal efficiency of the SediPipe alone was 22%. The SediSorp+, which was not present in Münster, did improve the removal efficiency on the Rooseveltlaan service road, but only by 7%.

The settling velocity distribution makes the influence of particle size and density absolutely clear. Taking the average sediment density of 1144 kg/m^3 as a reference, the largest measured particle size fraction (138-200 µm) will settle on average in the SediPipe in less than 5 minutes. The smallest fraction, < 1 µm, will take over a year. To reach an overall 50% TSS removal during a rainfall event requires a residence time of 10 hours, a criterion that will be met in average flowrates of 0.3 m^3/h at maximum (equivalent to 0.06 mm/h falling on the effective connected area). In the summer season, which typically receives more intense rainfall events, this is a difficult criterion to meet.

The average removal efficiency for PO_4^{3-} in natural rainfall was satisfactory (50%), and even better for constantly pumped surface water (56-66%) with relatively low contact times (10-30 minutes maximum). The atypical geometry of the filter and related flow patterns in the end shaft impeded the determination of exact contact times, but this is nevertheless a promising result for decentralized stormwater filtration in the city. However, it appears that dissolved and colloidal organic phosphorus was generated in both the SediPipe and SediSorp+, driving significant negative removal efficiencies (see “Particulate and Organic P”, Table 7). As introduced in section 2.6, this may be expected in a system receiving organic-rich sediments which stimulating biological decomposition processes.

6.1.4 Total Load Removed

With a cumulative 398 m^3 of stormwater discharged across the experimental period, the average event influent TSS = 20 mg/L (Figure 24) and a flow-weighted removal efficiency of 34%, it is expected that 2.7 kg (dry wt.) sediments were captured across the 4-month period. The average runoff coefficient across the measured events is 0.41, yielding an estimated runoff discharge through the SediSubstrator of 1700 m^3/year (based on annual average precipitation of 851 mm) (*KNMI Klimaatsignaal'21*, 2021). This corresponds to a conservative estimate for the caught load of 11 kg/year.

In the SediPipe, with a removal efficiency of 22%, 7.5 kg/year is caught below the flow separator. Assuming a sediment density equivalent to the 1144 kg/m^3 measured on the Ookmeerweg a porosity of 30% and using the 0.4 m^3 storage volume below the flow separator, a cleaning interval of 42 years is recommended. This far exceeds the recommendations by the supplier, which consist of 1 year (*Product Brochure: SediPipe L / L plus; SediSubstrator L*, 2019).

A camera inspection conducted on November 3rd allowed for another method to estimate of the total caught load in the SediPipe (with images shown in Figure 29). The layer of solids gathered below the flow separator appeared to be 1 cm thick on average and spanned from the start shaft until 7 m into the system. Using the sediment density of 1144 kg/m^3 as measured on the Ookmeerweg (Nijman et al., 2015), a porosity of 30% and the width of the flow separator as the width of deposited material, this would indicate that an 27 kg of solids have been caught between April 29th and November 3rd 2022. This method generates a far higher estimate than that based on the summer average TSS concentration and removal efficiency, which yields a caught load below the flow separator of 3.1 kg for the same period (with 316 m^3 having passed through the SediSubstrator since the experimental period).

Should the autumn average influent TSS (from September 7th to November 3rd) be set to 100 mg/L, this caught load estimate becomes 34 kg, more similar to what was observed in the SediPipe. Alternatively, should the removal efficiency be assumed to be 50% for the SediPipe, 7.1 kg would be caught. The magnitude of the discrepancy between the TSS-generated estimation and the camera inspection estimation indicates the unknowns that are still present. The influence of seasonality (in terms of solids loading) is not captured in the annual caught load estimate in this study, nor is the influence of starting up the system clean. This is further discussed in Section 6.2. Between the end of the experimental period (September 7th) and the camera inspection (November 3rd), with less storage available in the gully pots and stormwater sewer (and with more settled solids which may be remobilized in heavy rainfall), more coarse or dense material likely entered the SediSubstrator with an improved removal efficiency to what was observed over the summer season.

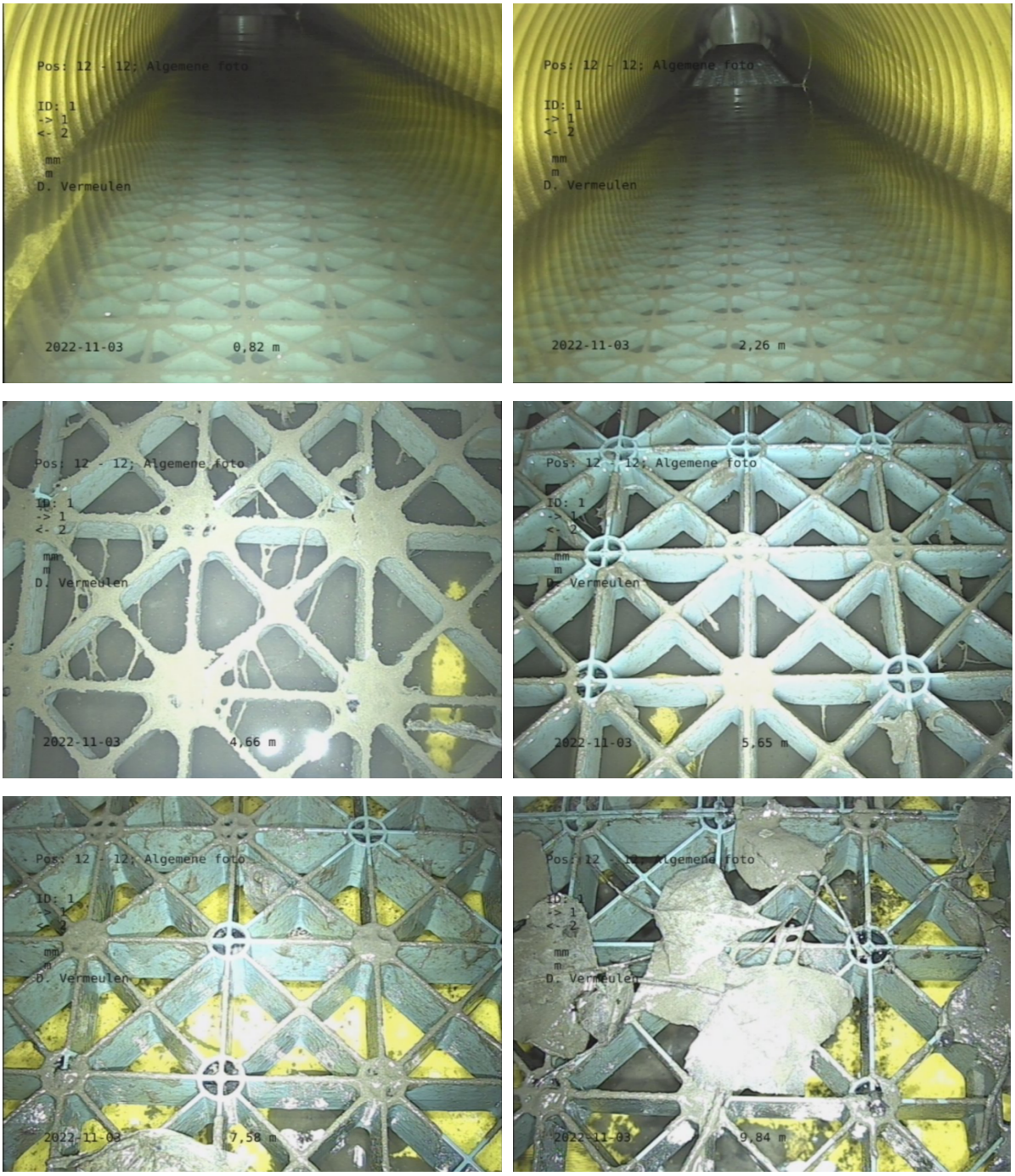

Figure 29: Camera inspection footage inside the system on November 3rd, at distances of 0.82 m, 2.26 m, 2.66 m, 5.65 m, 7.58 m and 9.84 m into the SediSubstrator

6.1.5 Factors Influencing Removal Efficiency

Of the factors studied, it appears that the influent concentration is the strongest predictor of the removal efficiency for TSS (R^2 = 0.31), as well as organic fraction (R^2 = 0.26) and length of the antecedent dry period (R^2 = 0.26) with no clear predictor generated for total P.

The antecedent dry period and influent concentration appear to both affect the removal efficiency but are both also interlinked. In theory, the longer the antecedent dry period, the

more solids gather on surfaces to be transported with the next rainfall which in turn increases the TSS concentrations measured.

Rainfall events in which the sediments have a lower organic fraction exhibit improved removal efficiencies due to the low density of organic materials (200-1350 kg/m^3 compared to mineral densities of 2040-2940 kg/m^3) (Gruber, 1985; Li et al., 2020; Swenson & Enquist, 2008).

The dissolved and particle bound P had too few points to analyze in a statistically correct manner. No strong relationship is shown between the maximum rainfall intensity, the mean rainfall intensity and the removal efficiency of TSS and total P.

6.1.6 System Dynamics

The simulated load dynamics for the event of September 7th (Figure 27) demonstrate the existence of a pronounced “first flush”, as flows early in the event contain high pollutant loads. This can occur as runoff washes accumulated matter off the catchment surface, in gully pots and a resuspends deposited sediments in the sewer line itself (Davies & Butler, 2011).

In the SediSubstrator, the cumulative loadings simulated from the change in turbidity across the system increase from the inlet (SP1) to the outlet (SP3). This is not reflected in the TSS measurements for this event, which indicate a net capturing of solids. This discrepancy suggests that there is a resuspension of fine solids which contribute disproportionately to the measured turbidity but are less significant by mass. For instance, these fine solids may be those that settle on the flow separator itself. They are shown in their original state in Figure 29, with resuspension observed in flowing water in Figure 30. The limitations of using turbidity as a proxy for TSS are further discussed in Section 6.2.

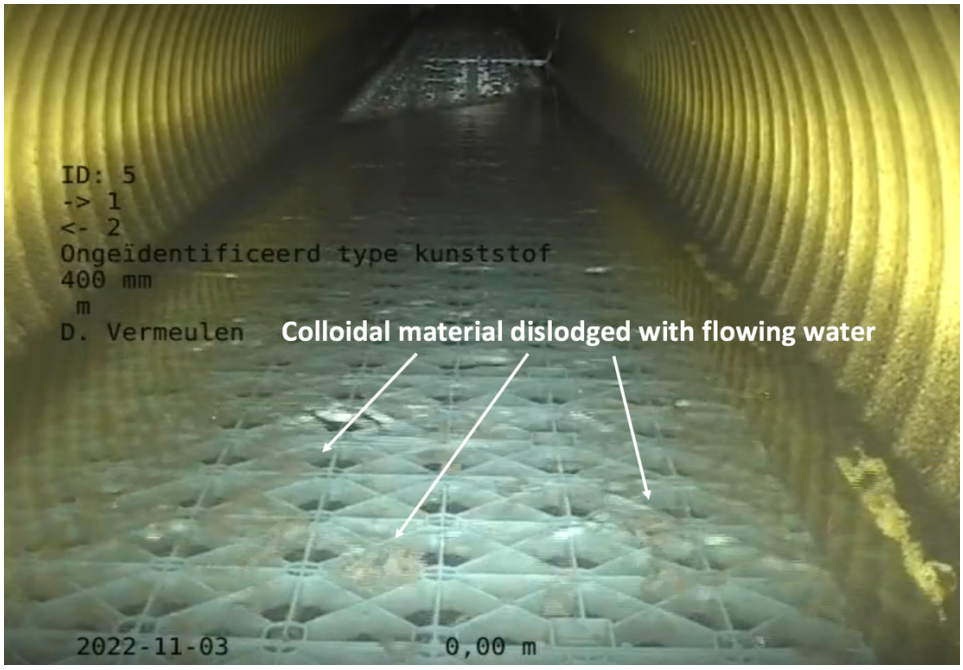

Figure 30: The removal of light colloidal solids from on the flow separator

6.1.7 Filter Performance

In Figure 28, the filter resistance per event can be inferred from the slope of the linear regression during the period of water level decline. The results show that after the first monitored event A (22.1 m^2/h), the slope is similar throughout the rest of the sampled events—which is not indicative of progressive clogging over time. The higher slope of event I (17.2 m^2/h), could be due to the high intensity and volume of discharge for this event, forcing water through the filter. Conversely, however, the slope of the extreme rainfall event ("Extreme") is uncharacteristically low (2.1 m^2/h), and the water level increases significantly with discharge from the very start of the event.

This behavior suggests there was either an acute clogging event between event I and the extreme rainfall event ("Extreme"), or that the AquaBASE infiltration system was overloaded. However, the water level at the outlet (SP3) was checked at 14:00 on September 28th, a point in which the gully pots were already flooded, and was visually estimated to be approximately NAP -0.3 m, which is more or less equal to the height of the overflow weir to the Waalstraat (NAP -0.35 m). On the side of the Rooseveltlaan service road connected to S3 (the non-studied SediSubstrator still connected to the AquaBASE but blocked off from S4, the studied system), the gully pots were draining normally with no water on the street. This suggests that the system was flowing freely and that there was not resistance from the AquaBASE system inhibiting flow.

A filter inspection took place on November 3rd 2022, and concrete was discovered in the slots of the bottom two cartridges and at the base of SP2. Concrete likely contributed to the increased filter resistance, but did not singly cause the high water levels during the "Extreme". It had previously been assumed that a filter cake would build up on the outer area of the bed material. However, the filter inspection revealed a substrate that was homogeneous, a little slimy and black, indicating the presence of organic material caught throughout the entire bed. The combination of organic material in the filter bed matrix, along with concrete are hypothesized to be the reasoning.

The hydraulic dynamics suggest that the design of the *SediSubstrator L* should be adapted, as the water level reaches the manhole cover (NAP +0.35 m) in three events (B, E and the "Extreme"). This appears to occur in events with a normal filter resistance (both early and late in the season).

6.2 Limitations

Within the experimental period (April 29th – September 7th), 9 out of 24 rainfall events were sampled and analyzed. Insufficient or incorrectly sampled volume for analysis, flowmeter malfunction and a limited budget were the causes of the events that were not sampled and analyzed. In this study, to best represent a long-term removal efficiency, a varied range of rainfall events (especially in terms of intensity, total runoff and duration) were sampled. Nevertheless, in order to be truly representative, both the number of rainfall events analyzed

and the duration of the experimental period should be increased. In the statistical analysis of the factors influencing the removal efficiency this is also the case. The relationships determined in section 5.4.1 provide a first indication, but already the dissolved phosphorus was not isolated in this analysis as there were only three natural rainfall events for which it was measured.

The handling of samples (section 4.3.3) was done in a timely manner, maintaining refrigerated conditions (4-6^{o}C) and avoiding agitation as much as possible. Still, the 10-minute bike route from the site to the laboratory drop-off and the sample preparation period was unrefrigerated, subject to shaking by nature of the transport method. Neglecting any heat insulation by the HDPE jugs which have insulating properties, the convective heat loss of one of the sample jugs in transit on a 20 ^{o}C summer day could amount up to 4 ^{o}C. The total phosphorus measurement is not expected to have been significantly impacted by this, as surface water experiments varying temperature and storage time have shown similar results (Moore & Locke, 2013). However, the filtered dissolved phosphorus measurements are likely to have been affected (compared to actual concentrations in-situ), due to interactions with the solids in the sample during storage. Agitation of the TSS in transport could have broken up some of the organic-based solids, lowering amount caught on the 0.45 µm filter, and artificially inflating the measured dissolved PO_4^{3-}. Immediate analysis (less than 3 hours after sampling) would have been the most reliable (Moore & Locke, 2013). However this was not possible due to the reservation setup at the TU Delft WaterLab and transportation times. Furthermore, the discrete analyzer available at Waternet yielded significantly varying phosphorus results when conducted in triplicate and for this reason was a less-preferred method.

The system start-up, beginning clean, likely reduced the influent TSS loading (Appendix C, Figure C - 5), as the street, gully pots and stormwater sewer were capturing coarse sediments (visibly organic and mineral in composition), as shown in Figure C - 5, Figure C - 6 and Figure C - 9. While the discharge at SP1 is referred to as the catchment runoff, the settling of large and/or dense particles has already taken place by this point in the system, driving the high fine fraction (TSS_{63}) that was measured as well. The influence of seasonality could not be separated from this effect as increased leaf litter deposition occurs over the summer.

Turbidity is frequently used as a proxy for continuous TSS measurements (Md et al., 2019; Packman et al., 1999; *Xylem Analytics | Turbidity Measurement with SI Analytics and WTW*, n.d.). However, this approach inherently has limitations, as coloured dissolved organic matter, air bubbles, particle size, shape, and composition all influence measurable light scattering and adsorption properties but are characteristics that are not distinguished in TSS (Downing, 1996). In the Münster SediPipe installation, Lieske et al. found that the measured fraction of TSS_{63} influences the applicability of the linear relation, but that this effect can be soundly mediated by removing points for which the TSS_{63} fraction exceeded 50% (Lieske et al., 2021). On the Rooseveltlaan, the TSS_{63} fraction was high and coloured dissolved organic matter could have been present in low levels with the degradation of organic material in the system. With only nine rainfall events sampled it is speculated that the TSS-turbidity relation

would not have been statistically strong. In the case of MP2 (the turbidity sensor at SP2), this is because cleaning didn't take place until September 8th due to parked cars blocking the manhole during scheduled maintenance visits (Appendix C, Table C - 3). MP3 exhibited frequent and extreme peaks which made the dynamics during rainfall events indiscernible, behavior which was only solved by adjusting the installation angle at the end of August. While MP1 and MP2 were installed on a slight axis, MP3 was vertical, trapping air bubbles from sparging in the recessed face of the instrument.

Suspended solids remaining in the SediSubstrator from previous rainfall may be pushed out in new rainfall events. As such, determining a per-event mass balance was not possible due to the working principle of the unit, so caught loads had to be estimated from the long-term average removal efficiency. This fact limits the applicability of the analysis of the factors affecting the removal efficiency (section 5.4). The actual caught load also cannot be retrieved and quantified due to the way in which the cleaning process (by vacuum truck) takes place. The inability to trace "old" water vs. "new" water on a per-event basis yields negative removal efficiencies of the finest fraction that remains from the previous rainfall. Nevertheless, more detailed analyses on the sediment properties by particle fraction would tune the settling behaviour in the model. In this research this was omitted as the low solids loading in the stormwater made the classification of the particle size distribution (by dry solids sieving) and density (by gas pycnometer) unfeasible in the lab.

In the SediSorp+ filter, clogging was quantified by the discharge-head relationship for the measured events across the system. While this relationship gives valuable information on the filter resistance, the actual pressure drop across the filter could not be quantified without continuous water level measurements on the other side of it as well. The mechanism and kinetics of adsorption and filtration in the SediSorp+ was not investigated as deeply as was initially desired. Adsorption isotherm information was only available for the supplier's other filter material, Ferrosorp Plus. The comparison between the two filters remains speculative.

6.3 Outlook

The performance of the full-scale *SediSubstrator L* on the Rooseveltlaan suggests that it would be an insufficient measure to meet the Water Framework Directive guideline in the Loosdrecht lakes (see Table 10). This is mainly due to the solubilization of particle-bound P in the settled sediments in the SediPipe (Table 7) and the low density of organic suspended solids in stormwater which settle slowly (as discussed in section 2.5).

Table 10: Predicted average concentrations of total P and dissolved P going in and out of a SediSubstrator treating road runoff in Loosdrecht

	Total P	PO
Inflow concentration [mg/L P] (Mandemakers & Holstein, 2019)	0.22	0.06
Estimated outlet concentration [mg/L P]	0.18	0.03
Water Framework Directive Limit [mg/L P]	0.03	0.03

It is worth noting that proposed alternatives to the SediSubstrator (Appendix A, Table A - 1) in a sensitive nature area like Loosdrecht also suffer from significant drawbacks. Over-dimensioning the stormwater sewer would lower flowrates to promote sedimentation—but, without a flow separator, not only would particle-bound P still be solubilized but the resuspension of sediments would also contribute to particle-bound loadings in the discharge. Inspection chambers would also effectively behave as sediment collectors and present the same risks in terms of P solubilization from settled solids. Gully pot filters are more prone to clogging as they receive coarser sediments in higher loadings than the SediSorp+. Infiltrating pavements would be effective in separating and stabilizing the particle-bound phosphorus, but risk clogging long-term, especially on the Loosdrecht horseshoe road, which bears relatively heavy truck traffic considering its size. The optimal intervention in sensitive nature areas appears to be bioswales, as they naturally mitigate clogging and have been shown to be effective in removing P from road runoff (84 ± 9%), most even within the first 1.5 m of the matrix (Shokri et al., 2021). However, in spatially-limited locations these may not be feasible.

Frequent street and sewer cleaning are the most effective in reducing the amount of gathered sediments that solubilize phosphorus in the system. In Amsterdam, the cleaning frequency for the stormwater sewer is 11 years (van der Keelen, personal communication, November 3, 2022). Considering the reactions of settled solids observed on just a 4-month period in this research, the time interval between cleanings should be reduced. A three-stage approach is therefore recommended: that regular cleaning of streets and gully pots continue to be enforced, that bioswales are installed where possible, and in remaining (dense) locations, that a SediSubstrator L design adapted for P sequestration is considered.

7 Conclusions and Recommendations

7.1 Conclusions

The purpose of this research was to monitor the operation of the *SediSubstrator L* in a full-scale installation in Amsterdam throughout the summer of 2022. To do so, stormwater runoff discharge on the Rooseveltlaan service road was characterized. The sediment (TSS) concentration was low, equivalent to 20 mg/L on average. The sediments were also light and fine—with an organic fraction of 66% and with 78% of diameter smaller than 63 µm. The stormwater contained elevated lead and zinc concentrations, of 54 µg/L and 790 µg/L respectively, which appear to be generated from the gutters and old roofing material on the adjacent residential buildings.

These sediment characteristics contribute to a lower than expected average sediment (TSS) removal efficiency of 34% for the unit. This corresponds to an estimated caught load of 2.7 kg for the May-September period. Per-event, the removal efficiency increased with increasing stormwater TSS concentrations, with longer antecedent dry periods and with lower TSS organic fractions. Turbidity dynamics in the system suggest that while a net sequestration of solids occurs in the SediPipe, there is a resuspension of fine and colloidal solids from on top of the flow separator grate. This behavior was later observed in a camera inspection. Resistance in the filter that caused water on the street on September 28th 2022 was uncharacteristic of gradual clogging, but is speculated to have been due to a combination of washed out solids, cement and decayed organic matter filling the matrix in this extreme rainfall event.

The average phosphorus removal efficiency was 18%, in particular 50% for ortho-phosphorus and -24% for the remaining organic and particle-bound phosphorus. Interactions with settled sediments in the SediPipe generated dissolved phosphorus, and fine particulate or colloidal organic phosphorus is also remobilized in both the SediPipe and SediSorp+, driving the negative removal efficiency. The SediSorp+ performance is relatively consistent at contact times between 10-30 minutes.

Sustainable urban drainage systems (SUDS) play a crucial role in climate adaptation in the city. Decisive action is needed to ensure sustainable management of urban water quality and quantity, both for the groundwater and surface water. While this research demonstrates that the SediSubstrator L performs differently in practice to predictions in models and at lab scale, it also reveals its importance as a safeguard for the subsequent, inaccessible AquaBASE infiltration system under the tram tracks. The findings of this research suggest that neighbourhood- or typology-based based implementation practices should be introduced in addition to more full-scale SUDS testing and monitoring programs to better inform site selection. As for the *SediSubstrator L* in sensitive nature areas, the colloidal and dissolved phosphorus discharged from organic-rich sediments suggests more research and design adaptations are still needed before its viability in this setting can be proven.

7.2 Recommendations for Further Research

7.2.1 Removal Efficiency

To increase the statistical significance of the calculated removal efficiency of sediments and phosphorus and to capture seasonal variability, the discharge should continue to be monitored, sampled and analyzed over a long-term period of at least one year, preferably two. In particular, more small rainfall events (in terms of cumulative discharge) should be sampled and analyzed, to better observe the effect of “pushing out” settled water from the SediSubstrator L.

A series of analyses should be run in which the current 16 L sampling bottles are replaced by 1 L bottles, to observe the existence of a “first flush” as well (confirming the turbidity dynamics observed in Figure 27). With more resolution in TSS (with concentrations per timestep rather than one event mean concentration), a TSS-turbidity regression may be run to observe the relation and ideally use turbidity as a reliable proxy for TSS, reducing laboratory analysis expenses and labour in sample preparation and transport.

Furthermore, it is recommended that sediments are sampled from below the flow separator in the SediPipe to be used in column experiments to construct an empirical settling velocity curve. This may then be compared to characteristics of the supplier’s design stormwater sediments, and the settling velocity curves from other sites in Germany.

The removal efficiency on more water quality indicators should be tested, in particular heavy metals due to the high concentrations measured in this study. In natural rainfall, these analyses are costly and logistically difficult. It is therefore recommended to run a pumped water experiment (considering the success of the pumped surface water experiment in this research), pumping water from the adjacent stormwater sewer on the Maasstraat or the Waalstraat into SP1 of the SediSubstrator S3, and measuring the difference in concentration across the system at different flowrates.

7.2.2 Estimation of Caught Load

The settled sediments in the SediPipe should be sampled and analyzed for their density, to translate the volume as observed in a camera inspection into a more reliable caught load [kg]. Another camera inspection is recommended at the end of the extended experimental period (after one to two years of operation).

7.2.3 Hydraulic Dynamics and Filter Performance

In this research, the properties of the SediSorp+ filter remained relatively unknown. Further work is still needed to define the phosphorus removal mechanisms that take place at the concentrations found in stormwater. Samples from the filter bed should be taken after one year of operation to measure the mass, the organic fraction of the caught solids and the adsorbed phosphorus. Each the virgin filter bed material in each cartridge has a wet weight

of 80 kg when supplied (*Product Brochure: SediPipe L / L plus; SediSubstrator L*, 2019), so the current mass may be compared to this. Desorption tests would involve submerging a sample of SediSorp+ in NaOH (Na et al., 2021), filtering the slurry and testing for the dissolved PO_4^{3-} remaining in the liquid.

To characterize the long-term clogging behavior and compare the impact of targeting fine particles (TSS_{63}) via other filter media with the adsorptive capabilities of the SediSorp+, the assembly of an ex-situ filter test set-up is recommended. This proposal is described in more detail in Appendix F. The removal efficiency of filters on various pollutants in real stormwater is of interest to many parties in the urban water cycle at the moment, and this set-up would compare different media in identical conditions, to accurately identify the best filter for a given scenario (ie. TSS removal for infiltration systems, P for the mitigation of eutrophication or heavy metals to counter environmental toxicity). In addition, in more long-term monitoring, a pressure transducer should be installed at SP3 to accurately gauge the clogging of the filter over time.

While the supplier has cited a design throughput for the filter over 100 m^3/h, this was never reached in the SediSubstrator. The hydraulic capacity of the filter should be tested in-situ, to observe whether it can withstand heavy, sediment-free flowrates within the range of expected rainfall without flooding the street. To do so it is recommended to dose clean water using the adjacent hydrant and to measure the water level before and after the SediSorp+.

7.2.4 SUDS in General

On the Rooseveltlaan, it is recommended to monitor the groundwater levels over the coming years and include these measurements and the infiltrated volume of stormwater in the AquaBASE in local models. This should be done to assess the impact of the SediSubstrator-AquaBASE system on the water levels in the area. As the current main interest in the SediSubstrator in the city is to improve the performance of infiltration systems, it must first also be proven that the SUDS is effective for its intended purpose.

To ensure a longer lifetime for SUDS in the city, it may be beneficial to design systems which receive inflows with only fine-particulates, or which are sufficiently dilute to reduce the risk of clogging. This would simplify the pre-treatment required. It is therefore recommended to sample and analyze the runoff from roofs in the area for TSS and its organic fraction to better inform this possibility.

7.3 Design Recommendations

Recommended adaptations to the design of the SediSubstrator L that emerged from results of monitoring across the experimental period are summarized in Figure 31. These recommendations consider safety, an improvement of the removal efficiency of TSS and P and discuss the type of connected area that would optimize its performance.

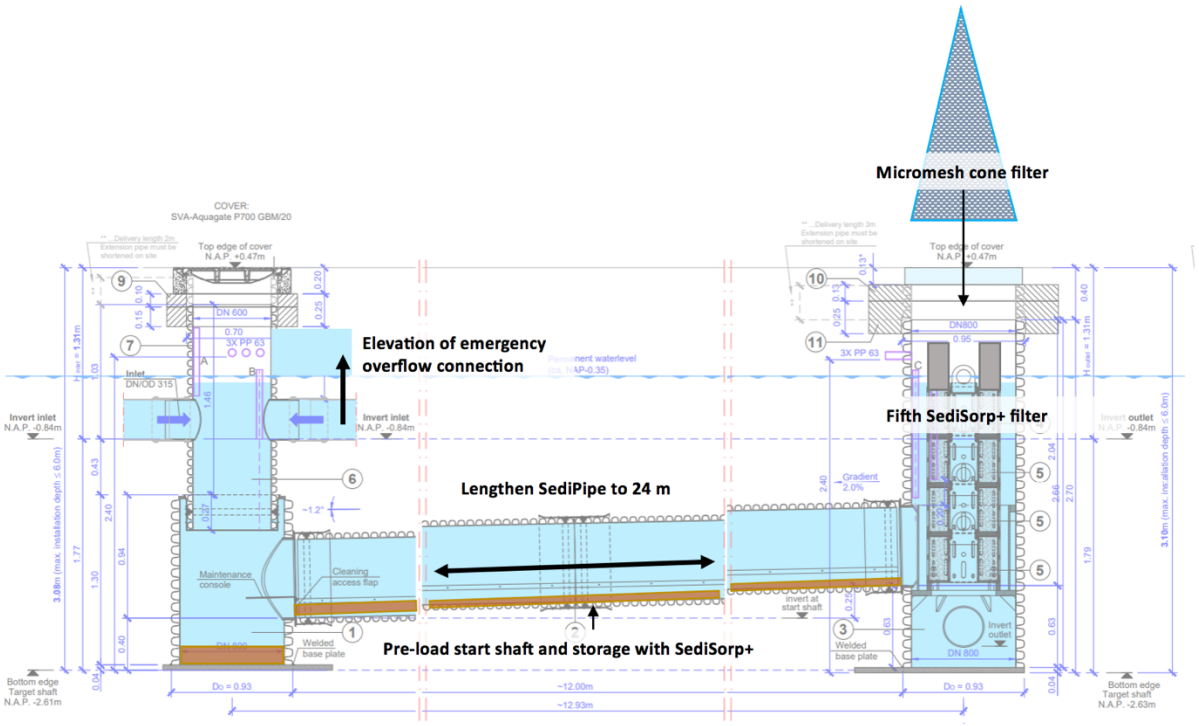

Figure 31: Design recommendations for the SediSubstrator L in Amsterdam

7.3.1 Removal Efficiency

The SediPipe should be lengthened to 24 m to improve the removal efficiency of TSS. This change alone would lead to an improvement of 16% for particles of diameter 63 µm in 10 L/s flows (Figure 26). However, it is recommended to run a cost-benefit analysis of this adaptation prior to implementation.

To achieve good removal efficiencies overall, the SediSorp+ would need to be adapted to target low-density (800-1500 kg/m^3) and fine (d_p < 63 µm) particulates. This warrants the use of either a filter with better fines retention than the SediSorp+ or the introduction of a second filter stage (micromesh cone filter on Figure 31) preferably without sacrificing hydraulic throughput. Interest in the filter bed material has motivated plans for further research (section 7.2.3). Furthermore, aquarium filters of mesh size 25 µm may be used as a design basis for the cone filter (aquariumkoelers, n.d.), for which throughput and ease of replacement are crucial.

To improve the phosphorus removal efficiency, in the Netherlands where solids loadings in stormwater are low, storage in the SediPipe system (both the sinker in SP1 and below the flow separator) can be preloaded with SediSorp+, to readily adsorb any PO_4^{3-} that is generated.

7.3.2 Emergency Overflow and Hydraulics

In Germany, where the SediSubstrator originates, the test principles of DIBt (the technical authority in the construction sector) do not require an emergency outflow (*Product Brochure:*

SediPipe L / L plus; SediSubstrator L, 2019). However, it is strongly urged that the Sedi-Substrator L in the Rooseveltlaan is equipped with one. The overflow in SP1 was temporarily blocked to maintain volume-proportional sampling across the system, and the water level rose up to the manhole cover at least three times during the monitoring period (NAP +0.35 m in the end shaft). Most of the sampled events have water levels exceeding NAP -0.35 m (Figure 28), indicating that the emergency overflow as designed would even consistently discharge untreated water in normal rainfall events, reducing the effective removal efficiency of the catchment runoff discharge. The shallow installation depth and groundwater levels in the Rooseveltlaan make improvements difficult, but the height of the weir may be optimized with a hydraulic model for the area. This needs to be tuned, as raising the weir would infiltrate more stormwater runoff, but also perhaps impede the ability to meet the target of 70 mm in one hour set by Amsterdam Rainproof.

The largest connected area recommended for a SediSubstrator L is 3000 m^2 (model 600/24 with four filter cartridge elements in the end shaft) (*Product Brochure: SediPipe L / L plus; SediSubstrator L*, 2019). The placement of blockages in the sewer entering into the modified SediSubstrator L 600/12 on the Rooseveltlaan service road expanded the connected area to 4753 m^2 which is substantially larger. The expansion of the connected area at the beginning of this study was done to push the boundaries of the system, being a quiet road with relatively low pollutant loadings compared to previous research. Restoring the connected area to the designed setup (area 3305 m^2) would also improve removal efficiencies. A 30% flowrate reduction would result and based on the maximum average inflow of the sampled events (by 5-minute timestep) equivalent to 4.5 L/s this would increase removal efficiencies for particles (d_p = 63 µm) by 10%.

A fifth SediSorp+ cartridge should be added in the end shaft to increase the area through which the stormwater is discharged, with the aim of reducing the pressure drop across the filter and improving hydraulic throughput. In stagnant conditions, this filter will remain above the water level, which will also foreseeably improve the aerobic decomposition of caught solids in this cartridge, reducing the clogging risk.

7.3.3 Site Selection

To mitigate clogging and optimize the sedimentation efficiency of the SediSubstrator L, heavily trafficked urban roads with few trees or sources of organic material should be selected as potential sites for the unit.

To generate a list of potential viable sites, it is recommended to overlay a GIS map of trees and vegetation in the city (for instance one could use the Normalized Difference Vegetation Index, or NDVI) on top of the Amsterdam Rainproof map (Figure 1). This would identify the sites with few trees that also urgently need SUDS interventions—locations in which the SediSubstrator should preferably be considered in the future.

The Ferdinand Bolstraat in de Pijp, for example, is a busy road with a tram line running through it (Figure 32), without space for bioswales. This could be an improved location for a SUDS installation similar to that on the Rooseveltlaan.

Figure 32: The Ferdinand Bolstraat in de Pijp (Lek, 2018)

References

Allison, R. A., Chiew, F. H. S., & McMahon, T. A. (1998). Nutrient contribution of leaf litter in urban stormwater. *Journal of Environmental Management*, *54*(4), 269–272. https://doi.org/10.1006/jema.1998.0334

Alves, C. A., Vicente, A. M. P., Calvo, A. I., Baumgardner, D., Amato, F., Querol, X., Pio, C., & Gustafsson, M. (2020). Physical and chemical properties of non-exhaust particles generated from wear between pavements and tyres. *Atmospheric Environment*, *224*, 117252. https://doi.org/10.1016/j.atmosenv.2019.117252

aquariumkoelers, O. S. | E., opvoerpompen, stromingspompen. (n.d.). *Gafzak, doorsnee 10cm. Dichtheid 25 micron | Gafzakken en houders | Filtersystemen*. Ocean Store | Uw online (zee)aquarium winkel. Retrieved November 8, 2022, from https://zeeaquarium-winkel.nl/gafzak-doorsnee-10cm-dichtheid-25-micron

Asano, T., Burton, F., & Leverenz, H. (2007). *Water Reuse: Issues, Technologies, and Applications*. McGraw-Hill Education. https://www.accessengineeringlibrary.com/content/book/9780071459273

Boogaard, F. (2015). *Stormwater characteristics and new testing methods for certain sustainable urban drainage systems in The Netherlands*. Technische Universiteit Delft.

Bratt, A., Finlay, J., Hobbie, S., Janke, B., Worm, A., & Kemmitt, K. (2017). Contribution of Leaf Litter to Nutrient Export during Winter Months in an Urban Residential Watershed. *Environmental Science & Technology*, *51*. https://doi.org/10.1021/acs.est.6b06299

Bunce, J. T., Ndam, E., Ofiteru, I. D., Moore, A., & Graham, D. W. (2018). A Review of Phosphorus Removal Technologies and Their Applicability to Small-Scale Domestic Wastewater Treatment Systems. *Frontiers in Environmental Science*, *6*. https://www.frontiersin.org/article/10.3389/fenvs.2018.00008

City of Amsterdam. (2022). *Rivierenbuurt: Nieuwe riolering en betere waterafvoer* [Webpagina]. Amsterdam.nl; City of Amsterdam. https://www.amsterdam.nl/projecten/rivierenbuurt/

Conley, G., Beck, N., Riihimaki, C. A., & Tanner, M. (2020). *Quantifying clogging patterns of infiltration systems to improve urban stormwater pollution reduction estimates*. 12.

Davies, J., & Butler, D. (2011). *Urban Drainage* (3rd ed.). Spon Press.

de Leeuw, A. (2022). *Rooseveltlaan Technical Drawings*. Waternet.

Deltares. (2022). *Fosfor speciaties kubus*.

Downing, J. (1996). *Suspended Sediment and Turbidity Measurements in Stream: What they do and do not Mean.*". Automatic Water Quality Monitoring Workshop.

Duffy, A., & McKay, G. (2015). A review of 20 years of SUDS in Scotland. *World Water Congress Conference XV*, 11.

EcoBASE A5. (n.d.). AquaBASE. Retrieved August 18, 2022, from https://www.aquabase.info/componenten/ecobase-a5/

Faizah, R., Priyosulistyo, H., & Aminullah, A. (2019). The Properties of Waste Rubber Tires in Increasing the Damping of Masonry Wall Structure. *Materials Science and Engineering*, 11.

Ferguson, R. I., & Church, M. (2004). A Simple Universal Equation for Grain Settling Velocity. *Journal of Sedimentary Research*, *74*(6), 933–937. https://doi.org/10.1306/051204740933

Fuchs, S., Kemper, M., & Morling, K. (2019). *REduktion des FEststoffeintrages durch Niederschlagswassereinleitungen Phase 2*.

Gelhardt, L., Dittmer, U., & Welker, A. (2021). Relationship of particle density and organic content in sieve fractions of road-deposited sediments from varying traffic sites based on a novel data set. *Science of The Total Environment*, *794*, 148812. https://doi.org/10.1016/j.scitotenv.2021.148812

Gemeente Wijdemeren. (2017). *Gemeentelijk Rioleringsplan Wijdemeren 2018-2021*.

Gemeentelijk-Rioleringsplan.pdf. (n.d.). Retrieved March 1, 2022, from https://www.wijdemeren.nl/4/grp/Gemeentelijk-Rioleringsplan.pdf

Göbel, P., Dierkes, C., & Coldewey, W. G. (2007). Storm water runoff concentration matrix for urban areas. *Journal of Contaminant Hydrology*, *91*(1), 26–42. https://doi.org/10.1016/j.jconhyd.2006.08.008

Goess-Enzenberg, I. (2020). *Determination of the removal efficiency of a decentralized stormwater treatment system—A theoretical approach to assess a modified SediSubstrator L*. TU Delft, Waternet.

Gruber, P. (1985). Die chemische und mineralogische Zusammensetzung des Flugstaubes im Linzer Raum. *Öko.L.*, *7*, 15–24.

Gunkel, G., Michels, U., & Scheideler, M. (2022). Climate Change: Water Temperature and Invertebrate Propagation in Drinking-Water Distribution Systems, Effects, and Risk Assessment. *Water*, *14*(8), Article 8. https://doi.org/10.3390/w14081246

Hobbie, S. E., Finlay, J. C., Janke, B. D., Nidzgorski, D. A., Millet, D. B., & Baker, L. A. (2017). *Contrasting nitrogen and phosphorus budgets in urban watersheds and implications for managing urban water pollution*. https://doi.org/10.1073/pnas.1618536114

Hofman-Caris, R., Bertelkamp, C., de Waal, L., van den Brand, T., Hofman, J., van der Aa, R., & van der Hoek, J. (2019). Rainwater Harvesting for Drinking Water Production: A Sustainable and Cost-Effective Solution in The Netherlands? *Water*, *11*(3), 511. https://doi.org/10.3390/w11030511

Jani, J., Yang, Y.-Y., Lusk, M. G., & Toor, G. S. (2020). Composition of nitrogen in urban residential stormwater runoff: Concentrations, loads, and source characterization of nitrate and organic nitrogen. *PloS One*, *15*(2), e0229715. https://doi.org/10.1371/journal.pone.0229715

Klappe, R. (2022). *Referentielijst SediPipe 2022*. Frelu B.V.

KNMI - Neerslagtekort / Droogte. (n.d.). Retrieved September 22, 2022, from https://www.knmi.nl/nederland-nu/klimatologie/geografische-overzichten/neerslagtekort_droogte

KNMI Klimaatsignaal'21. (2021). Koninklijk Nederlands Meteorologisch Instituut.

Lafuente, E., Lürig, M. D., Rövekamp, M., Matthews, B., Buser, C., Vorburger, C., & Räsänen, K. (2021). Building on 150 Years of Knowledge: The Freshwater Isopod Asellus aquaticus as an Integrative Eco-Evolutionary Model System. *Frontiers in Ecology and Evolution*, *9*. https://www.frontiersin.org/articles/10.3389/fevo.2021.748212

Lead sheet on monuments | Cultural Heritage Agency. (n.d.). Retrieved November 6, 2022, from https://kennis.cultureelerfgoed.nl/index.php/Bladlood_op_monumenten

Lek, S. (2018). *Toegang metrostation De Pijp aan de kruising Ceintuurbaan-Ferdinand Bolstraat*. https://nl.wikipedia.org/w/index.php?title=Ferdinand_Bolstraat&oldid=60964590

Li, D., Wan, J., Ma, Y., Wang, Y., Huang, M., & Chen, Y. (2015). Stormwater Runoff Pollutant Loading Distributions and Their Correlation with Rainfall and Catchment Characteristics in a Rapidly Industrialized City. *PLOS ONE*, *10*(3), e0118776. https://doi.org/10.1371/journal.pone.0118776

Li, W., O'Kelly, B. C., Yang, M., Fang, K., Li, X., & Li, H. (2020). Briefing: Specific gravity of solids relationship with ignition loss for peaty soils. *Geotechnical Research*, *7*(3), 134–145. https://doi.org/10.1680/jgere.20.00019

Liefting, H. J., Boogaard, F., & Langeveld, J. (2020). *Kwaliteit van afstromend hemelwater in Nederland*. RIONED & STOWA.

Lieske, C., Leutnant, D., & Uhl, M. (2021). Assessing the TSS Removal Efficiency of Decentralized Stormwater Treatment Systems by Long-Term In-Situ Monitoring. *Water*, *13*(7), Article 7. https://doi.org/10.3390/w13070908

Loosdrecht Site Visit. (2022).

Mandemakers, J. J., & Holstein, S. (2019). *Quality of rainwater runoff Loosdrecht*. Witteveen+Bos.

Md, S., Chowdhury, A., Haque, M. M., & Haque. (2019). *Using Turbidity to Determine Total Suspended Solids in an Urban Stream: A Case Study*. *Volume-67*, 83–88. https://doi.org/10.14445/22315381/IJETT-V67I9P214

Moore, M. T., & Locke, M. A. (2013). Effect of Storage Method and Associated Holding Time on Nitrogen and Phosphorus Concentrations in Surface Water Samples. *Bulletin of Environmental Contamination and Toxicology*, *91*(5), 493–498. https://doi.org/10.1007/s00128-013-1084-6

Na, C.-K., Park, G.-Y., & Park, H. J. (2021). Applicability of ferric(III) hydroxide as a phosphate-selective adsorbent for sewage treatment. *Water Science and Technology*, *83*(12), 2911–2920. https://doi.org/10.2166/wst.2021.180

Neupert, J. W., Lau, P., Venghaus, D., & Barjenbruch, M. (2021). Development of a New Testing Approach for Decentralised Technical Sustainable Drainage Systems. *Water*, *13*(5), Article 5. https://doi.org/10.3390/w13050722

Niëns, N. (2015). *Quantitative geohydrological effects of sustainable urban drainage systems (SUDS): Infiltration units and swale implemented in Stadstuin Overtoom, Amsterdam*. Vrije Universiteit Amsterdam and Waternet.

Nijman, M. (2022, July). *Gully pot study, SediSubstrator synergies* [Personal communication].

Nijman, M. (2022, July 11). *Questions about powerpoint "Efficiency of Sediment and Nutrient Removal."*

Nijman, M., El Ayadi, N., & Zandvoort, M. (2015). *Werking bezinkleiding Hemelwaterstelsel Ookmeerweg*. Waternet.

O'Callaghan, I., Harrison, S., Fitzpatrick, D., & Sullivan, T. (2019). The freshwater isopod Asellus aquaticus as a model biomonitor of environmental pollution: A review. *Chemosphere*, *235*, 498–509. Scopus. https://doi.org/10.1016/j.chemosphere.2019.06.217

Oostelijke Vechtplassen | Natura 2000. (n.d.). Retrieved March 1, 2022, from https://www.natura2000.nl/gebieden/noord-holland/oostelijke-vechtplassen

Packman, J., Comings, K., & Booth, D. (1999). *Using Turbidity to Determine Total Suspended Solids in Urbanizing Streams in the Puget Lowlands*.

Product brochure: SediPipe L / L plus; SediSubstrator L. (2019). Fränkische Rohrwerke.

Product specification for quality monitoring SediSorp, 1.0-2.0 mm. (2012). HeGo Biotec GmbH.

Rip, W., van den Boer, T., Düren-Calvelage, I., Hagen, D., van Amstel, N., Buitenhuis, W., & Trast, S. (2021). *Ontwerp riolering, omgang afstromend hemelwater en fosfaatreductie binnen het project herinrichting Boomhoek-Muyeveld*.

Schönherr, S., Scheffler, S., & de Leeuw, A. (2020). *Longitudinal section/Top view + Overview map*. Fränkische Rohrwerke.

Schulz, K. L. (n.d.). *Limnology: Phosphorus*. SUNY College of Environmental Science and Forestry. Retrieved September 13, 2022, from https://www.esf.edu/efb/schulz/Limnology/Phosphorus.html

Schutz, M. (2022). *SediSubstrator Meeting* [Online].

SediSubstrator® L. (n.d.). SediSubstrator® L. Retrieved September 28, 2022, from https://www.fraenkische.com/en/product/sedisubstrator-l?context=sedimentation-adsorbtion

Shokri, M., Kibler, K., Hagglund, C., Corrado, A., Wang, D., Beazley, M., & Wanielista, M. (2021). Hydraulic and nutrient removal performance of vegetated filter strips with engineered infiltration media for treatment of roadway runoff. *Journal of Environmental Management*, *300*, 113747. https://doi.org/10.1016/j.jenvman.2021.113747

Si, Q., Lusk, M. G., & Inglett, P. W. (2021). Inorganic nitrogen production and removal along the sediment gradient of a stormwater infiltration basin. *Water (Switzerland)*, *13*(3), 1–12. Scopus. https://doi.org/10.3390/w13030320

Song, K., Xenopoulos, M. A., Marsalek, J., & Frost, P. C. (2015). The fingerprints of urban nutrients: Dynamics of phosphorus speciation in water flowing through developed landscapes. *Biogeochemistry*, *125*(1), 1–10. https://doi.org/10.1007/s10533-015-0114-3

Spaan, B., & BAG. (2015). *Buildings in the Netherlands, by year of construction* [Map]. Waag Society. http://code.waag.org/buildings/

Sperlich, A., Schimmelpfennig, S., Baumgarten, B., Genz, A., Amy, G., Worch, E., & Jekel, M. (2008). Predicting anion breakthrough in granular ferric hydroxide (GFH) adsorption filters. *Water Research*, *42*(8), 2073–2082. https://doi.org/10.1016/j.watres.2007.12.019

Stroom, J. (2022, September). *Phosphorus removal and speciation* [Personal communication].

Swenson, N. G., & Enquist, B. J. (2008). The relationship between stem and branch wood specific gravity and the ability of each measure to predict leaf area. *American Journal of Botany*, *95*(4), 516–519. https://doi.org/10.3732/ajb.95.4.516

TNO. (1986). *Verklarende hydrologische woordenlijst*.

van de Ven, F. (2016). *CIE 5510: Water Management in Urban Areas*. TU Delft.

van der Keelen, V. (2022, November 3). *SediSubstrator Cleaning and Inspection* [Personal communication].

van Dijk, J. C. (2020). *#07—Sedimentation*. TU Delft OpenCourseWare.

Vollaers, V., Nieuwenhuis, E., van de Ven, F., & Langeveld, J. (2021). Root causes of failures in sustainable urban drainage systems (SUDS): An exploratory study in 11 municipalities in the Netherlands. *Blue-Green Systems*, *3*(1), 31–48. Scopus. https://doi.org/10.2166/bgs.2021.002

Votel, M., El Ayadi, N., & Nijman, M. (2022). *Kennisdocument hemelwater- verwerkende voorzieningen* (p. 37). Waternet.

Wagemakers, C. (2022, June 1). *Lab Analyses at Stichting Waterproef* [Personal communication].

Wang, Y., Thompson, A. M., & Selbig, W. R. (2022). Predictive models of phosphorus concentration and load in stormwater runoff from small urban residential watersheds in fall season. *Journal of Environmental Management*, *315*, 115171. https://doi.org/10.1016/j.jenvman.2022.115171

Waterfall, P. H. (2004). *Harvesting Rainwater for Landscape Use, 2nd Edition*. University of Arizona.

Xylem Analytics | Turbidity measurement with SI Analytics and WTW. (n.d.). Retrieved September 26, 2022, from https://www.xylemanalytics.com/en/parameters/turbidity-and-tss

Yang, B., Lin, H., Bartlett, S. L., Houghton, E. M., Robertson, D. M., & Guo, L. (2021). Partitioning and transformation of organic and inorganic phosphorus among dissolved, colloidal and particulate phases in a hypereutrophic freshwater estuary. *Water Research*, *196*, 117025. https://doi.org/10.1016/j.watres.2021.117025

Yang, Y.-Y., & Toor, G. S. (2018). Stormwater runoff driven phosphorus transport in an urban residential catchment: Implications for protecting water quality in urban watersheds. *Scientific Reports*, *8*(1), Article 1. https://doi.org/10.1038/s41598-018-29857-x

Appendix A – Background, Supporting Information

Past Research on the SediSubstrator

The particle size distribution of Millisil®W4 compared to stormwater sediments from international literature is shown in Figure A - 1. The average as measured in the Netherlands (labeled as “average Holland”) appears to have a relatively consistent distribution with that of Millisil®W4.

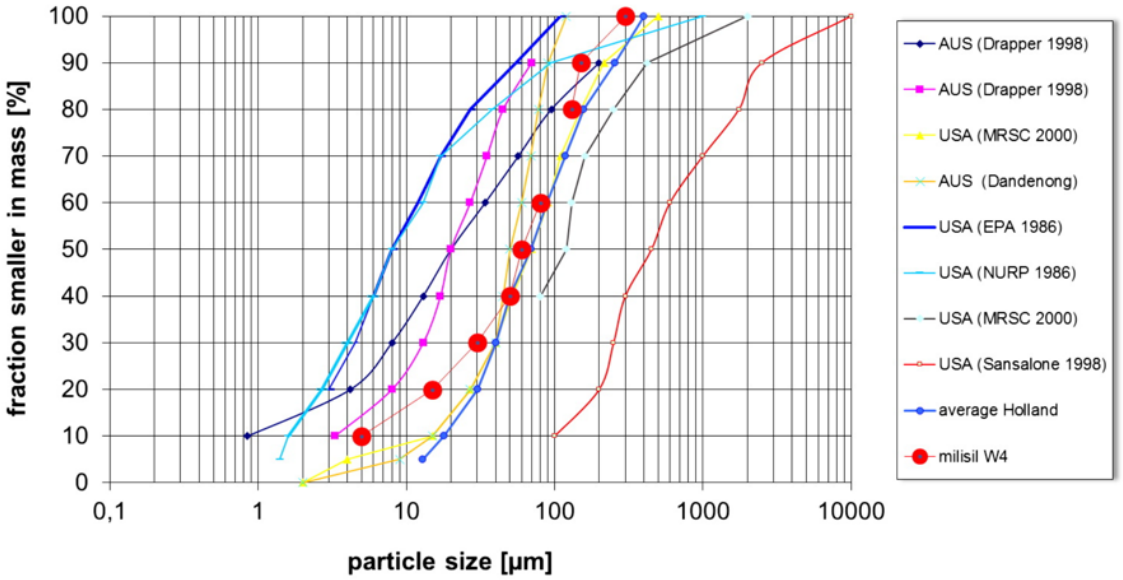

Figure A - 1: Comparison between particle size distribution of Millisil®W4 and real sediments (Boogaard, 2015)

The modeled impact of precipitation intensity and runoff volume on the sediment removal efficiency in the SediPipe L is shown in Figure A - 2. The removal efficiency in this event improves at low flows but only by a maximum of 9%.

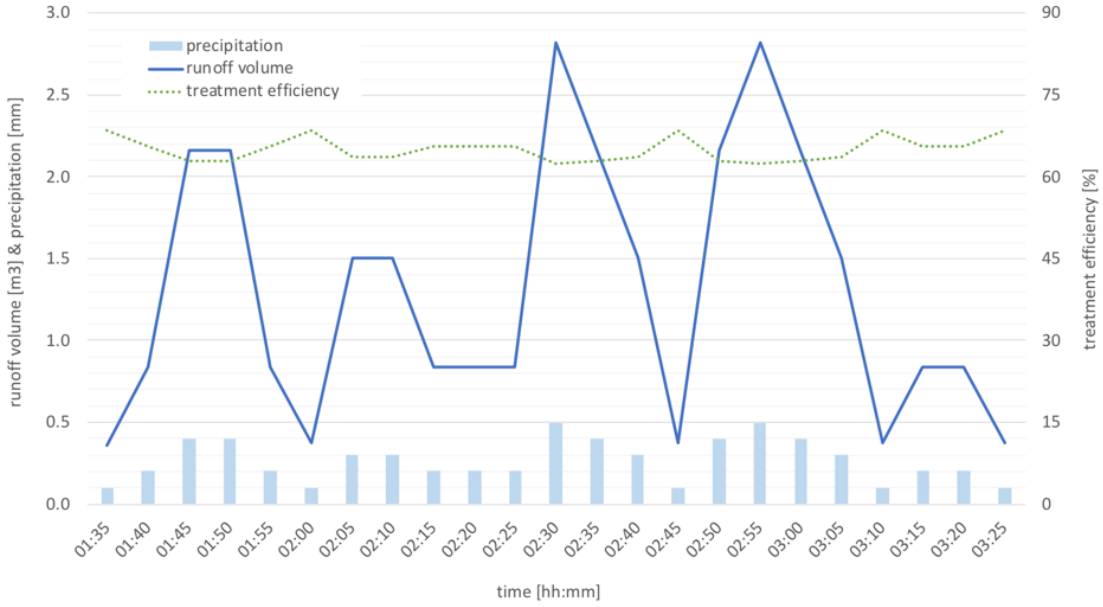

Figure A - 2: Modeled removal efficiency with varied runoff and inflow to a SediPipe L (Goess-Enzenberg, 2020)

Phosphorus Loadings to the Loosdrecht Lakes

A multidisciplinary project group has been consulted by the Municipality of Wijdemeren, where Loosdrecht is situated, on the issue of phosphorus loadings and stormwater sewer discharges. The catchment in question is shown in Figure A - 3 (outlined in black). The location of the Nieuw- and Oud-Loosdrechtsedijk roads is highlighted in orange.

Figure A - 3: Location of the Nieuw- and Oud-Loosdrechtsedijk roads in Loosdrecht (orange), with numbered measurement locations from the previous study. Adapted from Mandemakers and Holsteijn (2019)

In September 2021 it was decided that the removal of phosphorus in the urban water cycle at full-scale is still under development and therefore simple source-based measures should first be taken (Rip et al., 2021). There was a recognition that government investments must be efficient and socially responsible ("utility and necessity must be weighed against social costs"), and that land use is diverse and the available space is limited.

Mitigation solutions were compiled by the team (Appendix A, Table A - 1), divided into source (upstream) and in-system (effectively end-of-pipe) treatment. In the 2020-2024 renewal the project team decided to pursue a source approach that they estimate will remove a maximum of 50% of the phosphate from the road runoff discharge (Rip et al., 2021). Vacant space for a Best Available Technology (BAT)—which has yet to emerge—and a complete monitoring budget is included with the potential to install an in-system facility at a later date.

Table A - 1: Mitigation measures identified for phosphate in stormwater (Rip et al., 2021)

Source Approach (Prevention)	In-System (Capture & Sequestration)
- Animal waste policy	- Gully pot filters
- Street sweeping	- Over-dimensioning the stormwater sewer
- Tree leaf collection campaign	- Inspection chambers with sand traps in the stormwater sewer
- Gully pot cleaning	
- Sewer cleaning	- Infiltrating pavements or green strips

Nevertheless, according to the Municipal Sewerage Plan 2018-2021 (GRP) and Climate Adaptation Memorandum (2020-2030), untreated stormwater cannot be discharged to surface water if the receiving system is vulnerable to the discharge, which is the case with phosphorus (Gemeente Wijdemeren, 2017). According to the Water Framework Directive (WFD), water managers may not permit activities that cause a deterioration in the current state of the surface water or impede the achievement of WFD guidelines. With these considerations, it is mandatory that the mitigation measures taken are consistent as the runoff discharge may not cause a deterioration in the water quality of the Loosdrecht lakes.

The quality of the stormwater runoff from the Nieuw- and Oud-Loosdrechtsedijk roads is shown in Table A - 2. Cd and Hg were also measured, but lie below the measurement limits of 0.4 and 0.1 µg/L respectively.

Table A - 2: Water quality in the stormwater discharge as measured at five locations along the Nieuw- and Oud-Loosdrechtsedijk roads in 2018 (adapted from (Mandemakers & Holstein, 2019))

	1a	1b	2	4	5
Ammonium, NH_4-N [mg/L]	0.61	1.61	0.75	0.65	0.99
Nitrate, NO_3-N [mg/L]	1.46	0.67	0.97	1.35	0.80
Nitrite, NO_2-N [mg/L]	0.11	0.03	0.04	0.09	0.05
Total Kjeldahl Nitrogen, TKN [mg/L]	1.3	5.3	1.9	1.6	2.6
Ortho-Phosphate, PO_4-P [mg/L]	0.06	0.08	0.04	0.22	0.13
Total Phosphorus, P [mg/L]	0.12	0.28	0.15	0.25	0.35
Arsenic, As [µg/L]	1.6	2.2	1.5	1.5	1.5
Cadmium, Cd [µg/L]	0.4	0.4	0.4	0.4	0.4
Chromium, Cr [µg/L]	5	5	7	5	5
Copper, Cu [µg/L]	11	37	7	18	12
Mercury, Hg [µg/L]	0.1	0.1	0.1	0.1	0.1
Lead, Pb [µg/L]	5	31	13	5	5
Nickel, Ni [µg/L]	5	5	7	5	5
Zinc, Zn [µg/L]	99	271	538	40	10
Mineral Oil, C_{10}-C_{40} [µg/L]	280	182	54	190	-
PAHs, total VROM (10) [µg/L]	22	0.15	0.11	0.58	-

The phosphorus concentration measured in the Loosdrecht Lakes themselves is shown in orange in Figure A - 4, compared to the Water Framework Directive (WFD) limit marked in red.

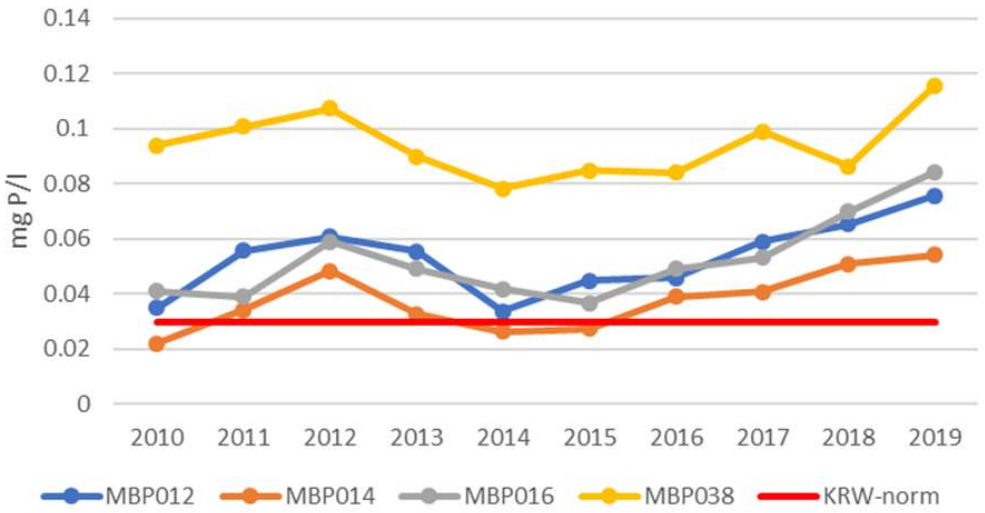

Figure A - 4: Total P concentrations in the Loosdrecht lakes (orange)(Mandemakers & Holstein, 2019)

Appendix B – Water Quality

Phosphorus Analysis

The phosphorus species detected depend on the laboratory analysis method used, as shown in Figure B - 1. The Waterproef laboratory used spectrophotometric methods (NEN-EN-150156812-2), measuring the dissolved reactive P, which includes the inorganic dissolved fraction (being PO_4^{3-} and polyphosphates) as well as the inorganic colloidal fraction. The measured dissolved reactive phosphorus is referred to as ortho-P (PO_4^{3-}) in this study. Although the dissolved reactive P is not true PO_4^{3-}, it is commonly referred to as such, as the contribution of the inorganic colloidal fraction is presumed to be small (Deltares, 2022; *C. Wagemakers, personal communication, June 1, 2022*; B. Yang et al., 2021).

When the dissolved reactive P is subtracted from total P, the remainder represents the particle-bound P as well as the organic dissolved and colloidal P. It is therefore impossible to isolate the particle-bound P alone, using the methods available in this study.

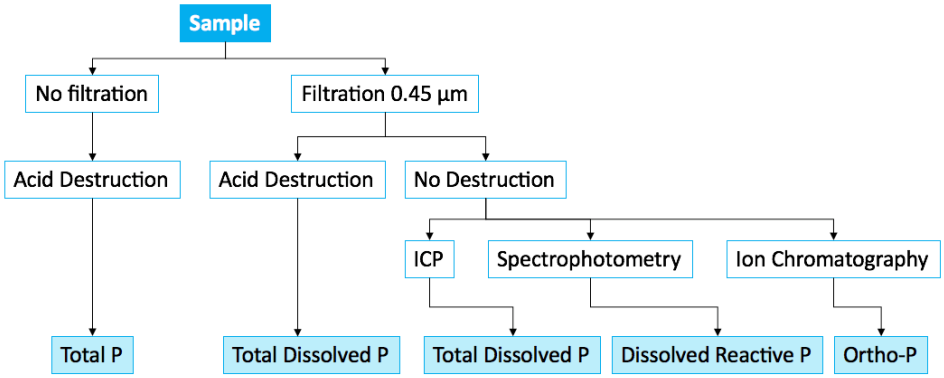

Dissolved organic phosphorus	✓	✓	✓		
Dissolved inorganic phosphorus	✓	✓	✓	✓	✓
Colloidal organic phosphorus	✓	✓	✓		
Colloidal inorganic phosphorus	✓	✓	✓	✓	
Particulate organic phosphorus	✓				
Particulate inorganic phosphorus	✓				

Figure B - 1: Phosphorus analysis methods and associated detectable forms, adapted from Deltares (2022)

Phosphorus Proficiency Tests

Prior to the opening of the SediSubstrator-AquaBASE system, stormwater from the sewer on the Rooseveltlaan service road in the next block (in front of house number 55) was sampled. This took place in stagnant conditions on April 28th, 2022.

Figure B - 2: Rooseveltlaan service road sampling location, approximately in front of house number 55

Samples were analyzed for total P and PO_4^{3-} by a HACH DR3900 spectrophotometer (test kit LCK349) at Waternet, and by discrete analyzer (NEN-ISO 15923-1 conform, measuring true PO_4^{3-}) at Het Water Laboratorium. The comparison between the levels measured in the service road stormwater and in Loosdrecht is shown in Table B - 1.

Table B - 1: Measured concentrations of P-species on the Rooseveltlaan and in Loosdrecht

Indicator	Rooseveltlaan service road	Loosdrecht roads 5-site avg. (Mandemakers & Holstein, 2019)
Ortho-P [mg/L P]	<0.02	0.04, 0.08
Total-P [mg/L P]	0.43	0.15, 0.28

Laboratory Analysis Reports (Stichting Waterproef)

Rapportnummer:
414086

Pagina
2 / 3

Volgnummer	Puntcode	Monsteromschrijving*
664714	oh080007	Overig SediSubtrator SP1
664715	oh080007	Overig SediSubtrator SP3

Volgnummer	664714	664715
Monstercode klant*	SP1	SP3
Monstertype*	Overige	Overige
Bemonsteringstype*	1 dag, volumeprop.	1 dag, volumeprop.
Monsternemer*	opdrachtgever	opdrachtgever
Monstername datum*	19-05-2022	19-05-2022
Monstername tijd*	18:00	18:00
Acceptatiedatum	20-05-2022	20-05-2022

Fysisch- Chemische analyses			Eenheid
Ortho-fosfaat	< 0,005 a	< 0,005 a	mg/l P
Totaal-fosfor in water	0,26 a	0,29 a	mg/l P

Opmerkingen
a Monster is in verkeerde verpakking aangeleverd.

Rapportnummer:
415379

Pagina
2 / 4

Volgnummer	Puntcode	Monsteromschrijving*
666851	oh080007	Overig SediSubstractor SP1
666852	oh080007	Overig SediSubstractor SP2
666853	oh080007	Overig SediSubstractor SP3
666854	oh080007	Overig SediSubstractor SP1

Volgnummer	666851	666852	666853	666854
Monstercode klant*	SP1-1	SP2-1	SP3-1	SP1-2
Monstertype*	Overige	Overige	Overige	Overige
Bemonsteringstype*	1 dag, volumeprop.	1 dag, volumeprop.	1 dag, volumeprop.	1 dag, volumeprop.
Monsternemer*	Emma Little	Emma Little	Emma Little	Emma Little
Monstername datum*	05-06-2022	05-06-2022	05-06-2022	06-06-2022
Monstername tijd*	21:00	21:00	21:00	17:00
Acceptatiedatum	07-06-2022	07-06-2022	07-06-2022	07-06-2022

Fysisch- Chemische analyses					Eenheid
Totaal-fosfor in water	0,12	0,14	< 0,05	0,10	mg/l P
Onopgeloste bestanddelen	10	10	9	9	mg/l
Gloeirest onopgeloste bestanddelen	38	37	42	35	% van dg

Rapportnummer:
415379

Pagina
3 / 4

Volgnummer	Puntcode	Monsteromschrijving*
666855	oh080007	Overig SediSubstractor SP2
666856	oh080007	Overig SediSubstractor SP3

Volgnummer	666855	666856
Monstercode klant*	SP2-2	SP3-2
Monstertype*	Overige	Overige
Bemonsteringstype*	1 dag, volumeprop.	1 dag, volumeprop.
Monsternemer*	Emma Little	Emma Little
Monstername datum*	06-06-2022	06-06-2022
Monstername tijd*	17:00	17:00
Acceptatiedatum	07-06-2022	07-06-2022

Fysisch- Chemische analyses			Eenheid
Totaal-fosfor in water	0,11	0,10	mg/l P
Onopgeloste bestanddelen	6	7	mg/l
Gloeirest onopgeloste bestanddelen	8	13	% van dg

Rapportnummer:
416866

Pagina
2 / 3

Volgnummer	Puntcode	Monsteromschrijving*
668755	oh080007	Overig SediSubstrator SP1
668756	oh080007	Overig SediSubstrator SP2
668757	oh080007	Overig SediSubstrator SP3

Volgnummer	668755	668756	668757
Monstercode klant*	SP1	SP2	SP3
Monstertype*	Overige	Overige	Overige
Bemonsteringstype*	1 dag, volumeprop.	1 dag, volumeprop.	1 dag, volumeprop.
Monsternemer*	Emma Little	Emma Little	Emma Little
Monstername datum*	19-06-2022	19-06-2022	19-06-2022
Monstername tijd*	04:00	04:00	04:00
Acceptatiedatum	20-06-2022	20-06-2022	20-06-2022

Fysisch- Chemische analyses				Eenheid
Totaal-fosfor in water	0,44	0,36	0,26	mg/l P
Onopgeloste bestanddelen	40	24	16	mg/l
Gloeirest onopgeloste bestanddelen	33	37	35	% van dg

Rapportnummer:
417123

Pagina
2 / 3

Volgnummer	Puntcode	Monsteromschrijving*
669385	oh080007	Overig SediSubstrator SP1
669386	oh080007	Overig SediSubstrator SP2
669387	oh080007	Overig SediSubstrator SP3

Volgnummer	669385	669386	669387
Monstercode klant*	SP1	SP2	SP3
Monstertype*	Overige	Overige	Overige
Bemonsteringstype*	1 dag, volumeprop.	1 dag, volumeprop.	1 dag, volumeprop.
Monsternemer*	Emma Little	Emma Little	Emma Little
Monstername datum*	24-06-2022	24-06-2022	24-06-2022
Monstername tijd*	04:00	04:00	04:00
Acceptatiedatum	24-06-2022	24-06-2022	24-06-2022

Fysisch- Chemische analyses				Eenheid
Totaal-fosfor in water	0,22	0,20	0,16	mg/l P
Onopgeloste bestanddelen	23	16	12	mg/l
Gloeirest onopgeloste bestanddelen	53	57	66	% van dg

Rapportnummer:
417417

Pagina
2 / 3

Volgnummer	Puntcode	Monsteromschrijving*
669391	oh080007	Overig SediSubstrator SP1
669392	oh080007	Overig SediSubstrator SP2
669393	oh080007	Overig SediSubstrator SP3

Volgnummer	669391	669392	669393
Monstercode klant*	SP1	SP2	SP3
Monstertype*	Overige	Overige	Overige
Bemonsteringstype*	1 dag, volumeprop.	1 dag, volumeprop.	1 dag, volumeprop.
Monsternemer*	Emma Little	Emma Little	Emma Little
Monstername datum*	26-06-2022	26-06-2022	26-06-2022
Monstername tijd*	12:01	12:01	12:01
Acceptatiedatum	27-06-2022	27-06-2022	27-06-2022

Fysisch- Chemische analyses				Eenheid
Totaal-fosfor in water	0,11	0,12	0,14	mg/l P
Onopgeloste bestanddelen	10	7	6	mg/l
Gloeirest onopgeloste bestanddelen	29	23	34	% van dg

Rapportnummer:
421162

Pagina
2 / 3

Volgnummer	Puntcode	Monsteromschrijving*
674461	oh080007	Overig SediSubstrator SP1
674462	oh080007	Overig SediSubstrator SP2
674463	oh080007	Overig SediSubstrator SP3

Volgnummer	674461	674462	674463
Monstercode klant*	SP1	SP2	SP3
Monstertype*	Overige	Overige	Overige
Bemonsteringstype*	1 dag, volumeprop.	1 dag, volumeprop.	1 dag, volumeprop.
Monsternemer*	Emma Little	Emma Little	Emma Little
Monstername datum*	31-07-2022	31-07-2022	31-07-2022
Monstername tijd*	20:00	20:00	20:00
Acceptatiedatum	02-08-2022	02-08-2022	02-08-2022

Fysisch- Chemische analyses				Eenheid
Ortho-fosfaat	0,15	0,18	0,076	mg/l P
Totaal-fosfor in water	0,44	0,47	0,36	mg/l P
Onopgeloste bestanddelen	18	14	9	mg/l
Gloeirest onopgeloste bestanddelen	21	28	29	% van dg

Rapportnummer:
422714

Pagina
2 / 3

Volgnummer	Puntcode	Monsteromschrijving*
676286	oh080007	Overig Sedisubstrator SP1
676287	oh080007	Overig Sedisubstrator SP2
676288	oh080007	Overig Sedisubstrator SP3

Volgnummer	676286	676287	676288
Monstercode klant*	SP1	SP2	SP3
Monstertype*	Overige	Overige	Overige
Bemonsteringstype*	1 dag, volumeprop.	1 dag, volumeprop.	1 dag, volumeprop.
Monsternemer*	Emma Little	Emma Little	Emma Little
Monstername datum*	15-08-2022	15-08-2022	15-08-2022
Monstername tijd*	22:00	22:00	22:00
Acceptatiedatum	16-08-2022	16-08-2022	16-08-2022

Fysisch- Chemische analyses				Eenheid
Ortho-fosfaat	0,29	0,25	0,076	mg/l P
Totaal-fosfor in water	0,60	0,56	0,41	mg/l P
Onopgeloste bestanddelen	31	18	16	mg/l
Gloeirest onopgeloste bestanddelen	23	33	43	% van dg

Rapportnummer:
422715

Pagina
2 / 4

Volgnummer	Puntcode	Monsteromschrijving*
676280	oh080007	Overig SediSubstator SP2 low flow
676281	oh080007	Overig SediSubstator SP2 med flow
676282	oh080007	Overig SediSubstator SP2 high flow
676283	oh080007	Overig SediSubstator SP3 low flow

Volgnummer	676280	676281	676282	676283
Monstercode klant*	SP2-3	SP2-4	SP2-9	SP3-3
Monstertype*	Overige	Overige	Overige	Overige
Bemonsteringstype*	1 dag, volumeprop.	1 dag, volumeprop.	1 dag, volumeprop.	1 dag, volumeprop.
Monsternemer*	Emma Little	Emma Little	Emma Little	Emma Little
Monstername datum*	15-08-2022	15-08-2022	15-08-2022	15-08-2022
Monstername tijd*	13:30	14:00	14:30	13:30
Acceptatiedatum	16-08-2022	16-08-2022	16-08-2022	16-08-2022

Fysisch- Chemische analyses					Eenheid
Ortho-fosfaat	0,32	0,30	0,36	0,11	mg/l P
Totaal-fosfor in water	0,44	0,46	0,48	0,26	mg/l P

Rapportnummer:
422715

Pagina
3 / 4

Volgnummer	Puntcode	Monsteromschrijving*
676284	oh080007	Overig SediSubstator SP3 med flow
676285	oh080007	Overig SediSubstator SP3 high flow

Volgnummer	676284	676285
Monstercode klant*	SP3-4	SP3-9
Monstertype*	Overige	Overige
Bemonsteringstype*	1 dag, volumeprop.	1 dag, volumeprop.
Monsternemer*	Emma Little	Emma Little
Monstername datum*	15-08-2022	15-08-2022
Monstername tijd*	14:00	14:30
Acceptatiedatum	16-08-2022	16-08-2022

Fysisch- Chemische analyses			Eenheid
Ortho-fosfaat	0,11	0,16	mg/l P
Totaal-fosfor in water	0,30	0,28	mg/l P

Rapportnummer:
426302

Pagina
2 / 4

Volgnummer	Puntcode	Monsteromschrijving*
678999	oh080007	Overig SediSubstrator SP1
679000	oh080007	Overig SediSubstrator SP2
679001	oh080007	Overig SediSubstrator SP3

Volgnummer	678999	679000	679001
Monstercode klant*	SP1	SP2	SP3
Monstertype*	Overige	Overige	Overige
Bemonsteringstype*	1 dag, volumeprop.	1 dag, volumeprop.	1 dag, volumeprop.
Monsternemer*	Emma Little	Emma Little	Emma Little
Monstername datum*	07-09-2022	07-09-2022	07-09-2022
Monstername tijd*	02:00	02:00	02:00
Acceptatiedatum	08-09-2022	08-09-2022	08-09-2022

Fysisch- Chemische analyses				Eenheid
Nitriet	0,03	0,02	0,03	mg/l N
Som nitriet + nitraat	0,53	0,50	0,40	mg/l N
Ammonium	2,0	2,1	2,3	mg/l N
Som ammonium- en organisch gebonden stikstof	3,3	3,4	3,7	mg/l N
Ortho-fosfaat	0,13	0,13	0,066	mg/l P
Totaal-fosfor in water	0,29	0,32	0,29	mg/l P
Onopgeloste bestanddelen	17	13	11	mg/l
Gloeirest onopgeloste bestanddelen	38	27	33	% van dg

Metaal analyses				Eenheid
Chroom in afvalwater na destructie	< 2	< 2	< 2	ug/l
Koper in afvalwater na destructie	< 5	< 5	< 5	ug/l
Lood in afvalwater na destructie	53	53	45	ug/l
Nikkel in afvalwater na destructie	< 5	170	< 5	ug/l
Zink in afvalwater na destructie	790	840	710	ug/l

Organische analyses				Eenheid
Minerale olie in water	0,06	< 0,05	< 0,05	mg/l
PAK VROM in afvalwater				
Anthraceen	< 0,01	< 0,01	< 0,01	ug/l
Benzo(a)antraceen	< 0,01	< 0,01	< 0,01	ug/l
Benzo(a)pyreen	< 0,01	< 0,01	< 0,01	ug/l
Benzo(g,h,i)peryleen	< 0,01	< 0,01	< 0,01	ug/l
Benzo(k)fluorantheen	< 0,01	< 0,01	< 0,01	ug/l
Chryseen	< 0,01	< 0,01	< 0,01	ug/l
Fenanthreen	0,02	0,03	0,03	ug/l
Fluorantheen	0,02	0,03	0,02	ug/l
Indeno(1,2,3-c,d)pyreen	< 0,01	< 0,01	< 0,01	ug/l

Rapportnummer:
426302

Pagina
3 / 4

Volgnummer	678999	679000	679001	
Naftaleen	< 0,02	< 0,02	< 0,02	ug/l
Som 10 PAK Leidraad VROM	0,10	0,12	0,11	ug/l

Appendix C – Site Visits and Observations

SediPipe Installation (December 2021)

Figure C - 1: Installation of S4 on the Rooseveltlaan service road

SediSorp+ Installation (February 2022)

Figure C - 2: Installation of SediSorp+ cartridges in S3

Gully Pots Pre-SediSubstrator (March 2022)

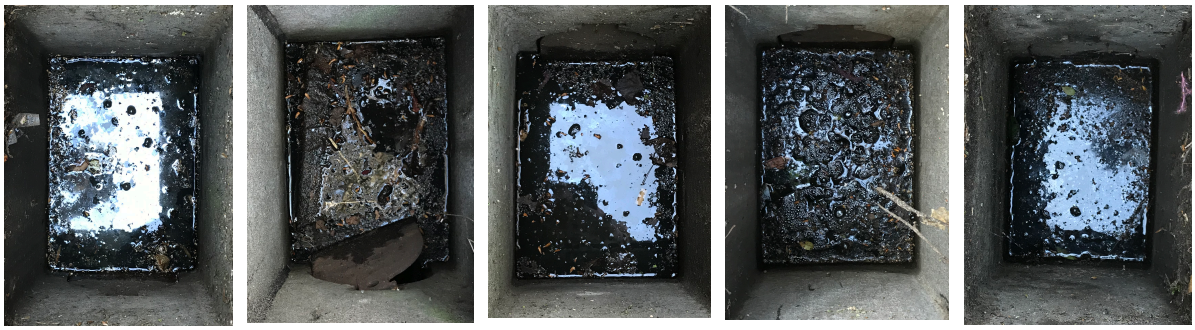

Figure C - 3: Gully pot check, with signs of late-stage decay (sludge-like solids) and bubbles present

Cleaning and Preparatory Works (April 2022)

Figure C - 4: Cleaning S4 for the first time (*left*, *center*); filling manhole sinkers with bricks prior to start-up (*right*)

Gully Pots and Road (May 2022)

Figure C - 5: Gully pot check, with coarse sediments gathering

Figure C - 6: Road gathering coarse sediments

Asellus aquaticus Sampling (June-July 2022)

Water lice (*Asellus aquaticus*) were observed in the SediSubstrator in June and July (Figure C - 7). At their peak, their population density in the system was estimated to be at least 1000 adult individuals per cubic metre.

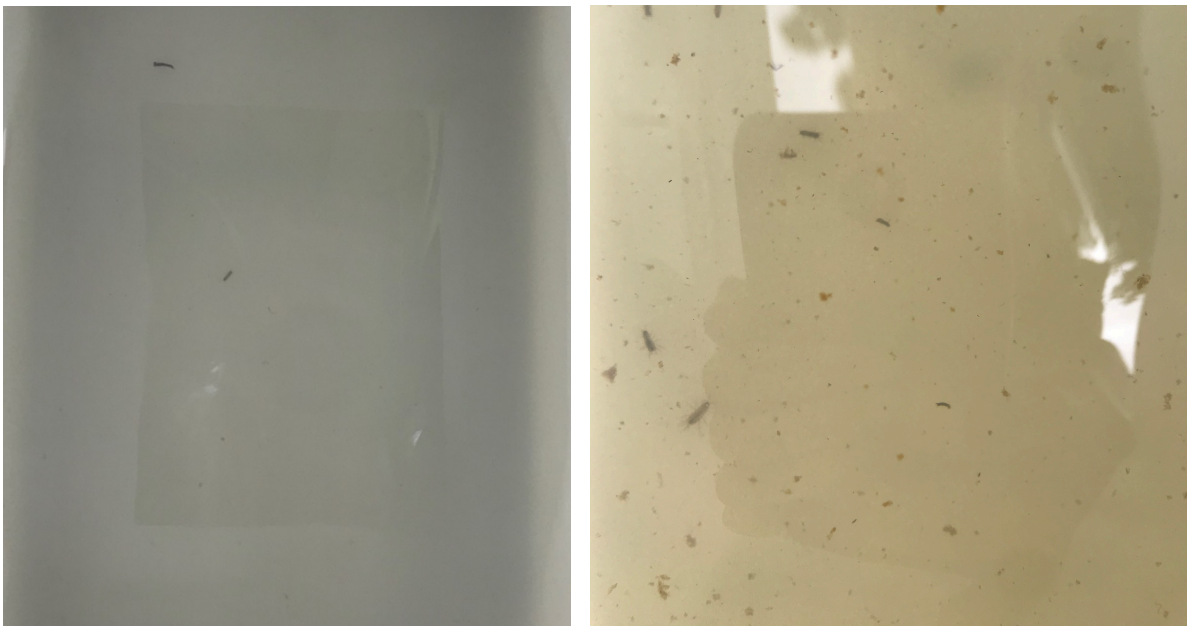

Figure C - 7: Water lice sampling in SP2 on June 27 (*left*) and SP3 on July 21 (*right*)

Water lice are known to feed on decaying organic matter as leaf litter, microscopic algae and small invertebrates and strongly accumulate trace metals in their tissues by ingestion and adsorption (O'Callaghan et al., 2019). They are able to degrade lignocellulose (of interest to the rate of decay of detritus in SUDS, reducing clogging), likely due to enzymes secreted in their gut microbiomes (Lafuente et al., 2021). In water distribution systems they now present themselves at three periods in the year (spring, summer and fall), as they grow at temperatures above 4 ^{o}C, reach maturation above 7 ^{o}C and reproduce above 12 ^{o}C (Gunkel et al., 2022).

Figure C - 8: Water lice visible on the walls of the end shaft, July 27th

Gully Pots (July 2022)

Figure C - 9: Gully pot status

Stormwater Appearance (July 21 2022)

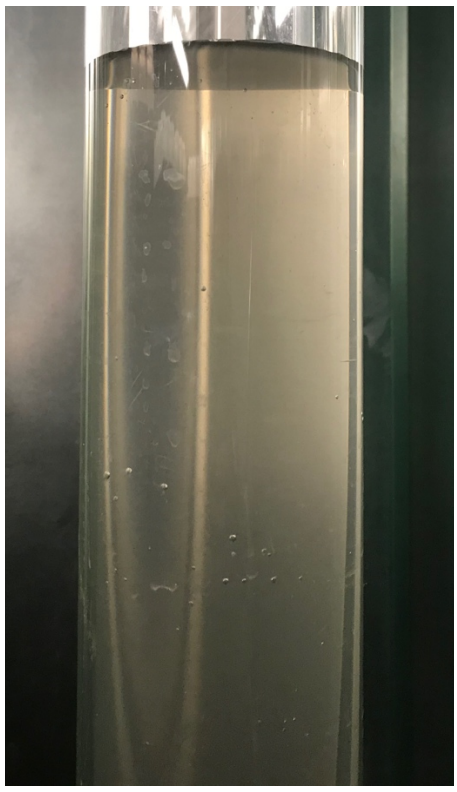

Figure C - 10: Stormwater (SP1) from the event of July 21 2022

Loosdrecht Site Visit

A site visit to the Oud- and Nieuw-Loosdrechtsedijk horseshoe roads took place in July 2022. The state of the gully pots entering the stormwater sewer at the measurement points used by Mandemakers and Holsteijn in 2018 suggested that cleaning had not taken place recently. The line gutter (bottom right) was completely full of leaf litter, while other gully pots showed signs of a process of decay (ie. dark, uniform sludge).

Figure C - 11: Gully pots and line gutter at the locations along the Loosdrecht horseshoe road monitored by Mandemakers and Holsteijn in 2018

Scheduled Instrumentation Maintenance (IMD)

Table C - 1: Scheduled maintenance 1

Maitenance Sedisubstrator
Date: 29-06-2022 Time: 12:00

Measuring point 1	Parameter / Type	Before (in water)	During (in air)	After (in water)	Remark
	Water Level	0,38 m	0 m	0,38 m	
	Turbidity	1,9 FNU	0,5 FNU	1,3 FNU	Only light pollution
	Conductivity	53 µS/cm	0 µS/cm	52 µS/cm	Steady, light pollution only.
	Sampling volume	85 ML		200 ml	New sampling volume
General remarks:					

Measuring point 2	Parameter / Type	Before (in water)	During (in air)	After (in water)	Remark
	Turbidity	10,4 FNU	-	10,3 FNU	Manhole was blocked, no maintenance
	Sampling volume	90 ml		200 ml	New sampling volume
General remarks:					

Measuring point 3	Parameter / Type	Before (in water)	During (in air)	After (in water)	Remark
	Turbidity	22,3 FNU	0,7 FNU	10,3FNU	Medium pollution.
	Sampling volume	100ml		200 ml	New sampling volume
General remarks: Turbidity MP 1 only slight visible pollution. Blockage prevented maintenance on MP 2. The mosted poluted turbidity sensor MP3 gives values simelar to MP 2 (seems confident). Increase on all sampling volumes in order to collect more water for analysis.					

Table C - 2: Scheduled maintenance 2

Maitenance Sedisubstrator
Date: 27-07-2022 Time: 12:00

Measuring point 1	Parameter / Type	Before (in water)	During (in air)	After (in water)	Remark
	Water Level	0,38 m	0 mNAP	0,38 m	
	Turbidity	3,1 FNU	0,4 FNU	3,5 FNU	
	Conductivity	53,2 µS/cm	0 µS/cm	55,2 µS/cm	
	Sampling volume	200 ml	x	200 ml	
General remarks:					

Measuring point 2	Parameter / Type	Before (in water)	During (in air)	After (in water)	Remark
	Turbidity	FNU	FNU	FNU	Manhole blocked by car
	Sampling volume	200 ml	x	200 ml	
General remarks:					

Measuring point 3	Parameter / Type	Before (in water)	During (in air)	After (in water)	Remark
	Turbidity	16,2 FNU	0,9 FNU	19,1 FNU	
	Sampling volume	200 ml	x	200 ml	

Figure C - 12: Turbidity sensor fouling (*top*), before (*left*) and after cleaning (*right*)

Table C - 3: Scheduled maintenance 3

Maitenance Sedisubstrator
Date: 07-09-2022 Time:13:00

Measuring point 1	Parameter / Type	Before (in water)	During (in air)	After (in water)	Remark
	Water Level	- 0,612 mNAP	-0,998 mNAP	- 0,613 mNAP	x
	Turbidity	12,1 FNU	0,4 FNU	12,7 FNU	Almost no visible pollution
	Conductivity	37,3 µS/cm	0 µS/cm	37,2 µS/cm	Light pollution, no effects on value
	Sampling volume	195 ml	x	198 ml	x
General remarks:					

Measuring point 2	Parameter / Type	Before (in water)	During (in air)	After (in water)	Remark
	Turbidity	6,3 FNU	0,6 FNU	5,7 FNU	Shortley after reaplacing high values (50 FNU), bacteria/sediments covering part of the sensor, removed.
	Sampling volume	180 ml	x	200 ml	
General remarks:					

Measuring point 3	Parameter / Type	Before (in water)	During (in air)	After (in water)	Remark
	Turbidity	11,2 FNU	0,7 FNU	12,4 FNU	
	Sampling volume	195 ml	x	200 ml	
General remarks:					

Figure C - 13: Biofouling on turbidity sensor 2 (MP2, September 9th)

Appendix D – Sloterplas Water Experiment Observations

Figure D - 1: Placement of blockages, on the service road (left) and the main road (right)

Figure D - 2: The end shaft (left) and the outlet (right) prior to the experiment (9:40 am).

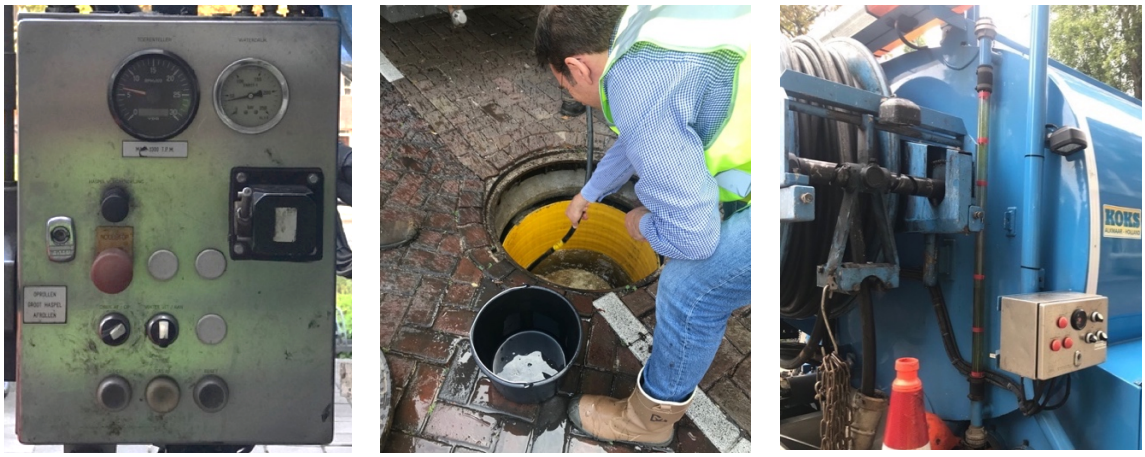

Figure D - 3: Truck pump pressure (left); bucket flowrate measurements (center) and water level (right)

Pumping began at 10:00 am, at a rate of 4 m^3/h. From this point, the water level in the end shaft rose from around NAP -0.4 m up to NAP +0.1 m as the water darkened with solids (most extreme at 10:30 am) and then stabilized at NAP -0.1 m (10:35 am onwards) (Figure D - 4). Fränkische Rohrwerke has asserted that the SediSorp+ filter is not designed to target TSS; however these findings suggest that with rainfall equivalent to just 0.7 mm/h, there is a significant increase in pressure head and some clogging.

Figure D - 4: Darkening of water as solids are resuspended in the end shaft during pumping. Visible change in water level and colour shown at 10:20 am (left), 10:27 am (middle) and 10:30 am (right).

At the end of the experiment the marked water level indicated approximately 3 m^3 remaining in the truck.

Appendix E – Results, Supporting Information

Precipitation Deficit and Groundwater Levels

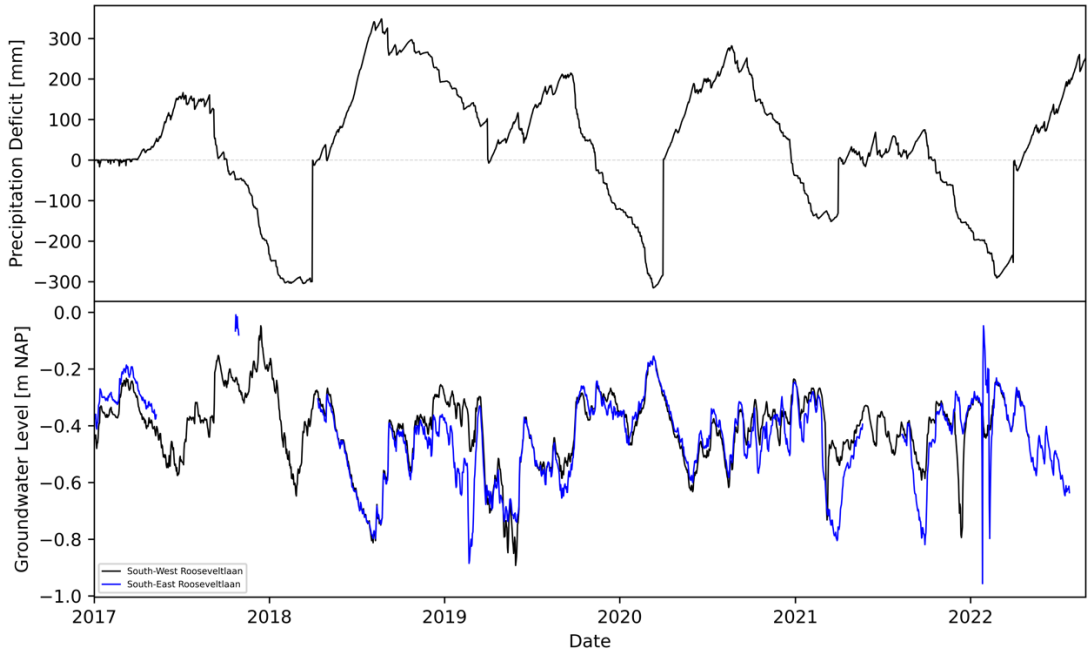

Figure E - 1: Precipitation deficit (from measurements at KNMI Station Schiphol) [mm] and measured groundwater levels on the southern service road of the Rooseveltlaan [m NAP])

Removal Efficiency

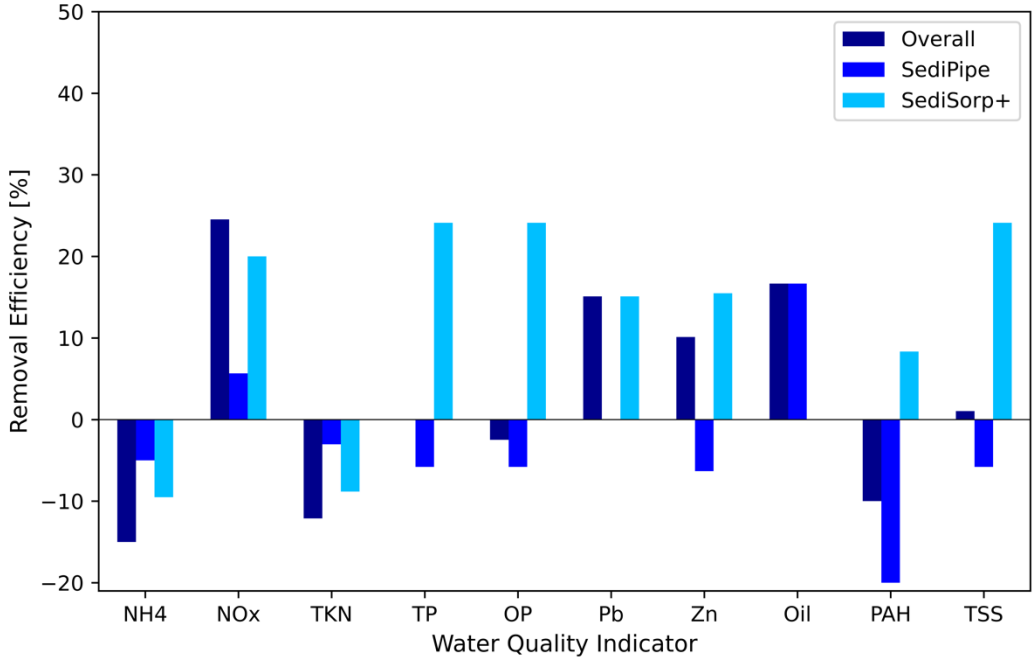

Figure E - 2: Removal efficiency of stormwater quality indicators (*n=1 event*), September 7th 2022

Appendix F – Concepts for Future Research

Ex-Situ Filtration Testing

Knowledge gaps remaining in terms of the long-term performance of the SediSorp+ (relating to clogging, exhaustion of its adsorptive capacity, maintenance, etc.) have driven the following research proposal and associated conceptual process design (Figure F - 1 and F - 2). In particular, the optimization of fine particulate TSS_{63} removal possible in other filters compared to the SediSorp+'s adsorptive and filtration mechanism is of interest.

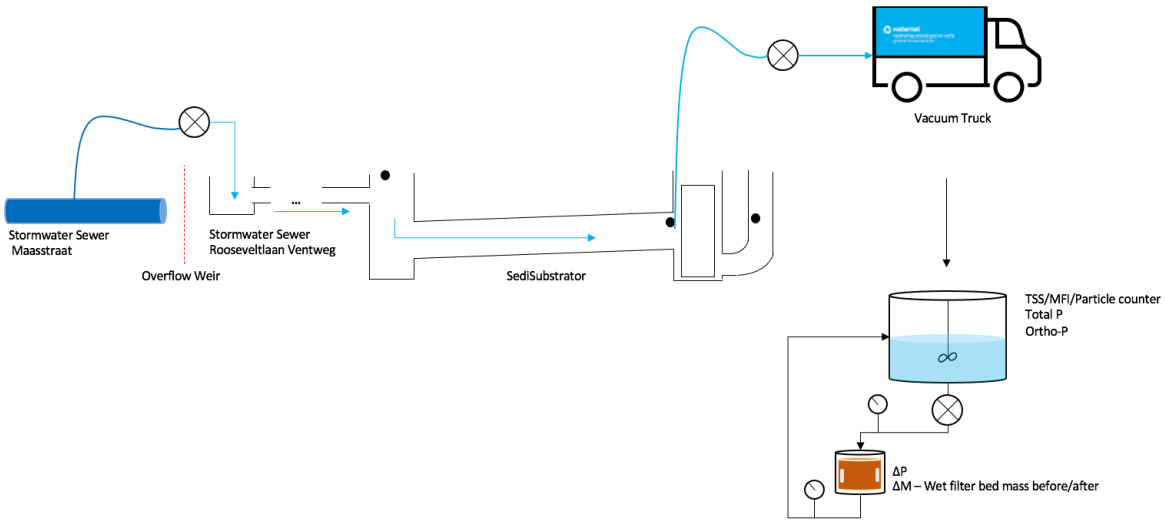

Figure F - 1: Experiment scheme and proposed filter test setup 1

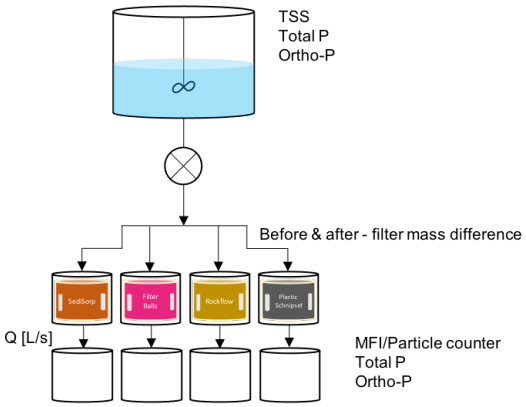

Figure F - 2: Proposed filter test setup 2

In these experiments, stormwater from the adjacent Maasstraat sewer would be pumped through the SediSubstrator at a rate equivalent to the average for inflows to the system in natural rainfall (approximately 4 m^3/h). Water would be pumped out of the system simultaneously at SP2 and trucked to a Waternet facility to be used in a free-standing filter test setup.

Of the two filter test setup concepts designed, the filter test setup 2 is simpler, with less instrumentation needed (measuring the pressure drop by the water level that accumulates

above the filter bed instead of pressure indicators) and allows for the comparison of filters side by side simultaneously using an identical mixed influent. The stirred tank of approx.-imately 2 m^3 (or two 1 m^3 PVC tanks) may be pumped through scaled down filter cartridges (H = D = 20 cm) with the effluent collected and separated by time increment (ie. 5 minutes). The TSS, total P and PO_4^{3-} will be measured before and after the filter, with the option to also analyze using the Membrane Fouling Index (MFI), to infer the stormwater ease of passing through a filter, and particle counter to see what size fraction are predominantly removed. The mass of the wet filter before and after the experiment can be measured to gauge the pollutant removal.

Targeting adsorption, this set-up would also allow for the comparison of the SediSorp+ to the easily-available and alternatively-used iron sand. As a water-treatment residual—consisting of iron oxide-coated sand remaining from the drinking water industry's rapid sand filtration process—it may demonstrate similar removal efficiencies for P, at a lower cost. Desorption tests using 1.0 M NaOH may be run to remove the majority of the adsorbed PO_4^{3-} and quantify the amount adsorbed throughout the experiment (Na et al., 2021).